

A-617  
First Scientific Report - AFCRC-TN-56-961  
ASTIA Document No.: AD 110157

AD-110157

UNITED STATES AIR FORCE  
CAMBRIDGE RESEARCH CENTER  
DOCUMENTS UNIT

## HANDBOOK OF

# TRI-PLATE®

## MICROWAVE COMPONENTS

November 30, 1956

The research reported in this document covers the period from June 1954 to June 1956, and was sponsored by Air Force Cambridge Research Center, Air Research and Development Command, under Contract AF 19(604)1154. Tri-Plate transmission line development was also sponsored in part by the National Bureau of Standards under Contract CST-1365, and developments resulting from this and other contracts held by Sanders Associates, Inc. have been included in this book.

**SANDERS ASSOCIATES, Inc.**

® Sanders Trademark

A-617

First Scientific Report - AFCRC-TN-56-961  
ASTIA Document No. : AD 110157

Copy A

## HANDBOOK OF

# TRI-PLATE<sup>®</sup>

## MICROWAVE COMPONENTS

November 30, 1956

The research reported in this document covers the period from June 1954 to June 1956, and was sponsored by Air Force Cambridge Research Center, Air Research and Development Command, under Contract AF 19(604)1154. Tri-Plate transmission line development was also sponsored in part by the National Bureau of Standards under Contract CST-1365, and developments resulting from this and other contracts held by Sanders Associates, Inc. have been included in this book.

**SANDERS ASSOCIATES, Inc.**

® Sanders Trademark

Copyright 1956  
by

SANDERS ASSOCIATES, INC.  
Nashua, New Hampshire

Except as authorized under  
rights of the United States Govern-  
ment, this book, or any parts there-  
of, may not be reproduced in any  
form without written permission  
of SANDERS ASSOCIATES, INC.,  
NASHUA, NEW HAMPSHIRE.



Comparison of Tri-Plate line and waveguide realizations of the same RF front end unit. The Tri-Plate line fabrication has one-eighth the weight and one-sixth the volume of its waveguide counterpart.



**Contributing Authors**

**Norman R. Wild**

**Jesse L. Butler**

**Kenneth P. Nelligan**

**Donald J. Sommers**

**William J. Wilson**

**Editor**

**Richard W. Peters**

## FORWARD

Most of the material of the present handbook deals with work done at Sanders Associates, Inc. in the development of Tri-Plate<sup>®</sup> line, an advanced form of "flat-strip" microwave transmission line. Tri-Plate microwave components effectively meet the needs of engineers who are interested in achieving light-weight, compact, and economically designed microwave components. The present book is published in order to acquaint engineers with the necessary basic technical information that will enable them to evaluate the advantages and limitations of Tri-Plate components, and thus encourage the use of this type of circuitry in practical working equipment.

During World War II, a flat-strip transmission line was developed by V. H. Rumsey and H. W. Jamieson and applied as a power divider to an antenna system. However, the technique remained dormant for some time thereafter. Early in 1949, Robert M. Barrett of Air Force Cambridge Research Center suggested that flat-strip transmission lines could be used to make any and all types of microwave components; and that the new techniques of printed circuitry be adapted to their fabrication. He proposed several varieties of line, including "flat coaxial" lines with air and solid dielectrics.

Development of flat coaxial line under the name Tri-Plate line was extensively furthered at Sanders Associates, Inc. in a program initiated early in 1952. In August of that year, the work was continued by Sanders under sponsorship of the National Bureau of Standard as part of a contract for developing automatic production of electronic equipment. In June 1954, Tri-Plate transmission line development was furthered by a contract with Air Force Cambridge Research Center. The present handbook serves as a scientific report under both contracts. The basic design and performance of a large variety of components, as well as many items of test equipment are included. In some cases, step-by-step design procedures have been given. A list of references has been added.

® Sanders Associates, Inc. Registered Trademark

Several complete Tri-Plate line RF receiving systems have been developed since 1952 and other systems are being converted to Tri-Plate line under present contracts with industry as well as the Government.

Acknowledgements are due to the many individuals who participated in the preparation of this handbook.

Norman R. Wild  
November, 1956

## CONTENTS

<b>FOREWORD</b> by N. R. Wild	
<b>Chap. 1. GENERAL FORMULAS FOR TRI-PLATE LINE</b>	<b>1</b>
1-1. General Considerations	1
1-2. Field Configuration	2
1-3. Characteristic Impedance	6
1-4. Propagation and Attenuation Characteristics	9
1-5. Power Handling Capability	14
<b>Chap. 2. DISCONTINUITIES</b>	<b>17</b>
2-1. General Considerations	17
2-2. Bends	17
2-3. Transformers	19
2-4. Gaps and Holes	33
<b>Chap. 3. TRANSITIONS AND COUPLINGS</b>	<b>37</b>
3-1. General Considerations	37
3-2. Tri-Plate Line to Tri-Plate Line Couplings	37
3-3. Tri-Plate Line to Coaxial Line Transitions	40
3-4. Tri-Plate Line to Waveguide Transitions	44
<b>Chap. 4. COMPONENTS</b>	
4-1. General Considerations	53
4-2. Terminations and Attenuators	53
4-3. Variable Tuners	57
4-4. Crystal Holders	61
4-5. Power Dividers	66
4-6. Bridge Circuits	73
4-7. Directional Couplers	78
<b>Chap. 5. FILTERS</b>	<b>89</b>
5-1. General Considerations	89
5-2. Behavior of Simple Sections of Line	89
5-3. Short-Line Filters	91
5-4. Practical Design Procedure for Low-Pass Filters	96
5-5. High-Pass Filters	102
5-6. Resonant-Line Filters	103
<b>Chap. 6. ANTENNAS</b>	<b>109</b>
6-1. General Considerations	109
6-2. Single Resonant Slots	109
6-3. Slot Arrays	115
<b>Chap. 7. MEASUREMENTS, MATERIALS, AND FABRICATION TECHNIQUES</b>	<b>127</b>
7-1. General Considerations	127
7-2. Measurement Techniques	128
7-3. Dielectric Materials	133
7-4. Metallic Materials and Bonding	136
7-5. Fabrication	137
<b>REFERENCES</b>	<b>147</b>

## LIST OF ILLUSTRATIONS

Fig.		Page
<b>Chapter 1. GENERAL FORMULAS</b>		
1-1	Evolution of flat-strip transmission line.	2
1-2	Cut-off wavelength for first higher-order mode.	3
1-3	Double centerstrip in Tri-Plate line.	3
1-4	Variation in coupling with lateral spacing between adjacent lines.	5
1-5	Capacitance data for Tri-Plate line.	6
1-6	Exact fringing capacitance for a semi-infinite plate between parallel ground-planes.	7
1-7	Graph of $Z_0$ versus $w/b$ for various values of $t/b$	8
1-8	Equivalence between a rectangular and circular cross-section for a center conductor.	12
1-9	Theoretical attenuation of copper-shielded strip-line in a dielectric medium $E_r$ .	13
1-10	Theoretical Q of copper-shielded strip-line in a dielectric medium $E_r$ .	14
1-11	Average power-rating of Tri-Plate line.	15
<b>Chapter 2. DISCONTINUITIES</b>		
2-1	Standing wave ratio of sharp bends in strip-line.	18
2-2	Input VSWR of mitered right-angle bends.	18
2-3	Contrasted equivalent circuits for center-conductor discontinuities in coaxial and Tri-Plate lines.	20
2-4	Cross-sectional view of coaxial and Tri-Plate lines showing dimensions governing characteristic impedance.	21
2-5	VSWR for $Z_{01}''/Z_{01}' < 1$ at X-band.	23
2-6	VSWR for $Z_{01}''/Z_{01}' > 1$ at X-band.	23
Fig.		Page
2-7	VSWR for $Z_{01}''/Z_{01}' < 1$ at S-band.	23
2-8	VSWR for $Z_{01}''/Z_{01}' > 1$ at S-band.	23
2-9	Single and double Tri-Plate transformers.	25
2-10	Comparison of measured input VSWR with theory for various lengths of taper.	27
2-11	VSWR versus stub-length for an open-circuited shunt-stub.	32

2-12	Admittance plot of shunt-stub as a function of $L/\lambda_{TP}$ .	32
2-13	Gap in Tri-Plate center-conductor and equivalent lumped circuit.	34
2-14	Round hole in Tri-Plate center-conductor and equivalent lumped circuit.	34
2-15	Two methods of increasing the center-conductor gap capacitance in Tri-Plate line.	35

### Chapter 3. TRANSITIONS AND COUPLINGS

3-1	Assembly of a typical Tri-Plate lap-junction with clamp.	38
3-2	Configuration of a typical mitered Tri-Plate junction.	39
3-3	In-line transition from Tri-Plate line to coaxial line.	40
3-4	Tri-Plate male and female coaxial connectors.	41
3-5	Broadband performance of connector shown in Fig. 3-4.	42
3-6	Comparison of right-angle Tri-Plate and waveguide transitions to coaxial line.	42
3-7	Exploded view of Tri-Plate Type-N coaxial connector.	43
3-8	Tri-Plate-line to coaxial-line transition, modified for use through X-band.	44
3-9	Exploded view of X-band Tri-Plate-line to waveguide transition showing series-slot feed element.	45
3-10	Input VSWR for slot-coupled X-band Tri-Plate-line to waveguide transition.	46
3-11	Tri-Plate-line to waveguide X-band probe transition.	47
3-12	Input VSWR for Tri-Plate-line to waveguide probe transition.	48
3-13	C-band Tri-plate-line to waveguide transition.	49
3-14	Input VSWR for C-band probe transition.	50
3-15	X-band Tri-Plate-line to waveguide transition employing magnetic coupling.	51
3-16	Input VSWR for X-band transition to waveguide.	52

### Chapter 4. COMPONENTS

4-1	Two methods of fabricating matched loads and fixed attenuators with resistive coated material.	54
4-2	Typical Tri-Plate termination.	54
4-3	VSWR of a typical Tri-Plate termination.	55

4-4	Disk load fabricated in Tri-Plate line.	55
4-5	Variable attenuator in Tri-Plate line.	56
4-6	Attenuating card and etched centerstrip configuration of Tri-Plate variable attenuator.	57
4-7	Input VSWR of a Tri-Plate variable attenuator.	57
4-8	Tri-Plate short-circuited single-and double-stub tuners.	59
4-9	Open-circuited double-shunt-stub tuner.	59
4-10	Maximum normalized conductance obtained with a double-stub tuner.	60
4-11	Tri-Plate "line-stretcher."	61
4-12	Tri-Plate "tab tuner."	62
4-13	Simple, fixed, tuned, Tri-Plate crystal mount.	63
4-14	Crystal holders in Tri-Plate line.	64
4-15	Admittance plot for crystals shown in Fig. 4-14.	65
4-16	VSWR for crystals shown in Fig. 4-14.	65
4-17	Crystal holder for "Tripolar" crystal.	66
4-18	VSWR for four "Tripolar" crystals in Tri-Plate holder.	67
4-19	Centerstrip configurations for simple power dividers.	67
4-20	VSWR for power dividers shown in Fig. 4-19.	68
4-21	Two possible combinations of power dividers.	70
4-22	Series of three unequal power divisions resulting in equal power in each of four parallel arms.	70
4-23	Power division network with quarter-wave line sections.	71
4-24	Four-way power division in Tri-Plate line.	72
4-25	VSWR for power divider shown in Fig. 4-24.	72
4-26	Symmetrical four-terminal-pair network.	73
4-28	Center-conductor configuration of a band-balanced mixer.	74
4-29	Isolation and VSWR for L-band hybrid ring.	75
4-30	Isolation and VSWR for S-band hybrid ring.	76
4-31	Coupling and VSWR for C-band hybrid ring.	77
4-32	Isolation and VSWR for X-band hybrid ring.	78
4-33	Tri-Plate branch-line coupler.	79
4-34	Coupling and directivity for branch-line coupler.	80

4-35	3-DB branch-line coupler in Tri-Plate line.	80
4-36	VSWR and isolation for 3-DB coupler.	81
4-37	Tri-Plate quarter-wave stub-coupler.	81
4-38	Parallel-line directional coupler.	82
4-39	Coupling, VSWR, and directivity for parallel-line coupler.	83
4-40	Construction of long slot in Tri-Plate line.	83
4-41	Bethe-hole coupler in Tri-Plate line.	84
4-42	Coupling versus hole size etched in ground-plane common to two Tri-Plate lines.	85
4-43	Coupling and directivity for Bethe-hole coupler with $\frac{3}{8}$ " coupling hole.	85
4-44	Multihole coupler in Tri-Plate line.	86
4-45	Frequency characteristics of multihole coupler.	86

#### Chapter 5. FILTERS

5-1	Reactance for short-circuited line and susceptance for open-circuited line.	91
5-2	Comparison of low-frequency low-pass filter network with Tri-Plate configuration.	92
5-3	Comparison of low-frequency high-pass filter network with Tri-Plate configuration.	93
5-4	Comparison of symmetrical lumped-constant T-section for low-pass filter with equivalent configuration in Tri-Plate line.	97
5-5	Centerstrip configurations of three low-pass filters.	100
5-6	Tri-Plate low-pass filter.	101
5-7	Attenuation versus frequency for Tri-Plate low-pass filters.	101
5-8	Cross-sectional view of a series-capacitance in Tri-Plate line.	102
5-9	Impedance of single-element resonant line filter.	104
5-10	Transmission loss at resonance for TEM transmission line filters.	107

#### Chapter 6. ANTENNAS

6-1	Various radiating devices in Tri-Plate line.	109
6-2	Two dipole radiating devices in Tri-Plate line.	110
6-3	Resistance of L-band standing-wave slot.	112



6-4	Resistance of L-band traveling-wave slot.	112
6-5	Reactance of L-band standing-wave slot.	113
6-6	Reactance of L-band traveling-wave slot.	113
6-7	Typical L-band series-fed slot.	114
6-8	Impedance of L-band slot.	115
6-9	Structural drawing of L-band slot.	116
6-10	X-band series slot.	117
6-11	VSWR for X-band series slot.	117
6-12	4-slot E-Plane array.	118
6-13	4-slot H-plane array.	118
6-14	Input VSWR for four-slot arrays.	119
6-15	Pattern for four-slot E-plane array.	119
6-16	Pattern for four-slot H-plane array.	119
6-17	Composite 4 x 4 slot array.	120
6-18	Input VSWR for 4 x 4 slot array.	121
6-19	E-plane pattern for 4 x 4 slot array.	121
6-20	H-plane pattern for 4 x 4 slot array.	121
6-21	4 x 6 slot array.	123
6-22	E-plane pattern for 4 x 6 array.	123
6-23	H-plane pattern for 4 x 6 array.	123
6-24	Admittance plots for two 4 x 6 arrays.	124
6-25	Input VSWR for two halves of twin X-band array.	124
6-26	Twin X-band Tri-Plate array.	125

#### Chapter 7. MEASUREMENTS, MATERIALS, AND FABRICATION TECHNIQUES

7-1	Probe, slotted metal case and Tri-Plate line with top ground-plane etched away.	128
7-2	Field distribution in Tri-Plate line.	129
7-3	Measurement of current on outer plates of Tri-Plate line.	130
7-4	Cross-sectional view of line in slotted metal section.	131
7-5	Tri-Plate slotted line.	132

7-6	Attenuation in DB per foot for four different Tri-Plate lines.	135
7-7	Unloaded Q values for four different 50-ohm Tri-Plate lines.	136
7-8	Finishing touches on base-plate for S-band hybrid ring.	138
7-9	Technician placing S-band hybrid ring baseplate in copy camera vacuum frame.	140
7-10	Preparations for exposing sensitized copper plane.	142
7-11	Washing dye off exposed Tri-Plate components.	143
7-12	Etched components being removed from etching tank.	143
7-13	Final cleaning to remove photo-resist from copper.	143
7-14	Roughing out S-band hybrid ring along cutlines.	145
7-15	Shaving hybrid ring down to cut-lines.	145
7-16	High speed drill bores eyelet holes.	146
7-17	Assembly of hybrid ring: peening eyelets.	146
7-18	Trimming termination of hybrid ring.	146

This document contains information on matters proprietary to Sanders Associates, Inc., subject to the rights of the U. S. Government and any other parties as defined by the contracts applicable hereto. Subject to the above-referenced rights, no portion of this document may be disclosed, used, or reproduced without the written consent of Sanders. Nothing in this document shall be construed as in any way modifying the rights or responsibilities of Sanders Associates, Inc. as defined by the applicable contracts.

## CHAPTER ONE

### GENERAL FORMULAS FOR TRI-PLATE LINE

#### 1-1 General Considerations

An important recent trend in microwave engineering has been the development of "flat-strip" microwave components fabricated with printed-circuit techniques. The type of flat-strip transition line used for making these components must be carefully chosen, since most types of flat-strip line are characterized by considerable leakage of RF energy, seriously limiting their performance. Components fabricated in Tri-Plate<sup>®</sup> line, however, have ground-planes which are at equal potential, and no such leakage exists. As a result, Tri-Plate line components have been developed which operate successfully up to 11,000 megacycles.

In Tri-Plate line, electromagnetic energy is guided by a flat center-conductor through a dielectric medium sandwiched between flat ground-planes. Energy is carried in the TEM mode. Discussions throughout this book are restricted to this mode of transmission since the configuration of the line effectively cancels out other modes. As in all transmission lines, variation of the line geometry at any point will create discontinuities. Properly dimensioned, these discontinuities become the useful devices discussed in succeeding chapters.

Tri-Plate line allows the expression of design concepts that are impracticable or even unattainable in conventional coaxial and waveguide systems. The most complex device can be manufactured in Tri-Plate line as easily as the simplest. The flat design of Tri-Plate components permits fabrication directly on the dielectric medium by conventional printed-circuit techniques. Greatly simplified production of microwave components of unusual light-weight and compactness is thus made possible, as shown in the frontispiece.

### 1-2 Field Configuration

The field configuration in Tri-Plate line is shown in Fig. 1-1 as the final stage in a progressive modification by flattening of the conventional coaxial line. The inner conductor of the coaxial line becomes a flat strip of finite thickness, while the outer conductor is broken into two semi-infinite ground-planes. The solid lines in the figure are used to indicate the electric field; and broken lines, the magnetic field. These lines are entirely in the transverse plane.

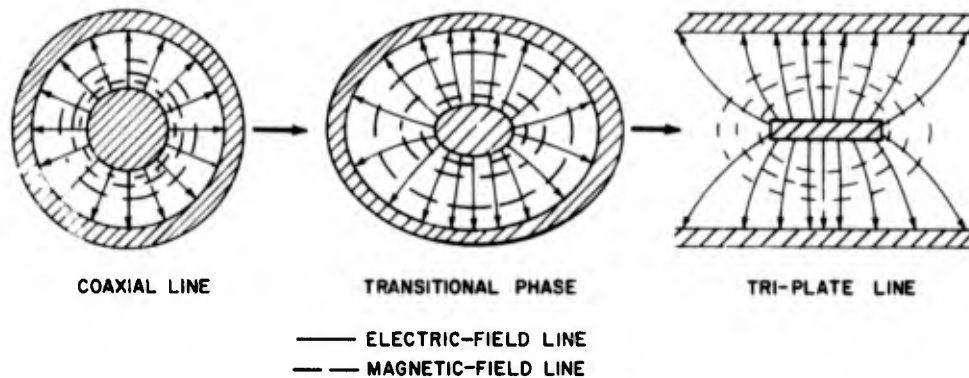


Fig. 1-1 Evolution of flat-strip transmission line.

The electric field is entirely bounded by the flat outer-conductors in the region of the centerstrip and is relatively uniform within the space directly between centerstrip and outer plates. The fringe field (or field external to the space directly between centerstrip and ground-planes) decays very rapidly. There is no electrical field-component lateral to the centerstrip. Thus, sidewalls are unnecessary.

Since the TEM mode is used in most practical applications of Tri-Plate line, limitations are imposed upon the dimensions of the line. Higher-order modes may propagate when the ground-plane spacing exceeds a half-wavelength. Thus, the spacing must be kept at less than a half-wavelength for the highest frequency desired, so that extraneous TE and TM modes excited in the line will be rapidly attenuated.

It has been shown<sup>1</sup> that propagation of higher-order modes is possible in a strip-transmission line, when a circumferential path, as shown in Fig. 1-2, described about the centerstrip and passing through the means between inner and outer conductors, is equal to or greater than one wavelength. This property of strip-transmission lines is analogous to that found in coaxial line where a circumference at the arithmetic mean between conductors must be held to less than one wavelength.

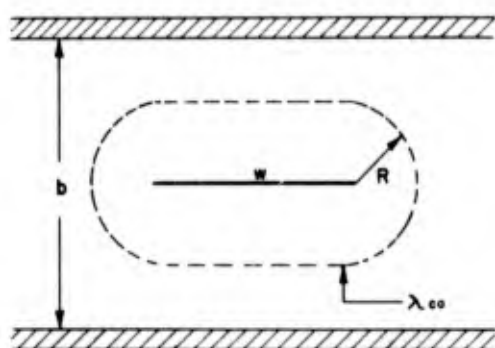


Fig. 1-2 Cut-off wavelength for first higher-order mode.

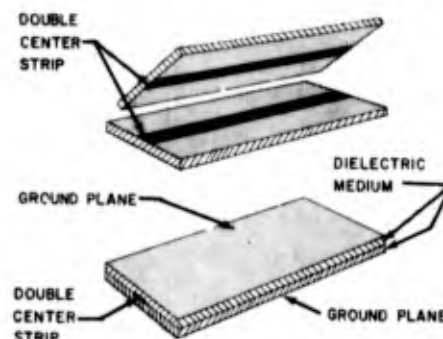


Fig. 1-3 Double centerstrip in Tri-Plate line: a) exploded view, and b) assembled.

Because of the inherent balance of the ideal strip line configuration, the fields above and below a central plane through the line are equal and opposite. No parallel-plate TEM, or TE zero-order modes exist as long as the symmetry of such structure is maintained. In the ordinary flat-strip line, however, longitudinal tilting of the centerstrip between the ground-planes excites higher-order modes. Tilting may arise under pressure or any condition which separates the ground-planes.

In Tri-Plate line, the problems of avoiding longitudinal tilting of the center-conductor, and of maintaining structural symmetry, are solved by the method of constructing the line, as shown in Fig. 1-3. The dielectric

<sup>1</sup>E. Fubini, W. Fromm, and H. Keen, "New Techniques for High-Q Strip Microwave Components," IRE Convention Record, March, 1955.

which fills each half of the line between the center-conductor and the ground-plane, maintains proper spacing between these conducting elements and affords a solid mechanical support for them. This structure facilitates photo-etching, and easy assembly of the line into a rugged and non-microphonic package. The configuration of the centerstrip is photo-etched on the inner faces of both laminates. Since there are two such etched lines, symmetry of the fields is maintained, even when the two halves of the line are separated. Each half of the line functions effectively as a single strip-conductor above a ground-plane, and the effects of "tilting" are almost entirely avoided. Assuming a reasonably homogeneous dielectric material and uniform strip to ground-plane spacing, an air gap between the two center-conductors will have little effect on the line and Tri-Plate line is thus not pressure-sensitive.

This ability to tolerate separation of the two halves of the line can be used to advantage. With gradual separation of the center-conductors so that reflections do not arise, variable devices, such as line-stretchers and lossy materials, may be inserted without upsetting the balance of the line. This leads directly to the development of unique and useful devices.

For this type of line configuration, the magnetic field decays at a rate inversely proportional to distance from the centerstrip, so that coupling between two adjacent lines should decay rapidly with separation. Experimental verification of this supposition has been obtained by measurements made at 4.2 KMC. A curve showing the variation of coupling with lateral spacing is shown in Fig. 1-4. The measurements were made for a length of line of about  $5 \frac{1}{4} \lambda$ , at various spacings between the lines. As the spacing between strips is increased from  $\frac{1}{32}$ " to  $\frac{1}{4}$ ", the coupling between strips drops from -10.8 DB to less than -70 DB. It can be seen from this curve that the lateral attenuation between two adjacent

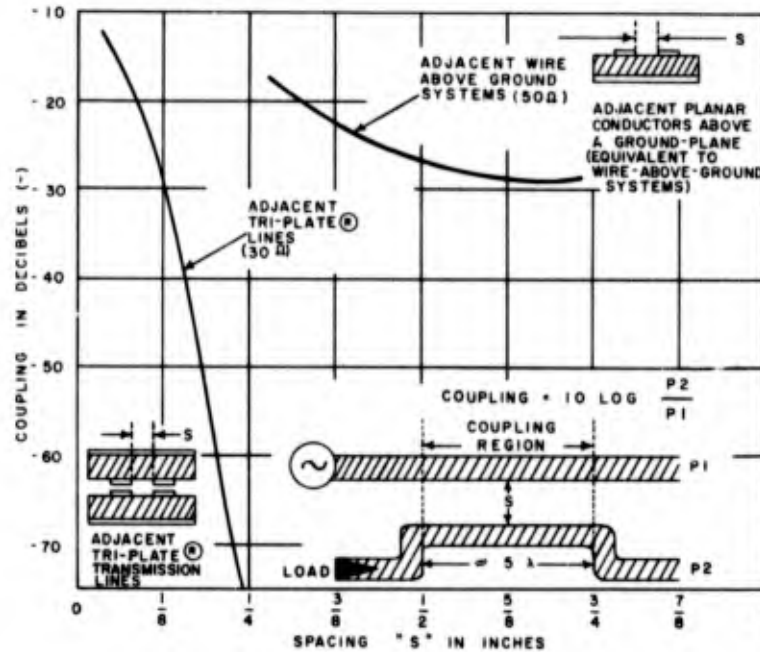


Fig. 1-4 Variation in coupling with lateral spacing between adjacent Tri-Plate lines compared with coupling between adjacent conductors-above-a-groundplane (equivalent to early two-plate strip-transmission lines).

strips at about 4.2 KMC is greater than 70 DB per 1/4" separation, which indicates that circuit components spaced as closely as one-fourth inch will not be appreciably affected by crosstalk.

It is often necessary to couple RF energy to a particular strip transmission line in a direction normal to the plane of the center-conductor. Such a transition would require opening one ground-plane and probing the field in an asymmetrical manner. The resulting field-disruption would excite undesirable modes which would propagate freely between the ground-planes and would not be confined to the region of the center-conductor. Such undesired modes may be suppressed by the insertion into the line of screws or eyelets which would short the ground-planes together in the region of the unbalance.



The spacing of these shorting bars is of particular importance. If the maximum distance between any two adjacent pins is kept less than  $\lambda/2$  in the dielectric medium, all modes but the desired TEM mode will be suppressed. The degree of suppression is, of course, increased when the number of pins is increased and when they are placed closer together.

### 1-3 Characteristic Impedance Capacitance

The capacitance of Tri-Plate line is equal to the plate-to-plate capacitance ( $C_{pp}$ ) plus the fringe field capacitance ( $4C'_f$ ) as shown in Fig. 1-5.

$$C = C_{pp} + 4C'_f \quad (1-1)$$

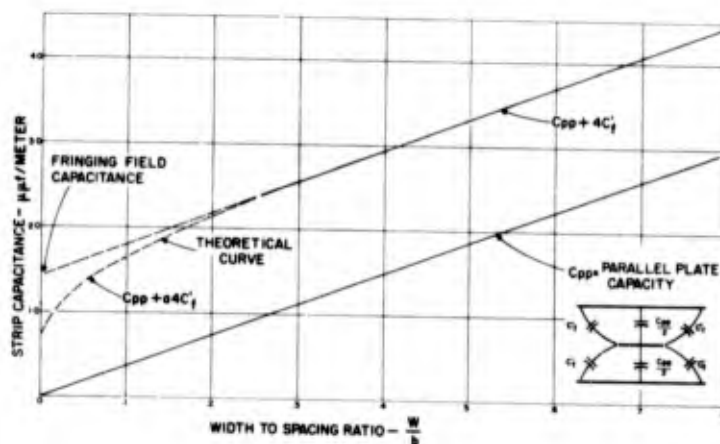


Fig. 1-5 Capacitance data for Tri-Plate line.

The fringe-capacitance becomes an increasingly large part of the total capacitance as the width of the center-strip is decreased. In a capacitor consisting of three parallel plates, such as Tri-Plate line:

$$C_{pp} = 35.4 \frac{w/b}{\left(1 - \frac{t}{b}\right)} \epsilon_r \mu\text{f/meter} \quad (1-2)$$

where:

$\epsilon_r$  = relative dielectric constant  
 $w$  = centerstrip width

b = ground-plane separation  
and t = centerstrip thickness,

and, for a center-conductor where the ratio of center-strip width to ground-plane separation ( $w/b$ ) is more than 0.35, the equation for fringing capacitance, as given by S. Cohn<sup>2</sup>, is

$$C'_f = \frac{0.0885}{\pi} \epsilon_r \left\{ \frac{2}{\left(1 - \frac{t}{b}\right)} \ln \left( \frac{1}{\left(1 - \frac{t}{b}\right)} + 1 \right) - \left( \frac{1}{\left(1 - \frac{t}{b}\right)} - 1 \right) \ln \left( \frac{1}{\left(1 - \frac{t}{b}\right)^2 - 1} \right) \right\} \mu\mu\text{f/cm.} \quad (1-3)$$

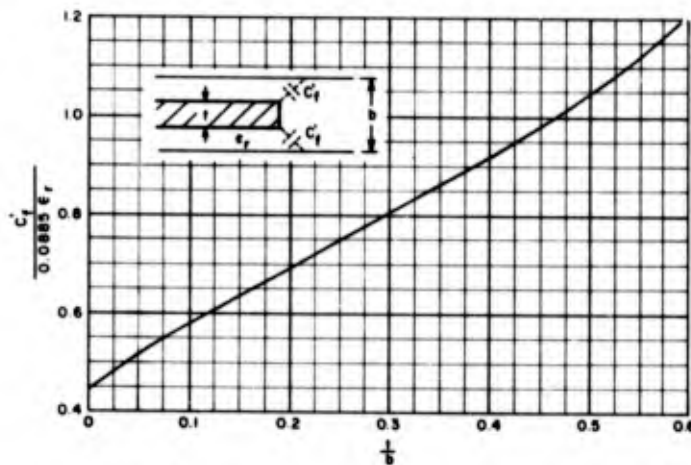


Fig. 1-6 Exact fringing capacitance for a semi-infinite plate between parallel ground-planes.

As centerstrip width decreased and  $w/b$  becomes less than 0.35, Eq. (1-3) is no longer accurate, due to the interaction which takes place between the fringe fields at the edges of the centerstrip. The effective fringe-field capacitance has been shown by Barrett<sup>3</sup> to rise to a limiting value. The curve<sup>2</sup> in Fig. 1-6 shows exact

fringing capacitance  $\frac{C'_f}{0.0885 \epsilon_r}$  in microfarads per cen-

timeter for a semi-infinite plane centered between parallel ground-planes.

<sup>2</sup>Seymour B. Cohn, "Problems in Strip Transmission Lines," IRE Transactions on Microwave Theory and Techniques, March, 1955.

<sup>3</sup>Robert M. Barrett, "Microwave Printed Circuits — A Historical Survey", IRE Transactions on Microwave Theory and Techniques, March, 1955.

**Impedance**

The characteristic impedance of Tri-Plate line, when the ratio of width ( $w$ ) of the centerstrip to the separation ( $b$ ) between the ground-planes ( $w/b$ ) is equal to or more than 0.35 (which is the case for comparatively wide centerstrips), is found as follows:

$$Z_o = \frac{94.15}{\sqrt{\epsilon_r} \left( \frac{w/b}{1-t/b} + \frac{C'_f}{0.0885\epsilon_r} \right)} \quad \text{ohms} \quad (1-4)$$

where  $C'_f$  is found as shown in Eq. (1-3).

For narrow centerstrip conductors, where the ratio ( $w/b$ ) is less than 0.35, the following formula<sup>4</sup> is accurate within 1.2%.

$$Z_o = \frac{60}{\sqrt{\epsilon_r}} \ln \frac{4b}{\pi d_o} \quad \text{ohms} \quad (1-5)$$

Characteristic impedance curves for various values of  $t/b$  are plotted against  $w/b$  in Fig. 1-7.

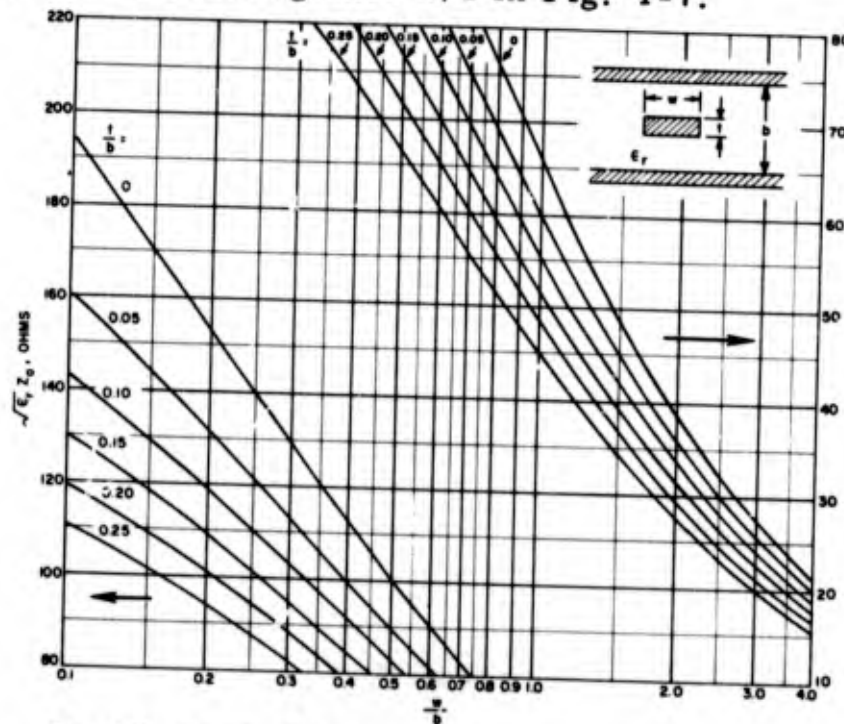


Fig. 1-7 Graph of  $Z_o$  versus  $w/b$  for various values of  $t/b$ .

<sup>4</sup>Cohn, loc. cit.

## 1-4 Propagation and Attenuation Characteristics

*Propagation in TRI-PLATE line*

The general expression for the propagation constant of a transmission line is given by:

$$\gamma = \sqrt{ZY} = \sqrt{(R + j\omega L)(G + j\omega C)} \quad (1-6)$$

$$\gamma = \alpha + j\beta \quad (1-7)$$

where:

$Z$  is the characteristic impedance,  
 $Y$  is the characteristic admittance,  
 $\alpha$  is the attenuation constant, and  
 $\beta$  is the phase constant.

It can be shown that for most practical transmission line problems the conductor and dielectric medium may be considered lossless when determining propagation characteristics. Thus: when  $R$  and  $G$  equal zero, and likewise  $\alpha$  equals zero, the expression for  $\gamma$  becomes:

$$\gamma = j\omega \sqrt{LC} = j\beta \quad (1-8)$$

The phase velocity is given by:

$$V_p = \frac{\omega}{\beta} = \frac{1}{\sqrt{LC}} \quad (1-9)$$

and is related to the speed of light ( $c$ ) by:

$$V_p = \frac{c}{\sqrt{\mu_r \epsilon_r}} \quad (1-10)$$

where  $\mu_r$  and  $\epsilon_r$  are the relative permeability and dielectric constant respectively of the transmission line medium. With the symbol  $\beta_L$  representing the phase constant for a line where losses are considered,  $\beta_L$  may be equated to the phase constant of a lossless line ( $\beta$ ) by:

$$\beta_L = \beta \left[ 1 + \frac{1}{2} \left( \frac{\alpha_c + \alpha_d}{\beta} \right)^2 \right] \quad (1-11)$$

in which  $\alpha_c$  and  $\alpha_d$  are respectively the conductor and dielectric losses expressed in nepers per unit length of line. Typical loss data measured at 10 KMC for a Tri-Plate line fabricated from copperclad teflon-fiberglass

laminates shows  $\alpha_c = .0311$  neper/feet and  $\alpha_d = .0955$  neper/feet. Substituting these attenuation values and 2.5 for the relative dielectric constant of teflon glass, Eq. (1-11) gives a value of  $.999995\beta$  for  $\beta_L$ . Thus for most practical applications, losses have no significant effect on the phase constant. It is interesting to note that when  $\alpha_c = \alpha_d$ ,  $\beta_L = \beta$ .

#### Wavelength in TRI-PLATE line

The wavelength in Tri-Plate line is related to the free space wavelength by:

$$\lambda_{TP} = \frac{\lambda}{\sqrt{\mu_r \epsilon_r}} \quad (1-12)$$

#### Attenuation

Two basic types of loss occur in Tri-Plate lines, namely: conductor loss and dielectric loss. The total loss may be expressed as the sum of these individually computed losses, as follows:

$$\alpha = \alpha_c + \alpha_d \quad (1-13)$$

where:  $\alpha$  = total loss per unit length  
 $\alpha_c$  = conductor loss per unit length  
 $\alpha_d$  = dielectric loss per unit length

The attenuation resulting from dielectric losses in any TEM transmission line is given by:

$$\begin{aligned} \alpha_d &= \frac{\pi}{\lambda} \sqrt{\epsilon_r} \tan \delta \text{ nepers/unit length} \\ &= \frac{27.3 \sqrt{\epsilon_r} \tan \delta}{\lambda} \text{ DB/unit length} \end{aligned} \quad (1-14)$$

where:

$\lambda$  = wavelength in free space,  
 $\epsilon$  = relative dielectric constant of the dielectric material, and  
 $\tan \delta$  = loss tangent of the dielectric material.

The attenuation resulting from copper losses is given by the following general expression:

$$a_c = \frac{0.0231 R_s \sqrt{\epsilon_r}}{Z_0} \left( \frac{\partial Z_0}{\partial b} - \frac{\partial Z_0}{\partial w} - \frac{\partial Z_0}{\partial t} \right) \text{ DB/unit length} \quad (1-15)$$

where

$R_s$  = surface resistivity in ohms/square

#### Wide Centerstrip

With a centerstrip width such that no interaction between the fringe-field capacitances exists, ( $w/b = 0.35$ ), then the formula for attenuation due to conductor loss in copper is

$$a_c = \frac{2.02 (10)^{-6} \sqrt{\epsilon_r} f(\text{KMC})(\sqrt{\epsilon_r} Z_0)}{b} \left[ \frac{1}{1 - \frac{t}{b}} + \frac{\frac{2w}{b}}{(1 - \frac{t}{b})^2} + \frac{1}{\pi} \frac{(1 + \frac{t}{b})}{(1 - \frac{t}{b})^2} \right] \ln \left( \frac{\frac{1}{1 - t/b} + 1}{\frac{1}{1 - t/b} - 1} \right) \text{ DB/unit length} \quad (1-16)$$

The term  $(\sqrt{\epsilon_r} Z_0)$  is determined as a function of the cross-sectional dimensions from Fig. 1-7.

#### Narrow Centerstrip

As centerstrip width is decreased enough to allow interaction between fringing fields on opposite sides of the strip, Eq. (1-16) becomes inaccurate. In order to evaluate the narrow-strip case, Cohn<sup>5</sup> has substituted the simplified approach of postulating an equivalent circular conductor with a diameter ( $d_0$ ) for the normal

<sup>5</sup>Cohn, loc. cit.

rectangular centerstrip. A plot of  $(d_o/w)$  versus  $(t/w)$  is shown in Fig. 1-8. Using this approach, when  $w/b - t \geq 0.35$ ,  $t/b \leq 0.25$  and either  $t/w$  or  $w/t \leq 0.11$ , the expression for conductor loss is as follows:

$$\alpha_c = \frac{0.011402 \sqrt{\epsilon_r} f \text{ KMC}}{(\sqrt{\epsilon_r} Z_0) b} \left\{ 1 + \frac{b}{d_o} \left[ \frac{1}{2} + 0.669 \frac{t}{w} - 0.255 \frac{t}{w} + \frac{1}{2\pi} \ln \left( \frac{4\pi w}{t} \right) \right] \right\} \text{DB/unit length} \quad (1-17)$$

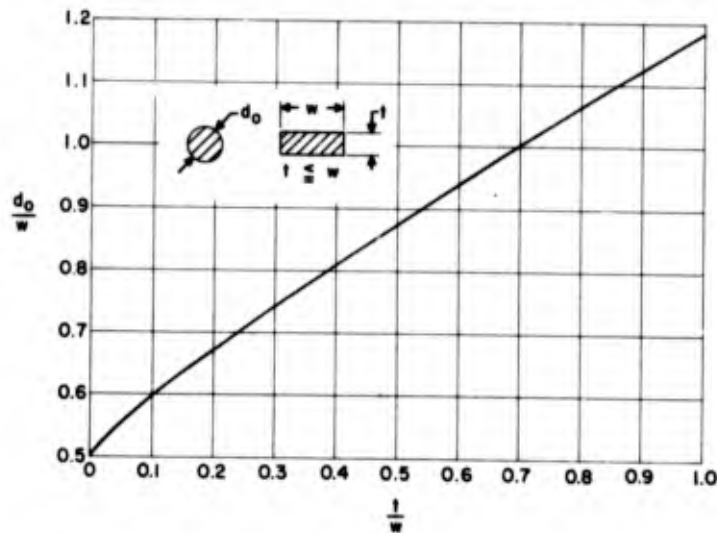


Fig. 1-8 Equivalence between a rectangular and circular cross-section for a center-conductor.

Fig. 1-9 shows the theoretical attenuation of copper-shielded strip line in a dielectric medium  $\epsilon_r$ . For other conductors, the attenuation should be scaled proportionately to  $R_s$ . Note that the ordinate gives  $\alpha_c$  directly in DB per inch at a frequency of 1 KMC when  $\epsilon = 1$  and  $b =$  one inch. The total attenuation when a dielectric material fills the line is given by:

$$\alpha = \alpha_c + \frac{27.3 \sqrt{\epsilon_r} \tan \delta}{\lambda} \text{DB/unit length} \quad (1-18)$$

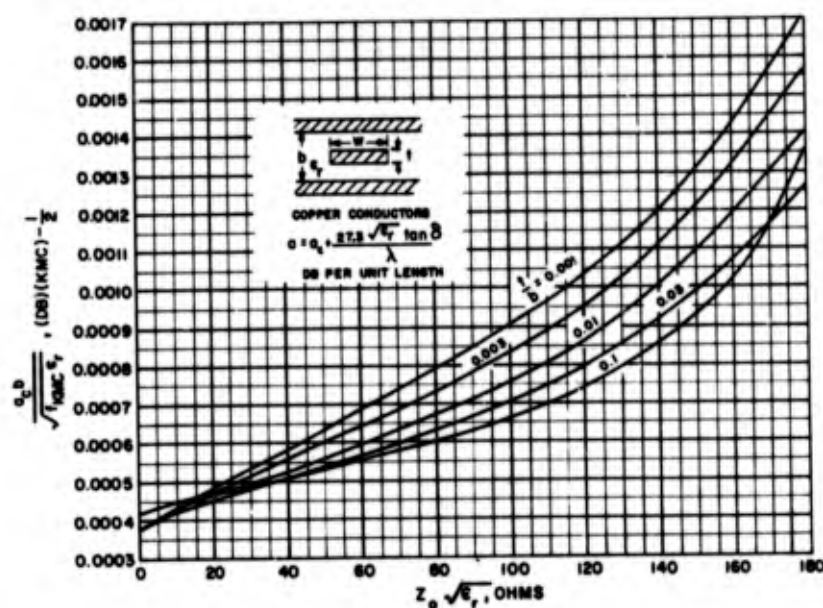


Fig. 1-9 Theoretical attenuation of copper-shielded strip-line in a dielectric medium  $\epsilon_r$ .

The quality of dielectric-filled line may be expressed<sup>6</sup> as follows:

$$\frac{1}{Q} = \frac{1}{Q_c} + \frac{1}{Q_d} \quad (1-19)$$

where  $Q_c$  and  $Q_d$  depend on conductor and dielectric loss.  $Q_c$  is found as follows:

$$Q_c = \frac{2\pi}{\lambda t p \alpha c} \quad (1-20)$$

where  $\alpha c$  is found in Eqs. (1-16) and (1-17), and  $\lambda_{TP} =$

$$\frac{\lambda}{\sqrt{\epsilon_r}}$$

$Q_d$  may be expressed as:

$$Q_d = \frac{1}{\tan \delta} \quad (1-21)$$

Curves<sup>7</sup> found in Fig. 1-10 show the theoretical  $Q_c$  of copper-shielded strip line in a dielectric medium  $\epsilon_r$ .  $Q_c$  is given directly for copper conductors at 1 KMC where (b) equals one inch. For conductors other than copper,  $Q_c$  is proportional to  $\frac{1}{R_s}$

<sup>6</sup>Cohn, loc. cit.

<sup>7</sup>Cohn, loc. cit.



By substituting  $\frac{1}{\tan \delta}$  for  $Q_d$  in Equation (1-19), we obtain

$$Q = \frac{Q_c}{1 - Q_c \tan \delta} \quad (1-22)$$

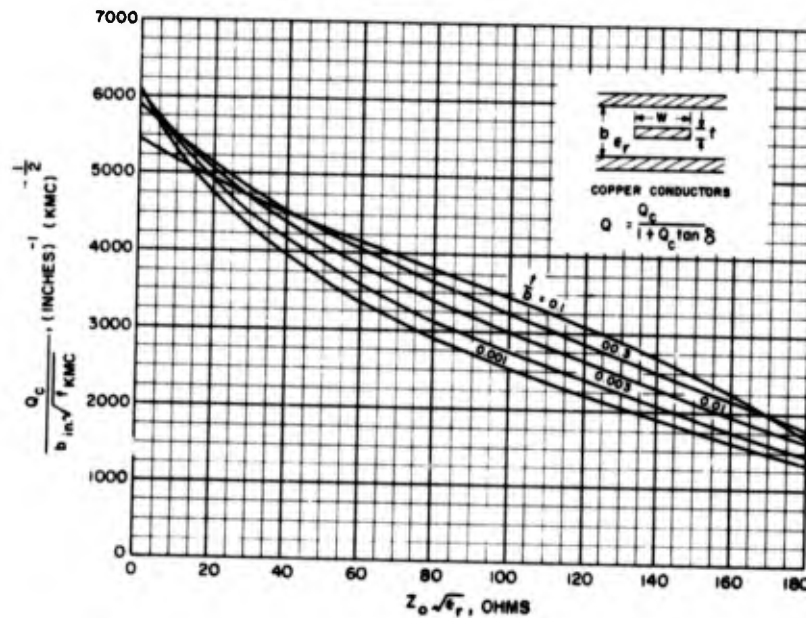


Fig. 1-10 Theoretical  $Q$  of copper-shielded strip-line in a dielectric medium  $E_r$ .

### 1-5 Power Handling Capability

The average power-handling capability of Tri-Plate line is limited primarily by the allowable temperature rise at the center of the line. (The heat is, of course, due to attenuation losses.) For a constant impedance and the same dielectric material, center-conductor temperature rise due to conductor losses is independent of ground-plane spacing. This is true because center-conductor losses and the rate at which heat is conducted away from the center-conductor are both inversely proportional to ground-plane spacing.

The center-conductor temperature rise for Tri-Plate transmission line and for coaxial transmission line with

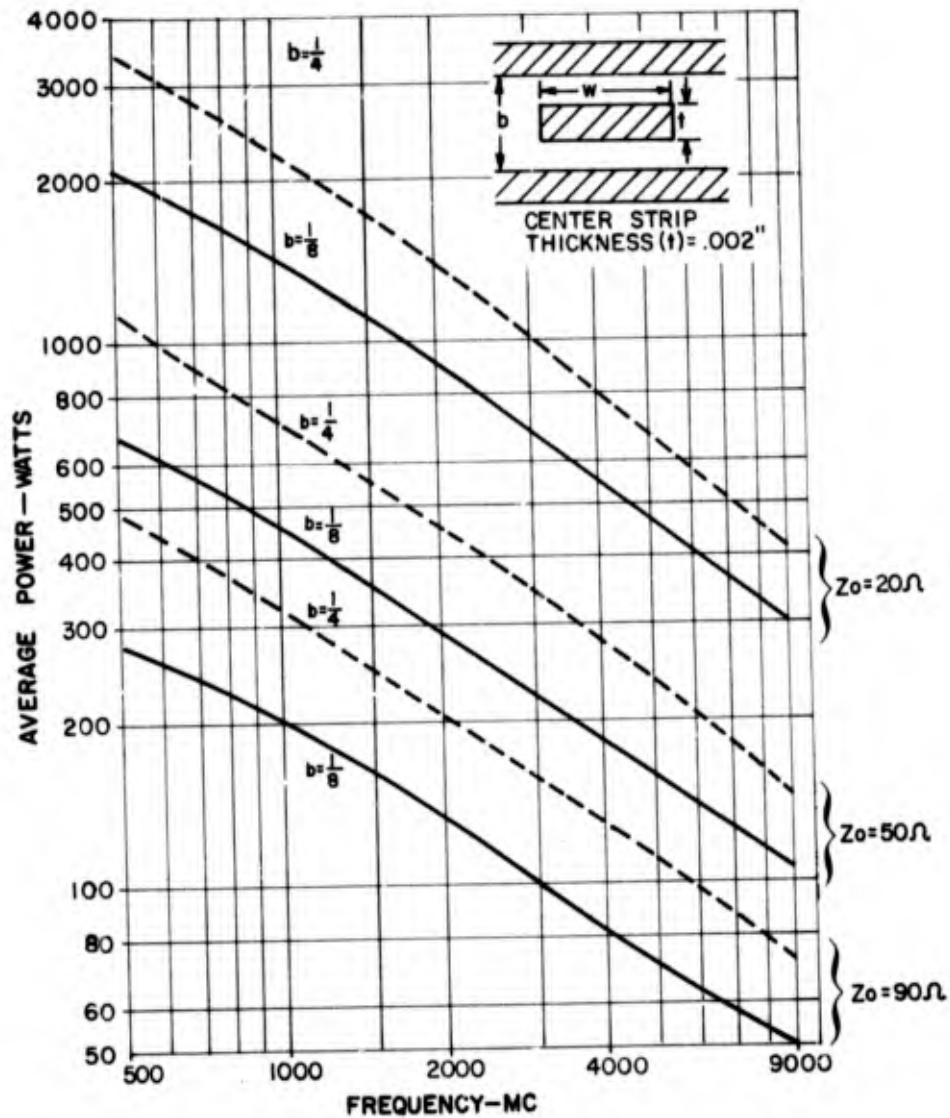


Fig. 1-11 Average power-rating of Tri-Plate line with a dielectric medium of Rexolite #1422.

the same characteristic impedance and the same attenuation per unit length are approximately equal. Fig. 1-11 shows calculated average power-ratings for a  $39\text{ C}^\circ$  center-conductor temperature-rise based on the thermal conductivity of Rexolite #1422 which is the dielectric medium for this particular Tri-Plate line. Outer-conductor temperature rise above ambient will depend on the outer-conductor finish, ground-plane area, atmos-

pheric pressure, and the amount of forced air circulation. Outer-conductor temperature rise is calculated to be 25 C° above ambient for one square-inch of heat radiating surface for each linear inch of 20-ohm line operating at maximum rated power, as shown in Fig. 1-11. Average power limitations imposed (in practice) will depend on the maximum ambient temperature and other environmental conditions expected during operation. Power limitations also depend on the conductor temperature at which the dielectric becomes excessively lossy, or at which the band between the dielectric and the conductor fails.

The peak power-handling capability of Tri-Plate line is limited by the sharp edge of the photo-etched center conductor and the air space that results when the copper on either edge of the center-conductor is etched away. If ground-plane separation (b) equals 0.125 inches, and the characteristic impedance equals fifty ohms for line filled with Rexolite #1422, a peak power-rating of 25 kilowatts includes at least a 2:1 safety factor. By encapsulating the center-conductor edges in a dielectric of strength comparable to Rexolite #1422, (600V/mil), the peak power-rating may be increased to 1.5 megawatts with a 2:1 safety factor. Thus, for most applications, the average power capability of the line will be the limiting factor provided suitable precautions are taken to prevent corona or breakdown along the edges of the center strip.

## CHAPTER TWO

### DISCONTINUITIES

#### 2-1 General Considerations

A knowledge of basic microwave configurations that will give desired reactance values or frequency characteristics is essential to microwave design. Such configurations - or discontinuities - will be used as components of matching networks. The components of these networks may be nothing more than lengths of transmission line, or they may be gaps, holes, tapers, or any combination of discontinuities which behave at high frequencies as do more conventional radio components at lower frequencies. Tunable units complete in themselves, which can be inserted between other components for the purpose of matching them, are especially useful in bench setups. Other matching networks may be integral parts of larger systems and may be either fixed reactance elements or tuneable devices.

#### 2-2 Bends

Certain rules of thumb can be set forth as a preliminary to a general discussion of bends. A right-angle bend is inherently mismatched at any frequency. For a particular right-angle bend (measured at Airborne Instruments Laboratory<sup>1</sup>) with an inner-conductor width of 0.625 inches and a ground-plane separation of 0.500 inches, the insertion VSWR measured 2.01 at 3 KMC. This value agreed closely with the theoretical value of 2.15. It can be shown that this mismatch will decrease along with an increase in wavelength<sup>1</sup>. Furthermore, as the angle of a bend is decreased from 90°, mismatch can be expected to decrease accordingly. Fig. 2-1 shows the theoretical variation in insertion VSWR versus the angle of bend at 3 KMC. The curve was calculated<sup>1</sup> for a bend of arbitrary angle in a line with inner conductor

<sup>1</sup>Arthur A. Oliner, "Equivalent Circuits for Discontinuities in Balanced Strip Transmission Line," IRE Transactions, March, 1955.

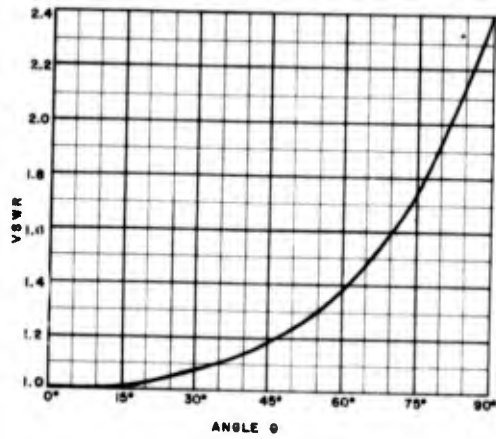


Fig. 2-1 Standing wave ratio of sharp bends in a strip-line versus the angle of bend.

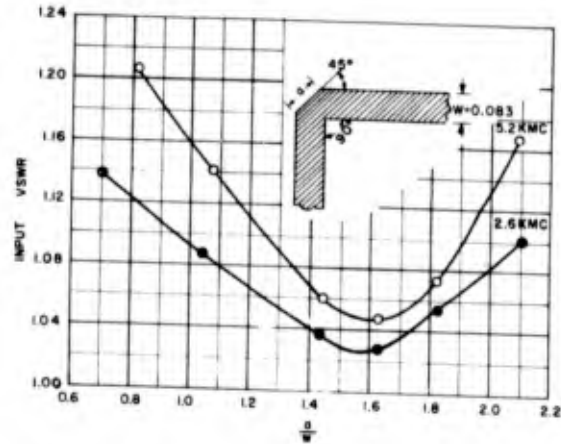


Fig. 2-2 Input VSWR versus  $a/w$  of mitered right-angle bends.

width of 0.400 inches and a ground-plane separation of 0.500 inches.

The mechanical convenience of the right-angle bend can be retained (while avoiding the penalties of inherent mismatch) by mitering the outside corner of the bend as shown in Fig. 2-2. This produces a useful configuration which can be matched at any frequency. Both radius (or curved) and mitered bends have useful applications to microwave strip-transmission lines. Above a transition frequency dependent on bending-radius, radius bends are superior to the mitered variety. A radius bend may be considered to be a series of very-small-angle bends; the larger the radius of the bend in terms of wavelength, the smaller the incremental angles and the better the match. However, as a frequency decreases, a given radius bend will decrease in performance and mismatch will increase. Although mitered bends can be matched at any frequency, they become more frequency-sensitive with higher frequencies, and as a consequence, construction tolerances become smaller. As far as bends of practical radii are concerned, the mitered bend is most broadband and therefore most useful at lower frequencies.

Mitered right-angle bends were investigated at Sanders Associates, Inc. at frequencies of 2.6 and 5.2 KMC. Seven bends, each with a different "a" dimension, were fabricated from double-copper-clad, 1/16-inch, 50-ohm line in teflon-fiberglass (GB112T). Input VSWR, as a function of  $a/w$  for the two frequencies, is shown in Fig. 2-2. In making these measurements, a 50-ohm Tri-Plate slotted line and a matched load (VSWR = 1.02 or less) consisting of a 50-ohm Tri-Plate to coaxial line transition, a double-stub tuner, and commercial coaxial load, were used. As a check on the physical symmetry of the bends and the reliability of the measurements, the input VSWR of each bend was first measured looking in one leg of the bend, and then looking in the other leg. Some slight difference was noted, and it is their average that is plotted in the above figure.

The curves for both 2.6 and 5.2 KMC show that for the particular line used, minimum mismatch occurred when the value of  $a/w$  was approximately 1.6. They tend to indicate, therefore, that this is the optimum value of  $a/w$  irrespective of frequency.

### 2-3 Transformers

Tri-Plate lends itself to the design of those types of transformers commonly associated with the conventional coaxial line, with the exception of those which employ a change in dielectric. In all instances, the center-conductor width is altered in a manner calculated to give the desired electrical results. Since this is readily accomplished by a simple, though precise, photo-etching process, expensive machining and fabrication are not required, as they are with normal coaxial transformers.

While conventional coaxial line and Tri-Plate are electrically quite similar, two differences should be noted prior to a discussion of specific examples of Tri-Plate transformers. First, an abrupt change in the diameter of the inner conductor of a coaxial line results in a discontinuity capacitance due to the fringing of the

fields in the vicinity of such a change. This discontinuity, or fringe, capacitance may or may not be negligible, depending on the magnitude of the step in the conductor. That its equivalent circuit is a shunt capacitance between inner and outer conductors is evident from the observation that the step is in the same plane as the radial electric field at that point. Consequently, it is the electric field that is altered, or perturbed, in that region, thereby exciting higher modes that give rise to a fringe capacitance. In the case of Tri-Plate, however, only the width of the center-conductor is abruptly changed, but in a direction perpendicular to the electric field. Assuming the center-conductor thickness to be negligible, there is, therefore, no perturbation of the electric field in this region. The magnetic field is affected however, and it has been shown<sup>2</sup> that the equivalent circuit for such a Tri-Plate discontinuity is a series inductance. This is illustrated in Fig. 2-3.

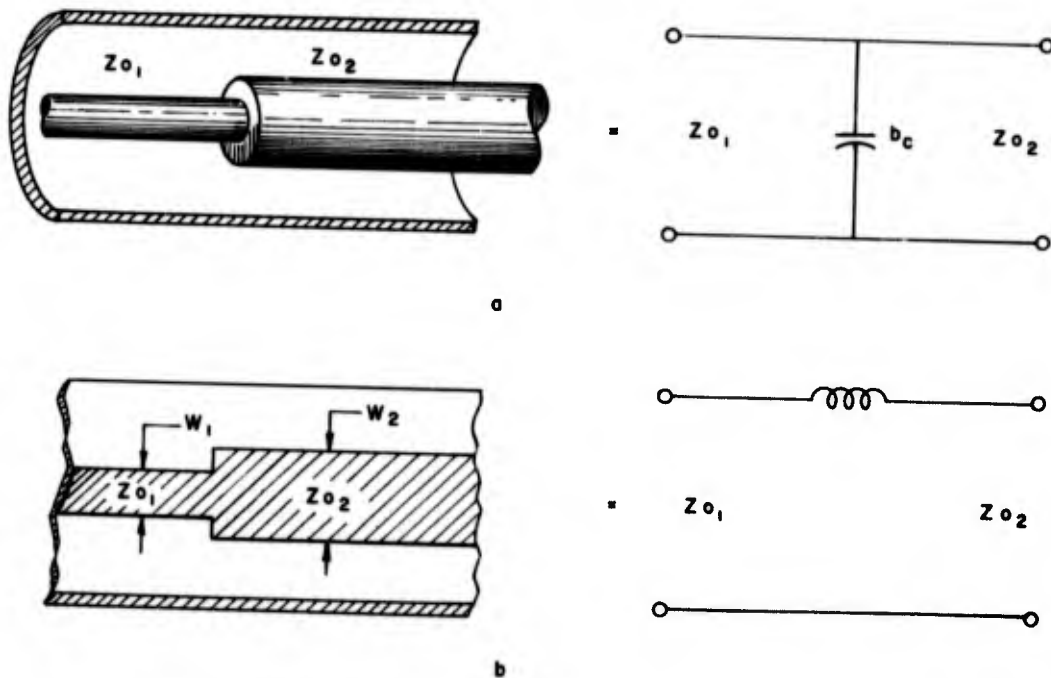


Fig. 2-3 Contrasted equivalent circuits for center-conductor discontinuities in a) coaxial, and b) Tri-Plate lines.

<sup>2</sup>A. A. Oliner, loc. cit.

In this figure, the series inductive reactance ( $X_L$ ) of the Tri-Plate discontinuity, normalized with respect to  $Z_{o2}$ , is equal to:

$$\frac{X_L}{Z_{o2}} = \left[ \frac{(2w_2 + \frac{4b}{\pi} \ln Z)}{\lambda_{TP}} \right] \ln \csc\left(\frac{\pi}{2}\right) \left(\frac{Z_{o2}}{Z_{o1}}\right) \quad (2-1)$$

A second difference is evident from the equations for the characteristic impedance of the two types of transmission line<sup>3</sup>. This difference will be taken into account in the determination of a theoretical curve of input VSWR versus length of taper for a particular Tri-Plate line. The formulas for impedance for coaxial line as well as for Tri-Plate can be understood better by referring to the sketches in Fig. 2-4. The characteristic impedance for the coaxial line is equal to:

$$Z = \frac{138.0}{\sqrt{\epsilon_r}} \log_{10} \frac{b}{a} \quad (2-2)$$

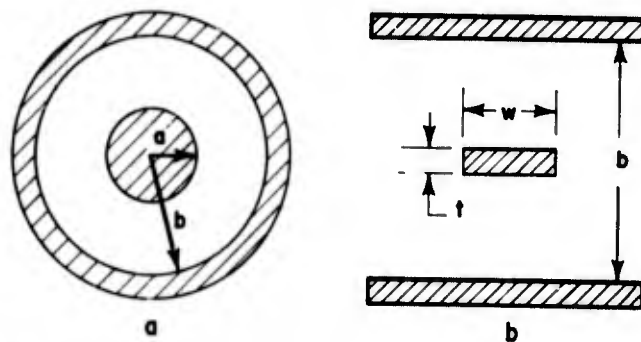


Fig. 2-4 Cross-sectional view of a) coaxial, and b) Tri-Plate lines, showing dimensions governing characteristic impedance.

Referring to the cross-sectional view of Tri-Plate line shown in Fig. 2-4, when  $\frac{w}{(b-t)}$  is greater than 0.35, then:

$$Z_o = \frac{94.15}{\sqrt{\epsilon_r} \left( \frac{w/b}{1-t/b} + \frac{C'_f}{0.0855 \epsilon_r} \right)}$$

<sup>3</sup>Seymour B. Cohn, "Problems in Strip Transmission Lines," IRE Transactions, March, 1955.



where  $C'_f$  is the fringing capacitance in micromicrofarads per centimeter from one corner of the strip to the adjacent ground plane. Here  $C'_f$  is independent of  $w$  and is a constant for a given  $\epsilon_r$  and  $\frac{t}{b}$ .

The simplest form of Tri-Plate impedance transformer has already been shown in Fig. 2-3. Neglecting junction reactance, this discontinuity is insensitive to frequency and will introduce a VSWR equal to the ratio  $Z_{01}/Z_{02}$ . If the required impedance step has negligible reactance, it can be used to match out a load at any particular frequency. To illustrate, let the normalized load impedance equal ( $\gamma$  max. ) at any voltage maximum and ( $\gamma$  min. ) at any voltage minimum. For an input VSWR equal to one, placing the transformer at a voltage maximum requires that  $Z_{01} = (\gamma \text{ max. })(Z_{02})$ , while placing it at a voltage minimum requires that  $Z_{01} = (\gamma \text{ min. })(Z_{02})$ . Note that the application of this device is limited not only by the range in which the junction reactance is negligible, but also by the very limited choice of the input-line characteristic impedance.

A second type of matching transformer incorporates two identical impedance steps in a symmetrical manner, thus permitting the input  $Z_0$  to equal the output  $Z_0$ . Measurements were made of thirty-five variations of this transformer at 9375 MC and forty-four variations at 3000 MC. The configurations and a comparison of measured values with theoretical curves for several different impedance ratios are presented in Figs. 2-5 through 2-8. Line attenuation was taken into account in the calculation of the theoretical points, but junction (or discontinuity) reactance ( $X_2$ ) is omitted in the determination of the theoretical curves.

It should be noted that, whereas all the experimental points agreed very well with the theoretical curves at 3000 MC, they differed considerably at 9375 MC for  $\frac{Z_{02}}{Z_{01}} = 0.5$  and  $\frac{Z_{02}}{Z_{01}} = 0.36$  in the region of  $l/\lambda_{TP} < 0.5$ .

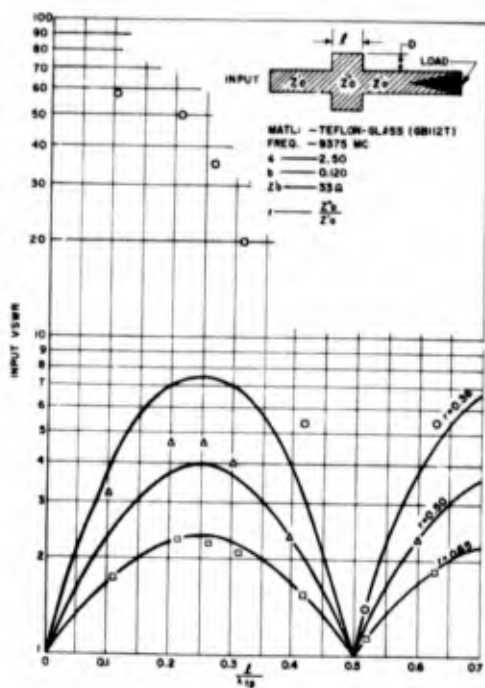


Fig. 2-5 VSWR versus  $l/\lambda_{TP}$  for  $Z_0''/Z_0' < 1$  at X-band (#1).

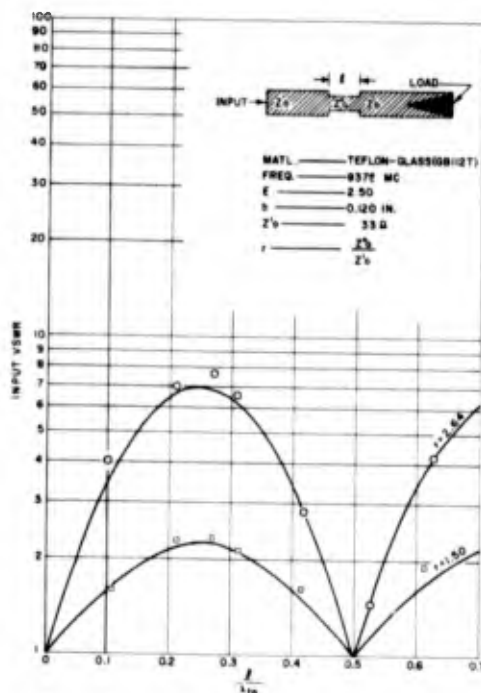


Fig. 2-6 VSWR versus  $l/\lambda_{TP}$  for  $Z_0''/Z_0' > 1$  at X-band (#2).

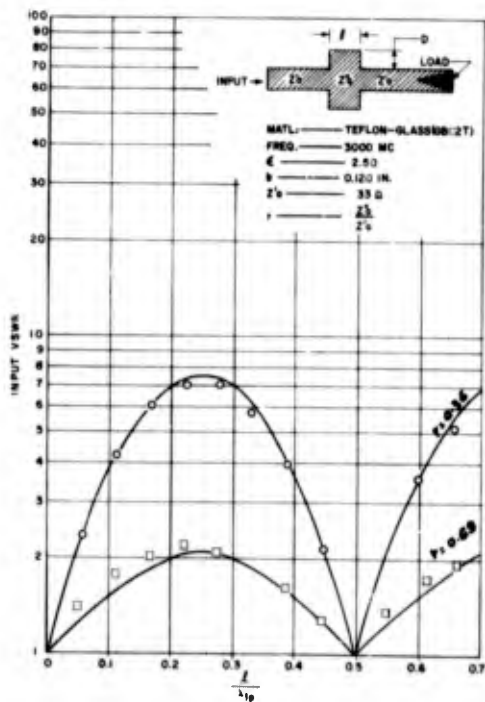


Fig. 2-7 VSWR versus  $l/\lambda_{TP}$  for  $Z_0''/Z_0' < 1$  at S-band (#1).

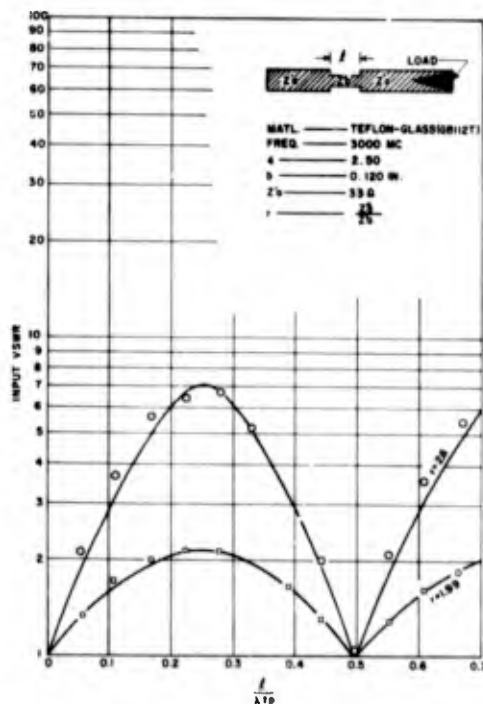


Fig. 2-8 VSWR versus  $l/\lambda_{TP}$  for  $Z_0''/Z_0' > 1$  at S-band (#2).

Three possibilities present themselves as an explanation of this occurrence. One is the omission, as shown in Fig. 2-5, of the junction reactance already mentioned. Another is the fact that when the effective electrical width of the center-conductor is greater than half a wavelength, higher-order modes can exist and be propagated. A third possibility is that the electrical configuration of this discontinuity very much resembles a relatively short but wide section of center-conductor with an open-circuited shunt stub attached to each side.

With respect to the first possibility, junction reactance is more than a negligible factor only at 9375 MC,

for  $\frac{Z_{o2}}{Z_{o1}} = 0.36$ , where  $w_2$  is  $0.707 \lambda_{TP}$ . Even here,

taking junction reactance into account, where  $\ell/\lambda_{TP} = 0.25$ , the theoretical figure for VSWR is 9.7, compared to a VSWR of 7.7 calculated on the basis of no junction reactance. Since the actual measured VSWR was about 36, it is obvious that the junction effect can account for only a small part of the discrepancy. Were the remainder due to the existence of higher-order modes (the second possibility) which resulted from the width of the center-conductor being well over a half-wavelength, then a considerable discrepancy would have occurred at  $\ell/\lambda_{TP} = 0.6$  as it did at  $\ell/\lambda_{TP} = 0.1$ . Such was not the case, and the second possibility must be dismissed.

The reasonable conclusion is that in this region of large discrepancy, the transformer is behaving primarily like a constant-width center-conductor having an identical open-circuited shunt stub attached to each side. As the dimension " $\ell$ " is varied, the characteristic

impedance of the stubs changes, but for  $\frac{Z_{o2}}{Z_{o1}} = 0.36$ ,

the length  $D$  of each stub remains a constant  $0.246 \lambda_{TP}$ . The fact that each open-circuited stub is, practically

speaking, a quarter-wavelength long makes it immediately obvious that the main line will be nearly short-circuited and consequently will have a very high VSWR.

If, then, this symmetrical transformer is to be used in a straight-forward manner as a load-matching device, care must be exercised that the  $Z_{02}/Z_{01}$  ratio chosen has negligible junction reactance, and also that its physical length is sufficient to prevent its behaving as a double-shunt stub. Compliance with the first requirement for any given frequency and main line  $Z_{01}$ , will, therefore, limit the maximum load VSWR that can be matched out. That this device is frequency sensitive is readily apparent.

Single and multiple-section quarter-wavelength transformers can be made in Tri-Plate simply by varying the width of the center-conductor. Single and double-section transformers are illustrated by the center-conductor configurations shown in Fig. 2-9.

These devices are particularly useful when it is necessary to connect an input line having a particular characteristic impedance, without causing an appreciable mismatch. If junction reactance is neglected, those equations which apply to coaxial line, and ignore junction susceptance, apply equally well to Tri-Plate. Therefore, for the single-section transformer, a theoretically perfect match is obtained at the design frequency when

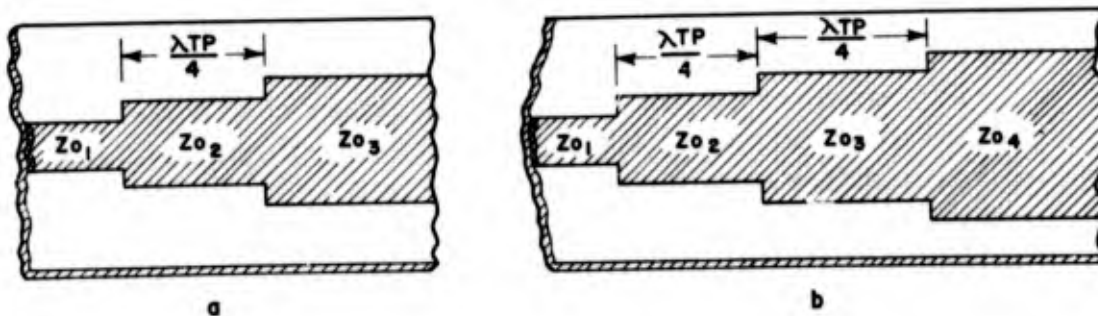


Fig. 2-9 Single and double-section Tri-Plate transformers.

$Z_{02} = \sqrt{Z_{01} Z_{03}}$ , while for the double-section transformer this is true when  $Z_{01} Z_{03}^2 = Z_{04} Z_{02}^2$ . Pertaining to the latter, Slater<sup>4</sup> shows that for low frequency sensitivity,  $Z_{02}$  and  $Z_{03}$  should be chosen to satisfy the further relationship that

$$\ln Z_{02}/Z_{03} = 2 \ln Z_{01}/Z_{02} = 2 \ln Z_{03}/Z_{04}.$$

Thus, the progressive changes in the logarithms of the characteristic impedances have the binomial relationship of 1:2:1. Optimum bandwidth characteristics are obtained using Tschebyscheff polynomials in computing the step parameters<sup>5</sup>.

Another method of connecting Tri-Plate lines (having dissimilar characteristic impedances) is to taper the width of the center-conductor joining the two lines, so that the characteristic impedance changes gradually. While all types of physical tapers can be made much more easily in Tri-Plate than in conventional coaxial line, the simplest is that which has a linear change of center-conductor-width with length. A thorough investigation of such a taper was made at 5400 MC using 12 separate transformers made from double copper-clad Rexolite #2200, each having a different length of taper. The input line impedance was 58.6 ohms ( $w = .059$  inches) and the output line impedance was 29.3 ohms ( $w = .172$  inches), giving an impedance ratio  $Z_{01}/Z_{02} = 2.0$ . Other pertinent information, and a comparison of measured values of input VSWR (corrected for line attenuation) with a theoretical curve, are presented in Fig. 2-10.

The manner in which the theoretical curve was obtained is of interest, since, here again, there is a significant difference between Tri-Plate and conventional coaxial line. Fig. 2-2 shows that the characteristic impedance of coaxial line is a logarithmic function of the center-conductor diameter while that of Tri-Plate does not have a logarithmic relationship to the center-conductor width. Frank<sup>6</sup> shows that for any uniform

<sup>4</sup>J. C. Slater, "Microwave Transmission", McGraw-Hill, New York, 1942, pg. 57.

<sup>5</sup>Seymour B. Cohn, "Optimum Design of Stripped Transmission-line Transformers, IRE Transactions on Microwave Theory and Techniques", April, 1955.

<sup>6</sup>N. H. Frank, "Reflections from Sections of Tapered Transmission Lines and Wave Guides", Radiation Laboratory Report 43-17, January, 1943.

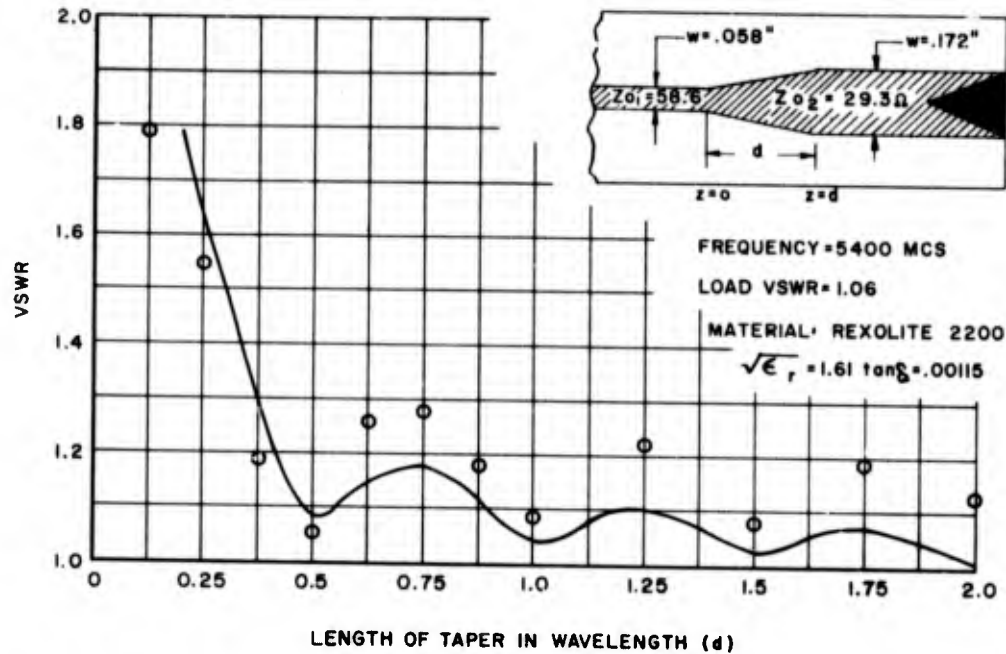


Fig. 2-10 Comparison of measured input VSWR with theory, for various lengths of taper.

transmission line terminated in a matched load and having a tapered center-section, the reflection coefficient for a taper of length  $d$ , within which the line constants are slowly varying, is approximately:

$$\Gamma = \frac{1}{4\gamma_0} \left[ \frac{d(\ln Z)}{dz} \right]_0 - \frac{1}{4\gamma_d} \left[ \frac{d(\ln Z)}{dz} \right]_d e^{-2 \int_0^d \gamma dz} \quad (2-4)$$

where  $\gamma = \alpha + j\beta$  = the propagation constant,  $Z$  = characteristic impedance, and the subscripts  $0$  and  $d$  denote values at the points ( $z = 0$ ) at the start of the taper and ( $z = d$ ) at the end of the taper. Obviously  $\Gamma$ , and therefore input VSWR, as a function of length of taper  $d$ , will vary differently for Tri-Plate than it does for coaxial line even though both employ physically linear tapers and have similar input and output impedances.

For this particular taper study,  $\frac{w}{b-t}$  is everywhere  $> 0.35$  and  $Z$  is therefore given by Eq. (1-4).  $\frac{C'f}{0.0885\epsilon_r}$  is found<sup>7</sup> to be equal to 0.48. The expression for  $w$  as a function of  $z$  is:

$$w = 0.059 + 2\left(\frac{0.0565}{d}\right)z \text{ inches.}$$

$$\therefore Z = \frac{94.15}{1.605 + \left(\frac{1.593}{d}\right)z} \quad (2-5)$$

where  $d = \text{inches} = \text{a constant for any given taper length.}$

Letting the denominator,  $1.605 + \left(\frac{1.593}{d}\right)z$ , equal  $X$ ,

and using the relationships  $d \frac{(\ln X)}{dX} \cdot \frac{dX}{dz} = d \frac{(\ln X)}{dz}$

results in:

$$\frac{d(\ln Z)}{dz} = - \frac{1.593/d}{1.605 + \left(\frac{1.593}{d}\right)z}$$

$$\therefore \left[ \frac{d(\ln Z)}{dz} \right]_0 = - \frac{0.993}{d} \text{ and}$$

$$\left[ \frac{d(\ln Z)}{dz} \right]_d = \frac{-0.498}{d} \quad (2-6)$$

Using Seymour B. Cohn's<sup>8</sup> theoretical curves for copper loss as a function of  $Z_0 \sqrt{\epsilon_r}$ , and assuming that the total attenuation  $\alpha$ , which includes both copper and di-

<sup>7</sup>Seymour B. Cohn, IRE Transactions, March, 1955.

<sup>8</sup>S. B. Cohn, loc. cit.

electric losses, is closely approximated by a linear variation with distance along the taper, total attenuation is:

$$\alpha = 0.0470 - 0.0024 z/d \text{ db/in.} \quad (2-7)$$

(It is of interest to note here that the calculated attenuation of 0.0446 db/in. for the 29.3 ohm line was only 7.1 per cent lower than that actually measured in an identical line at the same frequency of 5400 MC.)

Converting  $\alpha$  to nepers per inch:

$$\alpha = 54.1 \times 10^{-4} - 2.76 \times 10^{-4} z/d \text{ nepers/in.}$$

$$\begin{aligned} \therefore \int_0^d \gamma dz &= \int_0^d \left[ (54.1 \times 10^{-4} - 2.76 \times 10^{-4} z/d) \right. \\ &\quad \left. + j \frac{2\pi}{\lambda_{TP}} \right] dz \\ &= (52.7 \times 10^{-4} + j4.62)d \cong j4.62d \\ \therefore e^{-2 \int_0^d \gamma dz} &= e^{-j9.24d} = \cos(9.24d) - j \sin(9.24d) \end{aligned}$$

Since  $\alpha_o$  and  $\alpha_d$  are both  $\ll \beta$  :

$$\begin{aligned} \Gamma &= \frac{\left[ \frac{1}{4(j4.62)} \left( -\frac{0.0993}{d} \right) \right]}{(\cos 9.24d - j \sin 9.24d)} \left[ \frac{1}{4(j4.62)} \left( -\frac{0.498}{d} \right) \right] \\ \therefore \Gamma &= j d^{-1} (0.0537 - 0.0269 \cos 9.24d) - 0.0269 d^{-1} \sin 9.24d \end{aligned} \quad (2-8)$$



Substituting multiples of  $0.1 \lambda_{TP}$  in inches for  $d$ , and using the relationship that  $VSWR = \frac{1 + |\Gamma|}{1 - |\Gamma|}$ , results in the theoretical curve shown in Fig. 2-10. VSWR minima are obtained for taper lengths very slightly greater than multiples of a half-wavelength. The only reasonable explanation for the rather large differences between some of the experimental points and their corresponding theoretical values is that the lap joints on both ends of the taper sections were not reflectionless. Nevertheless, the experimental points very definitely demonstrate the nature of the curve. The theoretical curve was not drawn for values of  $d < 0.2 \lambda_{TP}$  since calculations showed that Eq. (2-4), which assumes very small reflections, was not valid in this region. In conclusion, it is worth noting that even a full-wavelength taper of this nature is no better than the much shorter double-section transformer that incorporates two quarter-wavelength sections.

#### Shunt Stub

Probably the most commonly used Tri-Plate transforming device is the simple open-circuit shunt stub. It is preferable to the short-circuit shunt stub since it does not present the fabrication problem of the latter. Theoretically, the normalized input admittance of a transmission line of length  $l$ , which has attenuation and is terminated in an open circuit, is given by:

$$\gamma_{oc} = \tanh (\alpha + j\beta) l, \quad (2-9)$$

where  $\alpha$  = attenuation per unit length and  $\beta = \frac{2 \pi}{\lambda_{TP}}$

For the usual case of  $l < \lambda_{TP}/2$ , the total attenuation for both Rexolite #2200 and teflon-fiberglass (GB112T), using a 1/8-inch plate-to-plate spacing, is less than 0.05 DB even at X-band frequencies. To a good approximation, such a shunt stub can be treated as a length of

lossless open-circuited transmission line whose normalized input admittance is a pure susceptance equal to:

$$b_{oc} = j \tan \beta l \quad (2-10)$$

Impedance transforming, or matching, by means of an open-circuit shunt stub is accomplished in the following manner. At the particular frequency of interest, the load admittance  $Y_L = g_L + jb_L$  is determined experimentally and plotted on a Smith chart. This admittance point is then rotated toward the generator on the chart until it lies on the  $g = 1$  circle. The input admittance at this plane is, therefore,  $Y_L = 1 + jb_L$ . An open-circuit shunt stub, having a characteristic impedance equal to that of the main line and a length  $l$ , such that  $b_{oc} = -b'_L$ , is connected to the main line at this plane. The total input admittance at this plane is equal to  $1 + j0$  and the input VSWR equals 1.0. Obviously, the stub is frequency sensitive, and the equivalent input admittance of the load and stub combination will exhibit a frequency dependency. While no specific example will be given here, it is theoretically possible in some instances to make the impedance match more broadband by making the stub long, thereby increasing its frequency sensitivity, and/or making the stub characteristic impedance differ from that of the main line. Both can be done quite readily in Tri-Plate.

The results of impedance measurements made at 3 KMC on an open-circuited shunt stub fabricated in Tri-Plate line are shown in Figs. 2-11 and 2-12. Fig. 2-11 shows VSWR versus shunt-stub length in inches, while Fig. 2-12 is a Smith chart admittance plot. These clearly indicate that the behavior of a shunt-stub in Tri-Plate is very close to the theoretical. However, two discrepancies are worth noting. First, the true stub length varies from the theoretical as the stub is increased from 0 to  $\lambda/4$ . When the stub length is  $\lambda/4$  or greater,

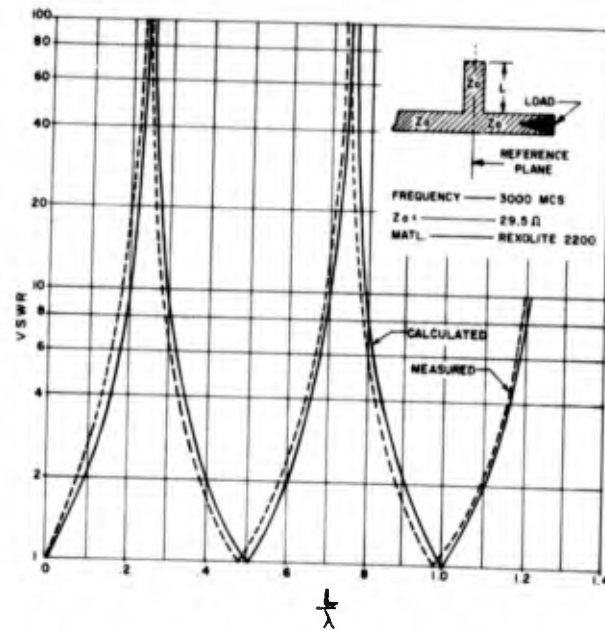


Fig. 2-11 VSWR versus stub-length for an open-circuited shunt-stub.

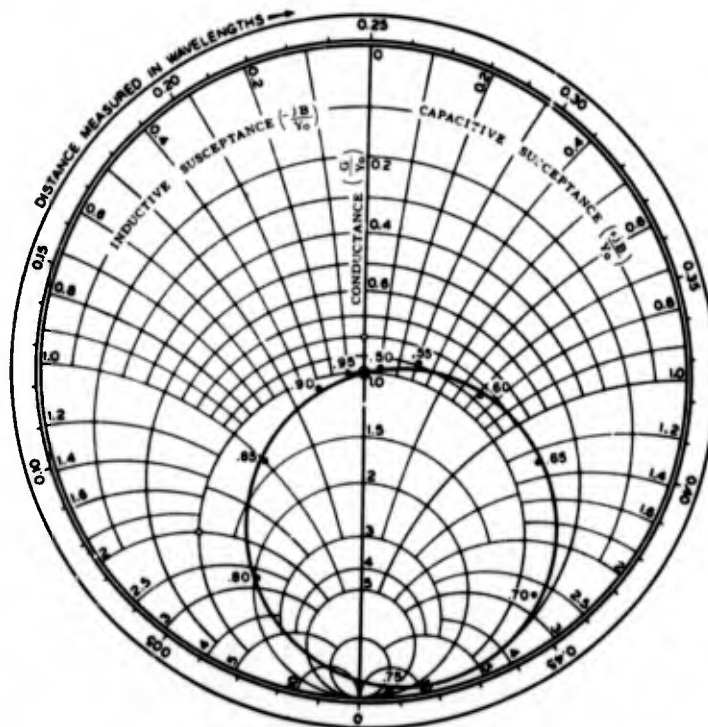


Fig. 2-12 Admittance plot of shunt-stub and matched load as a function of  $L/\lambda_{TP}$ .

it appears that a fixed correction can be made. In the case of a 30-ohm stub, shunting a 30-ohm line at 3 KMC, this discrepancy is about .022 (see Fig. 2-11). The correction will vary somewhat with frequency and change of characteristic impedance.

Fig. 2-12 is an admittance plot referred to the center line of the stub. It is evident that these plotted points would fall on the  $g = 1$  circle if the reference planes were shifted about  $0.02 \lambda$  toward the generator. Thus, the true phase-reference plane deviates slightly from theoretical.

#### 2-4 Gaps and Holes

Holes, and more especially gaps, in the center-conductor of a Tri-Plate line represent discontinuities which have considerable application to microwave filters. Arthur A. Oliner<sup>9</sup>, after making certain approximations, derived equivalent circuits for both a round hole and a gap in a zero-thickness center-conductor of a balanced strip-transmission line. The dielectric, whether air or otherwise, is assumed to be uniform throughout. Oliner's theoretical findings, given below and in Figs. 2-13 and 2-14, showed reasonably good agreement with measured data on these discontinuity structures.

##### *Circuit Parameters for Gap in the Center Conductor*

$$\frac{B_a}{Y_0} = \frac{2b}{\lambda} \ln \cosh \frac{\pi s}{2b}$$

$$\frac{B_b}{Y_0} = \frac{b}{\lambda} \ln \coth \frac{\pi s}{2b} \quad (2-11)$$

where  $b$  = ground plane separation.

Fig. 2-15 illustrates two methods of increasing center-conductor gap-capacitance in Tri-Plate line.

<sup>9</sup>A. A. Oliner, loc. cit.

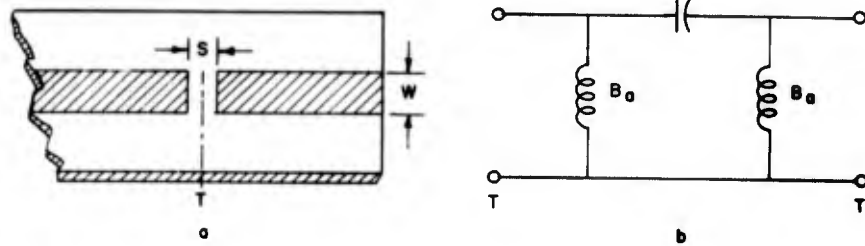


Fig. 2-13 a) Gap in Tri-Plate center-conductor, and b) equivalent lumped-circuit.

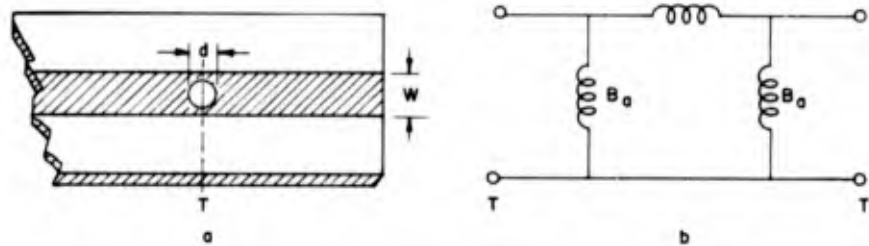


Fig. 2-14 a) Round hole in Tri-Plate center-conductor and b) equivalent lumped-circuit.

#### Circuit Parameters for a Round Hole in the Center Conductor

$$\frac{B_b}{Y_o} = \frac{-3\lambda b D}{4\pi d^3}$$

where  $D$  is approximately equal to  $W + \frac{2b}{\pi} \ln Z$  for  $Y_o = 70.01$ :

$$\frac{B_a}{Y_o} = \frac{1}{4 (B_b / Y_o)} \quad (2-12)$$

These parameters have been verified during the course of working with Tri-Plate line. Holes, it should be pointed out, are seldom used in Tri-Plate components, since they present a very small discontinuity. Gaps, on the other hand, have considerable application to the design of directional-couplers and to filters, and will be discussed more fully under these headings in Section 4-7 and in Chapter 5.

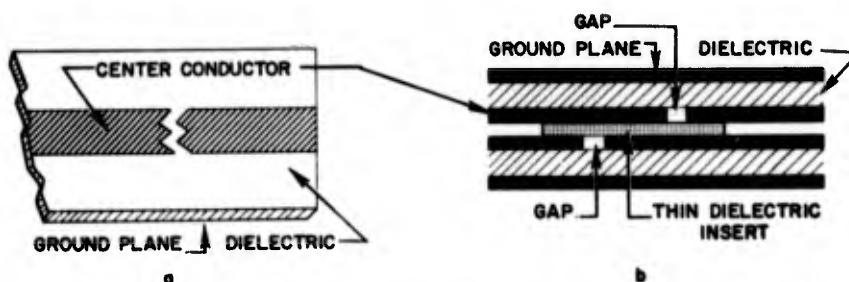


Fig. 2-15 Two methods of increasing the center-conductor gap capacitance in Tri-Plate line.

Variable devices, such as sliding short-circuits and rotary open-circuits, will similarly be discussed in Section 4-3. Simple short-circuits can be fabricated easily in two ways. The most convenient approach is to connect the ground-planes and center-conductors by soldering them to eyelets or rivets which are inserted through the line. Copper foil may be used for the same purpose, but only at the termination of the line. Two narrow strips of foil, equal in thickness to the ground-planes, are soldered one to each ground-plane, bent around the termination of the two separate laminated sheets and then soldered to the centerstrips etched on the inner face of each sheet, thus separately short-circuiting both halves of the line. The two short-circuited line-halves are then assembled together.



## CHAPTER THREE

### TRANSITIONS AND COUPLINGS

#### 3-1 General Considerations

Though the unit fabrication of entire RF systems is possible in Tri-Plate transmission line, yet the occasion for transitions to other Tri-Plate circuits or to waveguide or coaxial-lines often arises. Useful Tri-Plate components, for reasons of size, weight and economy, have found commercial application in conjunction with components fabricated in other types of transmission line. Tri-Plate devices for bench setups or laboratory work can be conveniently inserted into waveguide or coaxial-line circuits. Tri-Plate antenna arrays, for instance, due to their convenient flat form, have been inserted into diverse transmitting or receiving systems. The inclusion of photo-etched microwave devices in a large variety of RF systems will increase as the convenience of the flat-form of transmission line becomes better known. Therefore, the discussion of transitions and couplings warrants a chapter to itself.

#### 3-2 Tri-Plate to Tri-Plate Couplings

Reflectionless junctions between Tri-Plate lines are primarily used in development of individual components to be later incorporated as integral parts of complex systems. Transitions may be required to join two such systems or to allow certain components to be readily removable from a system.

Several factors are important to the design of useful connections in Tri-Plate transmission line. The most important are:

1. Mechanical facility in making and breaking the connection
2. Necessity for proper alignment.
3. Minimum leakage.



4. Mechanical strength.
5. Reversibility (the facility of mechanically reversing the faces of one of the components.)

A basic feature of these junctions is the overlap. An overlap is desirable for both mechanical and electrical reasons. Two versions of the overlap have been developed, each with its own advantages and disadvantages. The first is the ordinary lap-joint. In this form, the termination of the line is cut at right angles to the center line. One side-plate or laminate of the assembled line is cut a fixed-length longer than the other side, so that it overlaps. With good workmanship, this junction can be made to satisfy the listed requirements except that of reversibility. A photograph of a typical straight-lap junction with clamp is shown in Fig. 3-1.

As indicated, the two connected components are held together with a box clamp. The transmission line is cut to a width that, when boxed in, will be below cut-off for the  $TE_{1,0}$  mode at the highest frequency of interest. The edges are cut parallel to the centerline and equidistant from it. This ensures good alignment. The overlap of each component must, of course, be equal, so

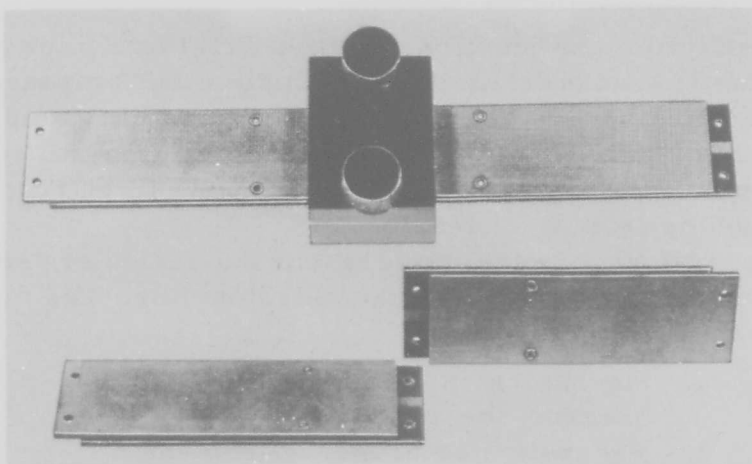


Fig. 3-1 Assembly of a typical Tri-Plate lap junction with clamp.

that, when joined, there will be no discontinuity in either center or outer conductors. As long as ground-plane separation is equal in the two components and center-strip width is the same, the seam between the dielectric surfaces (perpendicular to the centerstrip) is the only point of discontinuity. Careful fabrication and design of joint so that the maximum misalignment is less than a few mils will produce a junction that is practically reflectionless. The overlap itself is preferably short because of the desirability of using a single point of clamping pressure. (An overlap-length of  $3/16$ -inch has been commonly used with Tri-Plate transmission line having a ground-plane spacing (b) of one-eighth inch.) The overlap is not frequency sensitive.



Fig. 3-2 Configuration of a typical mitered Tri-Plate junction.

The mitered junction (first constructed by D. Fye of AFCRC) provides a reversible junction. In this form, the termination of each half of the Tri-Plate line is cut at an angle. The two side plates are assembled so that the mitered terminations, as shown in Fig. 3-2, are cut across each other at the centerline of the inner-conductor. Thus, either end of any two components cut in this fashion can be joined. There is sufficient overlap and, with a clamp, considerable strength. The disadvantages of the double-miter joint, however, include: less contact area between center-conductors; and a more critical alignment problem.

In either type of joint, a clamp is necessary for mechanical strength and to close the circuit. The clamp in common use consists of two interlocking pieces of aluminum approximately an inch-and-a-quarter across the

Tri-Plate line, and one inch along the line, and when assembled together, about  $11/16$  of an inch in thickness. In one of the two sections, there is a slot cut deep enough to accommodate the Tri-Plate line as well as to allow space for the ridge or tongue cut in the other piece of metal. The width of the slot is identical with the width of the Tri-Plate line.

The box clamp is held together by two thumb screws. One method for obtaining positive alignment between two sections of line is by means of pins which are inserted in one face of the clamp, through the overlap portion of each Tri-Plate laminated sheet, to the other side of the clamp. The inner surface of the clamp closes the electrical gap between the Tri-Plate outer-conductors.

### 3-3 Tri-Plate to Coaxial Line Transitions

There are several configurations which are suitable for a Tri-Plate to coaxial line transition. The in-line type, as shown in Fig. 3-3, provides optimum electrical characteristics, since the center conductors of both lines have a common axis at the point of transition.

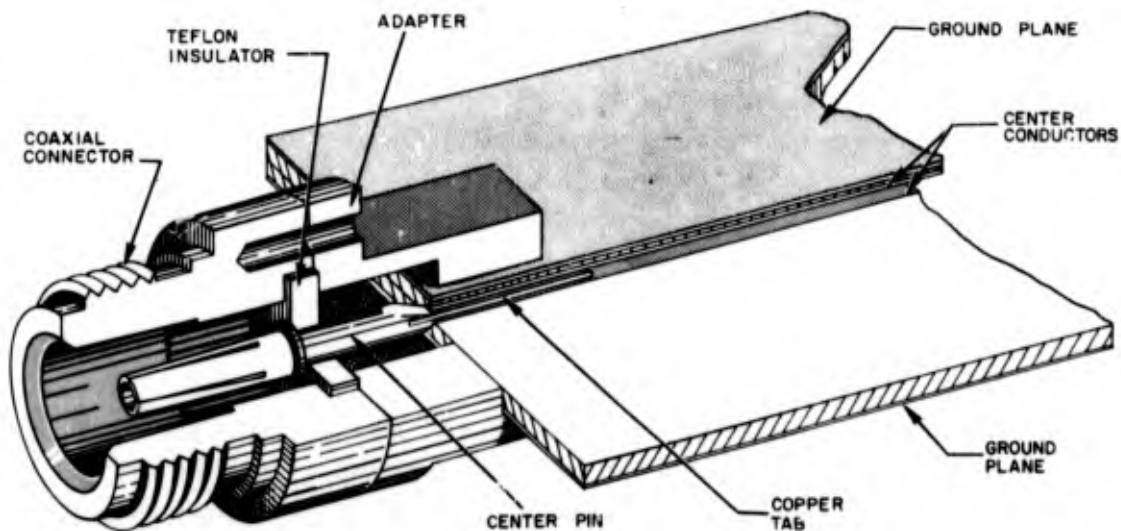


Fig. 3-3 In-Line transition from Tri-Plate line to coaxial line.

In-line transitions have been used with microwave air-dielectric lines with very good performance, but because of mechanical difficulties, due to extremely small dimensions in some solid dielectric-filled lines, this type of transition is less practical for ground-plane spacings less than 1/4 inch.

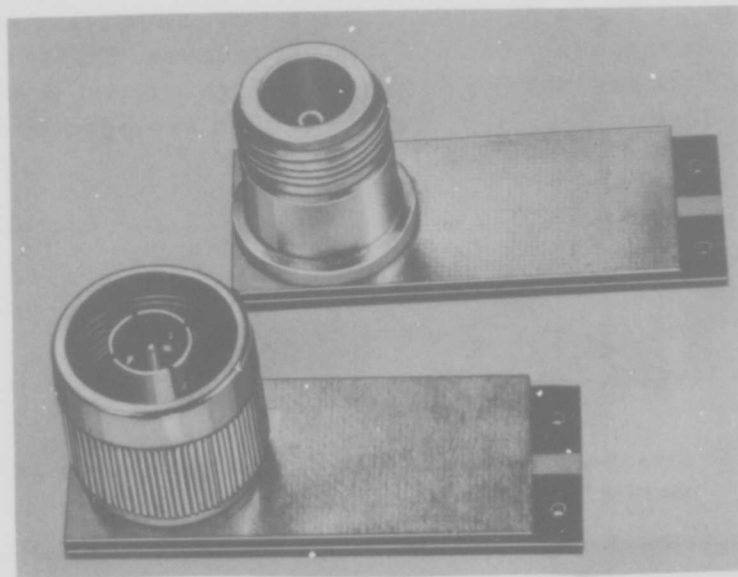


Fig. 3-4 Tri-Plate male and female coaxial connectors.

The right-angle male and female transitions to coaxial-line shown in Fig. 3-4 are a satisfactory solution to the mechanical problems encountered in the in-line type of transition.

In these transitions, the center-pins of the coaxial connectors are fastened to the centerstrip of one-half of the Tri-Plate line by means of an eyelet which is pressed through the Tri-Plate laminate into a hole in the end of the connector center-pin and then soldered. The Tri-Plate ground-plane around the connector center-pin is cut away to the same diameter as the insulator in the connector. The body of the connector is fastened to the line with screws which pass through both

halves of the Tri-Plate line and thread into the connector body. These screws serve also as shorting-pins to maintain proper voltage balance between the ground-planes of the line. The characteristic impedance of the Tri-Plate line is made to equal that of the coaxial line. The standing wave ratio of this transition, which is plotted in Fig. 3-5 as a function of frequency, shows that it has a usable frequency band of over two octaves. Right-angle Tri-Plate and waveguide transitions to coaxial line are compared in Fig. 3-6. Fig. 3-7 is an exploded view of a Tri-Plate female coaxial connector.

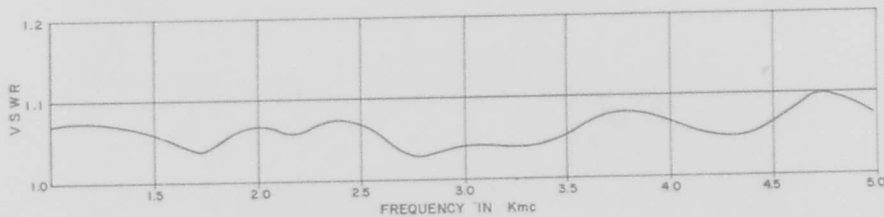


Fig. 3-5 Broadband performance of the type of female coaxial transition shown in Fig. 3-4.

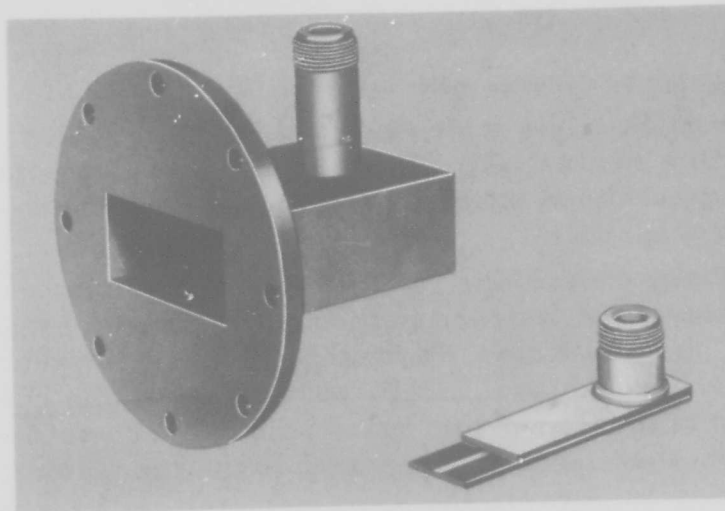


Fig. 3-6 Comparison of right-angle Tri-Plate and waveguide transitions to coaxial line.

In order to use a right-angle transition at X-band, more screws or other methods are needed to obtain adequate mode-suppression. A right-angle transition for use through X-band is shown in Fig. 3-8. This transition uses a solid metal wall and bottom plate instead of screws to obtain voltage balance between the ground-planes. The center-pin of the connector used in this X-band transition is fastened to the top half of the Tri-Plate line by means of an eyelet pressed through the dielectric filling into the end of the connector center-pin and then soldered, making a direct connection between the pin and the Tri-Plate centerstrip. The metal ground-plane of the top half of the Tri-Plate line is etched away, around the connector center-pin, to prevent a short circuit. The dielectric material of the Tri-Plate line replaces the insulator normally used with this type of connector. The bottom section of the Tri-Plate line is now attached, making a completed line, and a metal plate is screwed on or otherwise permanently attached, at the bottom, holding the entire assembly together. The metal plate, which is in direct contact with the bottom ground-plane and also with the body of the connector, adequately fulfills the function of maintaining voltage balance between the two ground-planes. Screws, in this case, do not double as shorting-pins. Although this is not the optimum design, this particular Tri-Plate to coaxial line transition has a voltage standing wave ratio under 2.0 from 3,000 to 11,000 megacycles.

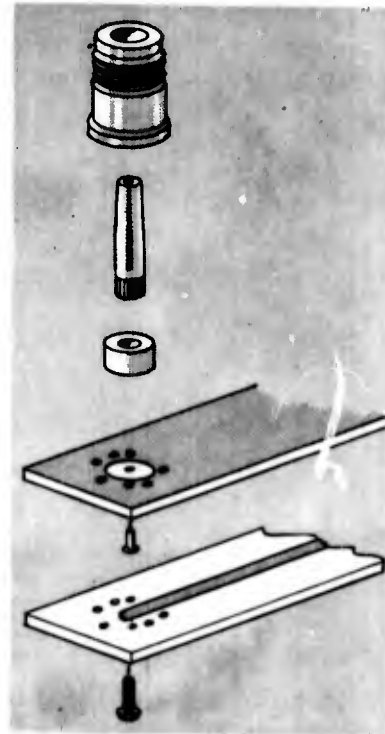


Fig. 3-7 Exploded view of Tri-Plate Type-N coaxial connector.

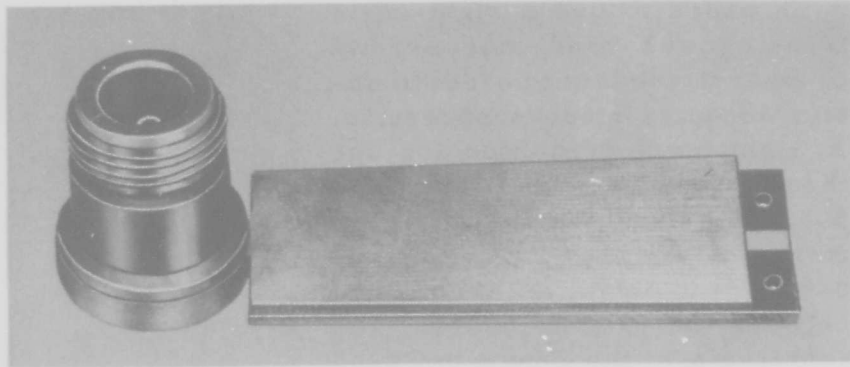


Fig. 3-8 Tri-Plate line to coaxial line transition, modified for use through X-band.

### 3-4 Tri-Plate to Waveguide Transitions

In chapter VII of this handbook; a Tri-Plate X-band series-slot antenna will be described. A natural consequence of its development was the application of such a slot as a transformer for coupling Tri-Plate to X-band waveguide. Although both utilize 1/16-inch copper-clad teflon-fiberglass (GB112T), their design parameters differ since the impedances presented to the slots are not the same. This transition, using a one-eighth by .90 inch series-slot, is illustrated in Fig. 3-9.

After etching the center-conductors, the slot, and eyelet locations: the two halves of the Tri-Plate line are fastened together with eight 1/16-inch eyelets around the slot. Four screws are then used to fasten the Tri-Plate sandwich to the waveguide flange. The slot is symmetrically positioned in the E-plane of the guide with the short dimension of the slot in the direction of the narrow dimension of the guide. This properly orients the transverse E-field of the series-fed slot for coupling to the waveguide.

Since a slot is etched on only one side of the line, it represents an unbalanced impedance discontinuity that normally would excite the parallel plate mode and result in some wasted power and undesirable radiation leakage

from the edge of the Tri-Plate line. To prevent this, both ground-planes in the vicinity of the slot are effectively shorted together by the eight rivets, thereby maintaining the outer-conductors at equi-potential as well as serving to hold the two halves of the Tri-Plate line together.

The 90-ohm line feeding the slot terminates in an open circuit 0.234 inches beyond the center-line of the slot. At the design frequency of 9375 MC, the electrical length of this open-circuited tuning element is approximately  $0.294 \lambda_{TP}$ . It therefore appears as a normalized inductive reactance of about  $j0.28$  in series with the slot resistance and capacitive reactance. Normally, the characteristic impedance of the input line is less than 90-ohms, necessitating the use of a matching transformer.

In arriving at the final design, systematic changes were made in the lengths of both the slot and the open-circuit termination, keeping the slot width and the feed-line impedance constant. Input VSWR as a function of frequency for the final design, as depicted in Fig. 3-9, is given in Fig. 3-10.

It should be mentioned that a tee, or two-way power-splitter, from waveguide to Tri-Plate could be made simply by making the Tri-Plate line continuous on both sides of the transition. For a reasonably good impedance match looking "in" the waveguide input, undoubtedly the characteristic impedance of the Tri-Plate line would have to be considerably greater than 90-ohms. (Characteristic impedance increases as centerstrip width is

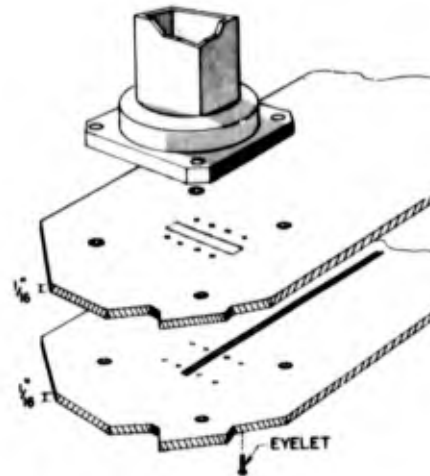


Fig. 3-9 Exploded view of X-band Tri-Plate line to waveguide transition, showing series-slot feed element.



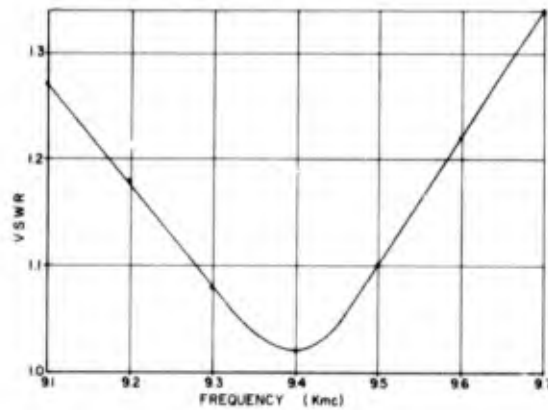


Fig. 3-10 Input VSWR for slot-coupled X-band Tri-Plate line to waveguide transition.

decreased.) However, for a small ground-plane spacing, such as 1/8-inch, the required center-conductor width might prove too narrow to be practical.

A considerably more broadband device is the Tri-Plate line waveguide probe-transition. Two versions have been developed and evaluated, one at X-band and the other at C-band. Both utilize a probe antenna-element which extends part way into the guide through a rectangular slot in the center of one of the broad walls of the waveguide. The probe is, therefore, parallel to the electric field for the dominant  $TE_{1,0}$  waveguide mode. The probe itself is simply a continuation of the 1/8-inch-thick, 30-ohm, teflon-fiberglass (GB112T), Tri-Plate line with the outer-conductors removed over the length of the probe. For X-band, the width of the probe is the same as that of the center-conductor, namely 0.172 inches, while for C-band, the width is 0.375 inches. In essence, then, the probe consists of the Tri-Plate center-conductor surrounded by dielectric material, the wide dimension of the probe being perpendicular to the longitudinal axis of the guide. The waveguide is terminated with a short circuit at a prescribed distance

from the centerline of the probe.

The construction of the one-half by one-inch waveguide X-band transition is illustrated in Fig. 3-11. In addition to clamping the 30-ohm Tri-Plate line securely against the waveguide flange, the metal backing-plate with a 0.250-inch-wide channel serves the purpose of suppressing the parallel-plate mode that would otherwise be excited in the vicinity of the slot and cause undesirable radiation from the edges of the Tri-Plate line. Since the slot width is not a negligible fraction of the

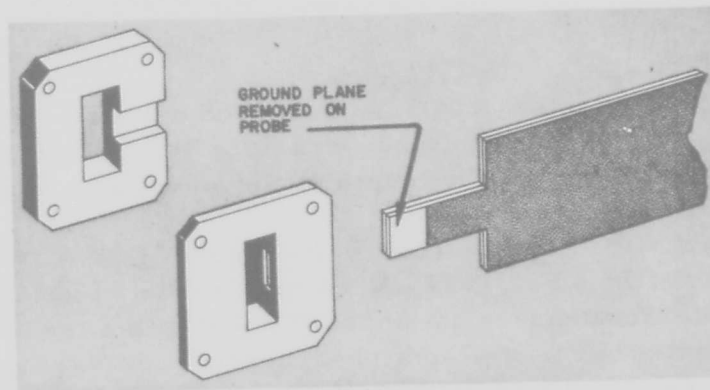


Fig. 3-11 Tri-Plate line to waveguide X-band probe transition.

guide wavelength, a potential difference exists across the slot. A waveguide mode therefore exists in this 0.050-inch-long (thickness of waveguide wall) section of waveguide below cut-off. This assumes that the outer-conductors of the Tri-Plate line make intimate contact with the slot. The power represented by this waveguide mode is only slightly attenuated over this short length, and if the confining channel were not present, it would propagate freely between the ground-planes and radiate at the edges. With the backing-plate present, however, the channel and waveguide-flange form a section of waveguide below cut-off that is sufficiently long and narrow to effectively attenuate all of the unwanted waveguide

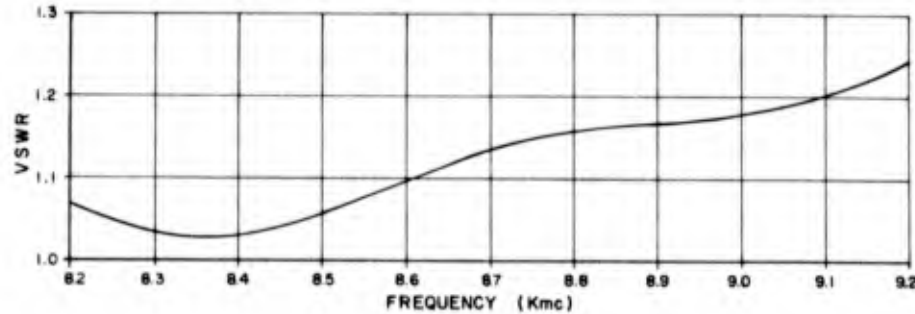


Fig. 3-12 Input VSWR for Tri-Plate line to waveguide probe transition of the type shown in Fig. 3-11.

mode. Once again this assumes good metallic contact at all critical points. Probe-depth for this transition is 0.229 inches while the length of the waveguide short is 0.195 inches.

Input VSWR as a function of frequency for this transition is shown in Fig. 3-12. A 30-ohm Tri-Plate slotted line was used to measure the input VSWR with the transition terminated in a well-matched, broadband waveguide load. Fig. 3-13 is a photograph of the C-band probe (one by two-inch waveguide). In principle, the latter is the same as the X-band transition. A 0.375-inch-wide channel in the backing-plate surrounds the Tri-Plate line and prevents radiation leakage. The 0.375-inch-wide probe extends 0.417 inches into the waveguide, and the distance from the centerline of the probe to the waveguide-short is 0.426 inches.

Input VSWR as a function of frequency for this transition is presented in Fig. 3-14. Again a 30-ohm Tri-Plate slotted-line was used to determine the input VSWR, while the transition was terminated in a matched, broadband waveguide load.

The method used to determine the proper depth of probe (and short) position for a minimum mismatch at the design frequency is of some interest. Normally,

the Tri-Plate line would be terminated in a matched Tri-Plate load, and for each of many different probe lengths the waveguide-short would be adjusted for a minimum input VSWR as measured on a waveguide slotted line. Ultimately, the required combination of probe-depth and short-position would be determined. In designing these transitions, however, it was recognized that the short would present a relatively pure shunt susceptance at the plane of the probe and serve

to cancel out the shunt susceptance of the probe, leaving a shunt conductance of 1.0 for the matched condition. Therefore, at the design frequency, the Tri-Plate line was terminated in a matched Tri-Plate load, while the waveguide was terminated in a matched waveguided slotted line, the probe depth was then adjusted so that the normalized conductance component of the input admittance, referred to the centerline of the probe, equalled 2.0, and the susceptance component was capacitive. The latter condition ensured minimum probe-depth and minimum distance of the short from the probe. Next, the waveguide load was replaced by a sliding short which was adjusted so that its inductive input susceptance at the plane of the probe cancelled out the capacitive susceptance of the probe. Effectively, this left a total normalized input admittance of  $g = 1.0$  and the transition was matched.

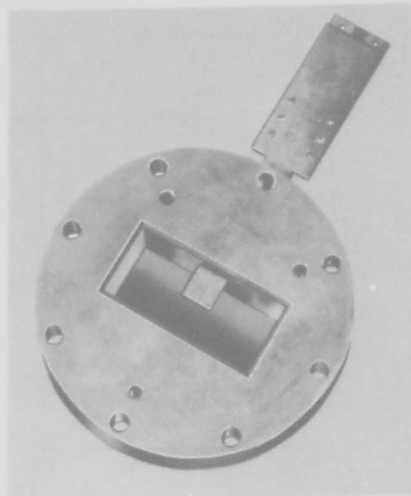


Fig. 3-13 C-band Tri-Plate line to waveguide probe transition.

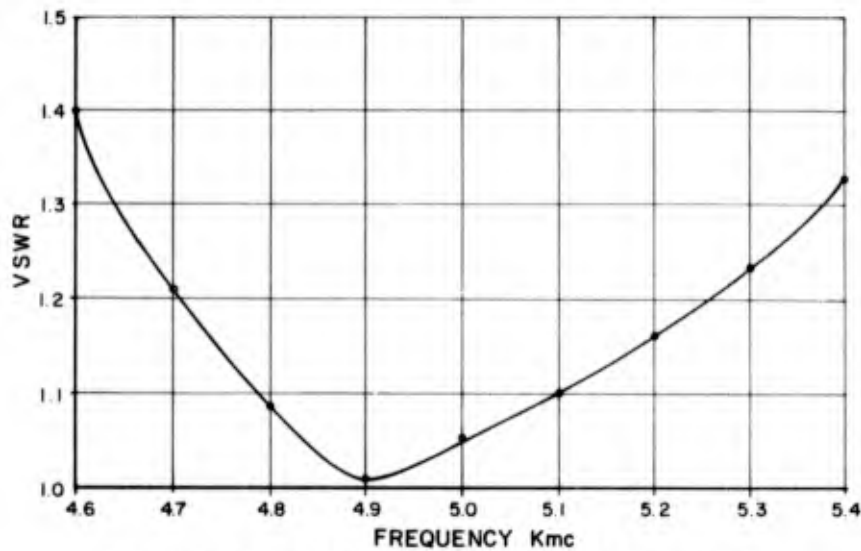


Fig. 3-14 Input VSWR for C-band probe transition.

Justification of this matching technique is clearly demonstrated by the bandpass of the C-band transition in Fig. 3-14. At the design frequency of 4.9 KMC, the input VSWR is only 1.01, and on both sides of this frequency, the curve exhibits a frequency sensitivity that is typical of similar coaxial to waveguide probe transitions. The sliding short of this experimental model was machined to ensure a good fit in the particular section of waveguide used, and, in addition, a clamp was used to ensure good contact between the broad walls of the guide and the short when it was finally positioned. (These precautions were not taken with the X-band experimental model. The data in Fig. 3-12 applies to a transition whose short was soldered in place. It is felt that its position was incorrect due to faulty contact between the experimental short and the waveguide, and therefore, the input VSWR did not vary as anticipated.)

In contrast to the "right-angle" electric-coupling probe-transition, an "in-line" Tri-Plate to standard X-band waveguide transition employing magnetic coupling was developed and evaluated. Its construction is illustrated in Fig. 3-15.

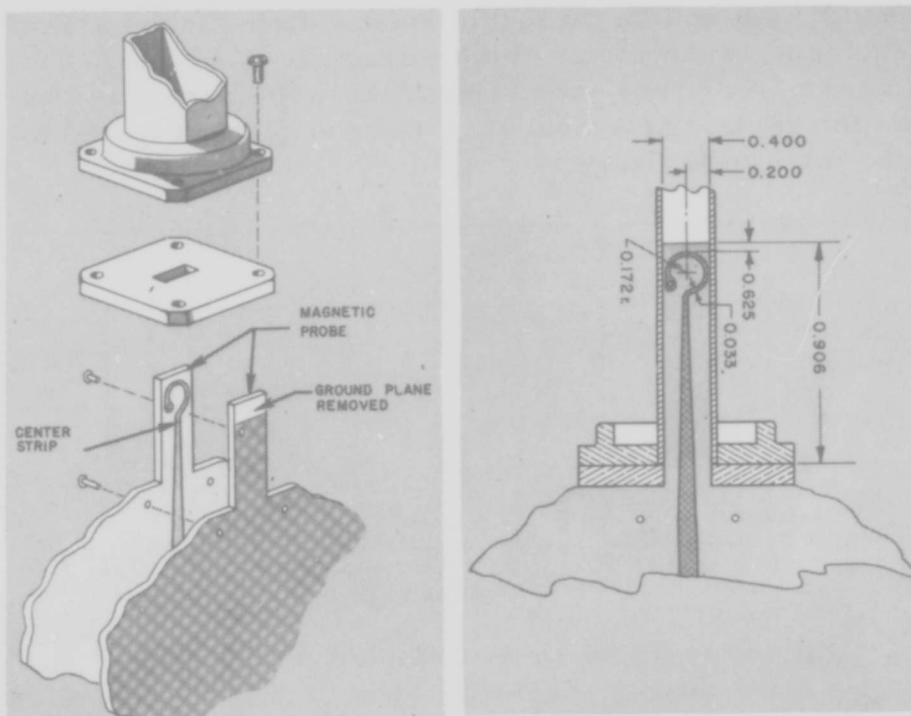


Fig. 3-15 X-band Tri-Plate to waveguide transition employing magnetic coupling.

As shown in Fig. 3-15, the center-conductor of the one-eighth-inch-thick, teflon fiberglass (GB112T), Tri-Plate line is gradually tapered to a width of 0.033 inches and terminates in a loop with an outside radius of 0.172 inches. Over-all line-width is symmetrically cut down to 0.4 inches over the required length to form a probe. Both Tri-Plate ground-planes are terminated a short distance away from the end of this probe, so that the loop in the center-conductor (sandwiched between the two sheets of dielectric material which form Tri-Plate line) extends into the waveguide, unbounded by the outer-conductors. A rivet is soldered to the termination of the loop and forms electrical contact with the ground-planes. The probe is then inserted the proper distance

into the waveguide through a one-eighth by four-tenths-inch slot in the center of the waveguide end-plate. (The plane of the probe-loop is parallel to the narrow walls of the guide.) As a final step, the end-plate is bolted to the waveguide flange.

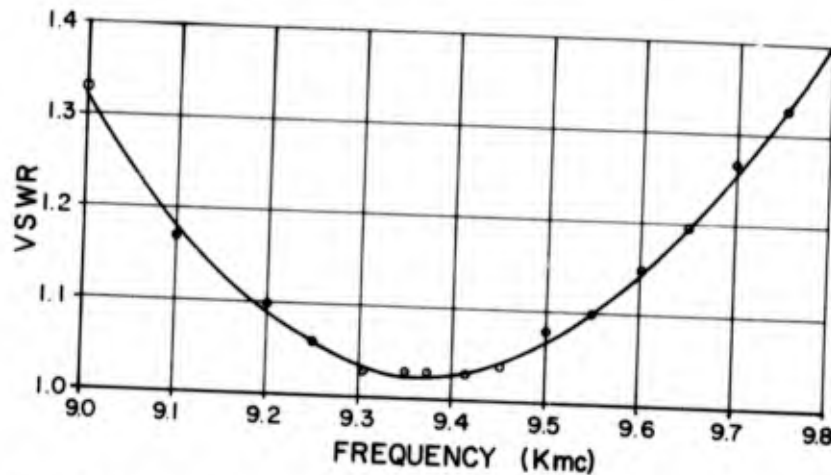


Fig. 3-16 Input VSWR for the X-band transition to waveguide shown in Fig. 3-15.

To prevent any radiation leakage, the Tri-Plate line should have a press-fit into the slot in the end-plate, and the end-plate should be sufficiently thick to ensure that the loop is in the center of the broad dimension of the guide. With respect to the dielectric-covered loop, it is apparent that it is perpendicular to the magnetic field for the dominant  $TE_{10}$  waveguide mode and is, therefore, capable of efficiently coupling energy from the guide to the Tri-Plate line. In respect to the Tri-Plate line, this is a balanced, or symmetrical, coupling device. There is no possibility of exciting the parallel-plate mode.

Input VSWR as a function of frequency for this transition is shown in Fig. 3-16. The values have been corrected for line attenuation. Prior to making these measurements, the insertion depth of the loop was adjusted for a minimum input VSWR at 9375 MC using a Tri-Plate slotted line and a matched-load waveguide termination.

## CHAPTER FOUR

### COMPONENTS

#### 4-1 General Considerations

Some of the basic elements of Tri-Plate design, which perform useful functions when properly proportioned, were discussed in Chapter II. Composite structures, fabricated at Sanders Associates, Inc. from such basic elements, are discussed in the present chapter, and include terminations and attenuators, variable tuners, crystal holders, power dividers, bridge circuits, and directional couplers.

#### 4-2 Terminations and Attenuators

Dissipative elements such as carbon-coated resistive-card (or tape) and thin, metallized, film-coated plastics have been used in the construction of matched loads and attenuators in Tri-Plate line. In general, attenuation varies considerably with frequency, in a linear fashion, in devices employing the carbon coating. Considerably less variation with frequency occurs when the metallized film is used. Two methods of fabricating matched loads in Tri-Plate line are shown in Fig. 4-1. The most common configuration is shown in Fig. 4-1a and consists of a sheet coated with absorbing material (such as IRC card or Uskon cloth) placed between the etched inner-faces of the two Tri-Plate laminates. As a result, the lossy material is situated within the fringe fields of the two center-conductors, thereby dissipating the power in the line. In order to obtain a good match with attenuators and terminations of this type, the lossy material should intercept the fringe energy in a gradual manner (exemplified by the tapered configuration shown in Fig. 4-2). Fig. 4-3 is a VSWR plot of a typical broadband load of this type. The match of this termination, which



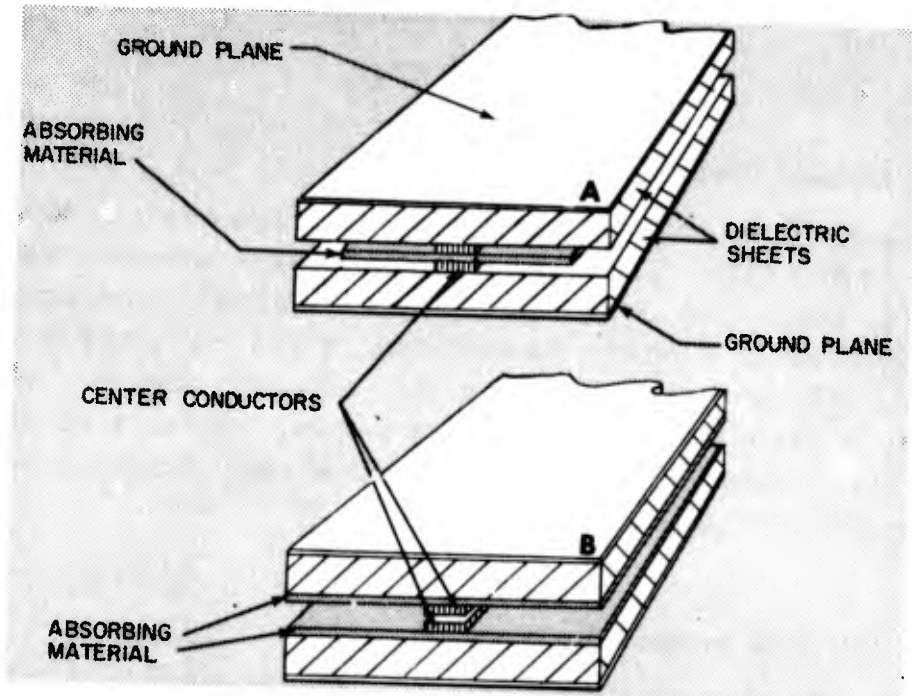


Fig. 4-1 Two methods of fabricating matched loads and fixed attenuators with resistive coated material

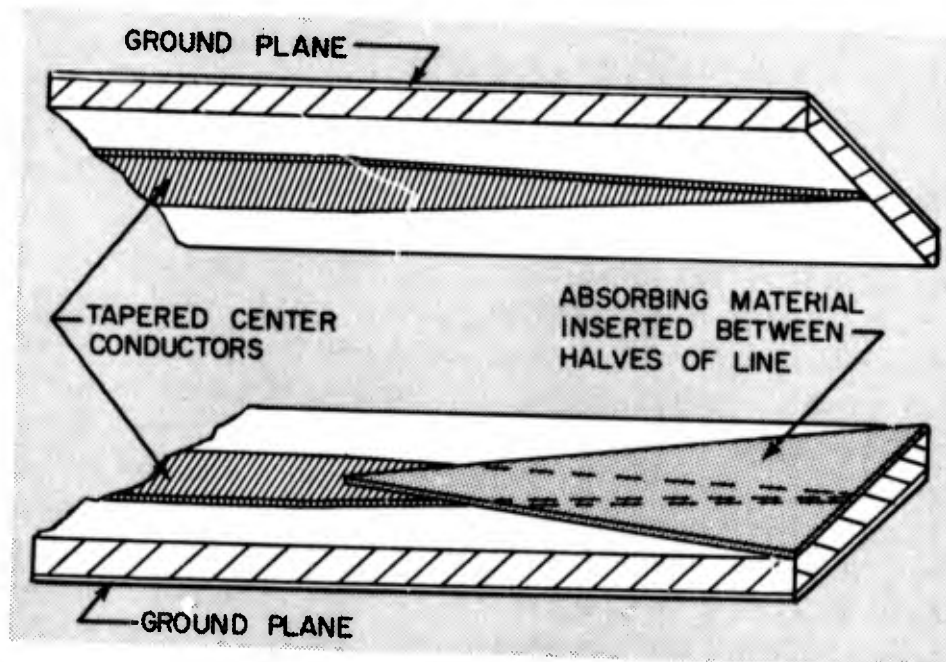


Fig. 4-2 Typical Tri-Plate termination

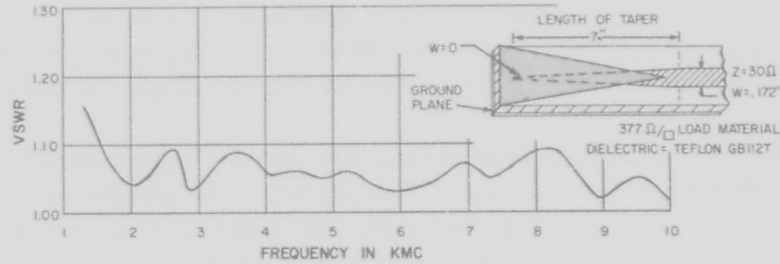


Fig. 4-3 VSWR of a typical Tri-Plate termination

uses a tapered length of  $377 \Omega / \square$  Uskon cloth, is under 1.1, from 1.6 KMC to at least 10 KMC.

The second method of constructing matched loads and fixed pads, shown at (b) in Fig. 4-1, consists in placing the lossy material in intimate contact with the current-carrying surface of the center-conductor. This requires separating the etched centerstrips from the dielectric, inserting the absorbing material, and replacing the centerstrips. An alternate technique would be to plate center-conductors on the surfaces of two short sections of lossy material and attach these lossy sheets to the inner faces of the two Tri-Plate laminates.

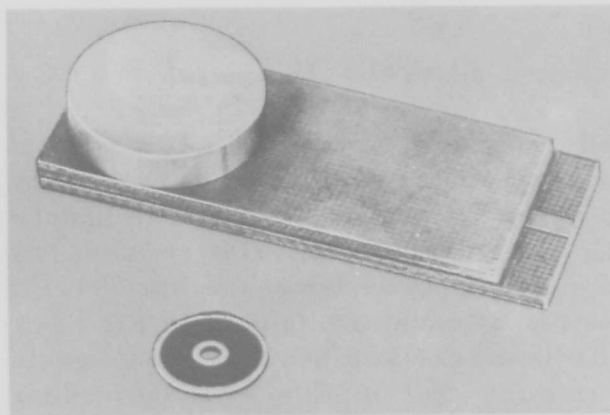


Fig. 4-4 Disk load fabricated in Tri-Plate line shown with commercial disk-type resistor

As a final step, the center-conductors plated on the lossy sheets would be connected to the contiguous etched-centerstrips of the regular line by short strips of copper foil.

Short coaxial terminations can be packaged neatly in Tri-Plate line. One such termination is shown in Fig. 4-4 and consists of a coaxial, carbon-coated, 50-ohm disk-resistor, the center of which is connected to the Tri-Plate center-conductor by an eyelet. The outer-conductor of the disk-resistor is shorted to the Tri-Plate ground-plane by a hollow cylindrical cap. Loads of this type have been made with a voltage standing wave ratio of less than 1.1 up to 4 KMC.

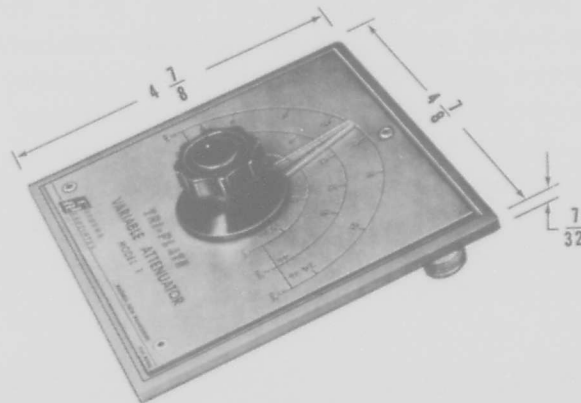


Fig. 4-5 Variable attenuator in Tri-Plate line

Printed strip-transmission lines have one unique advantage over other types of line in that the path along which the energy flows can be etched in practically any imaginable configuration with relative ease. This facility has made possible the design of the flat Tri-Plate variable resistive attenuator\* (shown in Fig. 4-5), which is currently being marketed by Sanders Associates, Inc. The center-conductor of this attenuator describes an arc. When a properly-shaped card made of lossy material is rotated over the center-conductor, it will cut this

\*Patent applied for.

conductor in a gradual manner. The design of the centerstrip and lossy card is shown in Fig. 4-6. The attenuator is particularly useful over the frequency band from 3 to 5 KMC, but can be used from L- to C-band. A typical VSWR plot over this frequency range is shown in Fig. 4-7. The degradation of match toward the lower end of the frequency band is attributed to the fact that the taper of the resistive card into the fringe field becomes more abrupt in terms of wavelength.

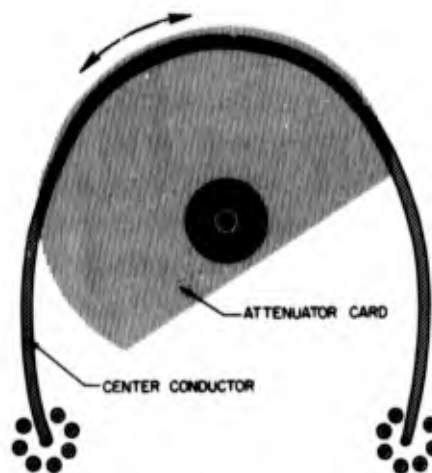


Fig. 4-6 Attenuating card and etched centerstrip configuration of Tri-Plate variable attenuator

### 4-3 Variable Tuners

Most of the work on variable impedance transformers,

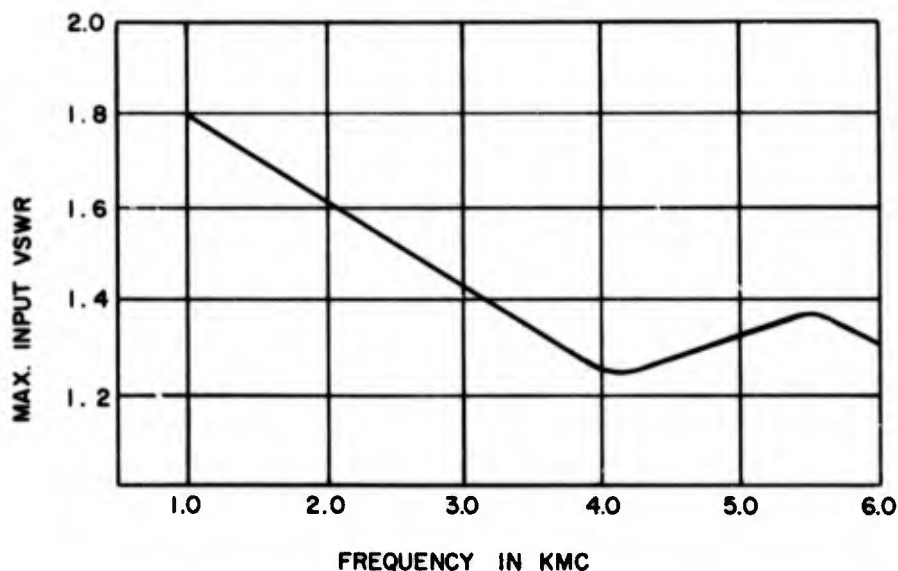


Fig. 4-7 Input VSWR of a Tri-Plate variable attenuator

or tuners, which have been fabricated in Tri-Plate line has been concentrated on stub-type tuners. The center-configuration of this type of tuner consists of a stub-line, perpendicular to the main transmission line, the length of which can be adjusted easily to vary the impedance in the main line. The stub-lines may be open or short-circuited, and there may be one or more variable stubs in the configuration. In both short and open-circuited types, a dielectric rotor about ten mils thick, with an arc-shaped conductor etched on both sides, is inserted between the halves of the Tri-Plate line. When the rotor is turned, the effective electrical length of the shunt-stub is changed. An especially compact arrangement of a multi-stub tuner is obtained by alternate placement of the stubs on each side of the main transmission line. Typical Tri-Plate single and double-stub short-circuit tuners are shown in Fig. 4-8. The fabrication of a double-stub open-circuit tuner is shown in Fig. 4-9.

The stub-line in the open-circuited configuration is longer than that of the short-circuited configuration since the first point of resonance is reached when the line is  $\lambda/2$  in length, while, for the short-circuited stub, the first point of resonance is reached when the stub line is  $\lambda/4$  in length. The shorter the stub line, the less the behavior of the line is frequency sensitive and this is an advantage for the short-circuited variety. However, the short-circuited rotor must maintain good contact with its axial pin and the ground-planes and this presents a greater fabrication problem than arises with an open-circuited rotor.

An analysis of the single-stub transformer in Tri-Plate line has been given in section 2-3, of this handbook. Theoretically, as an open-circuited shunt-line (of normalized conductance equal to one) is varied in length from zero to  $\lambda/2$ , the VSWR introduced in the main line varies from zero to infinity. The combination

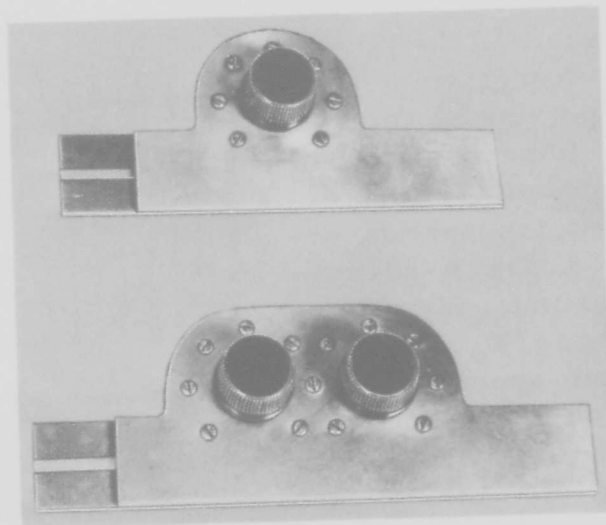


Fig. 4-8 Tri-Plate short-circuited single- and double-stub tuners

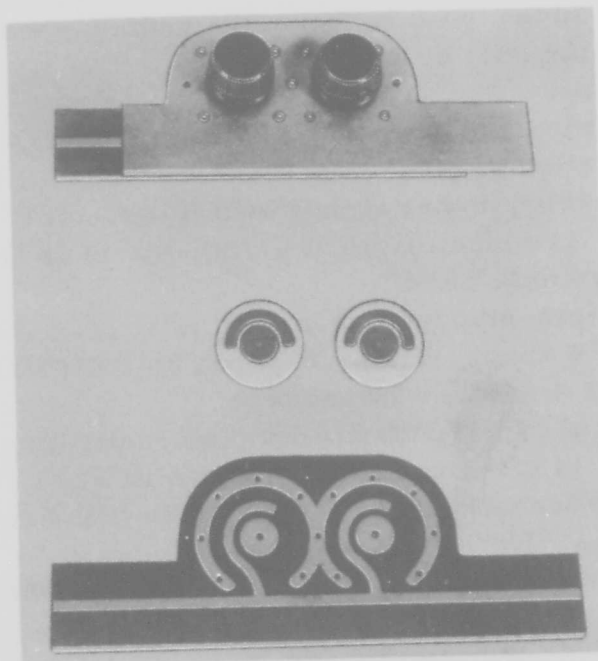


Fig. 4-9 Open-circuited double-shunt-stub tuner, showing a) assembled unit, b) open-circuited rotors, & c) centerstrip configuration

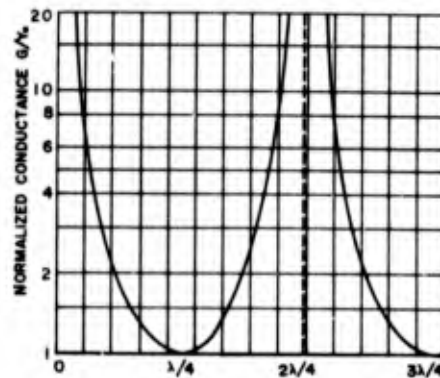
of two tunable-stubs gives a matching-transformer capable of presenting a wide range of impedances. The exact impedance-range depends upon the spacing between stubs. Fig. 4-10 illustrates maximum normalized conductance  $g/Y_0$  as a function of stub-spacing. From observation of this curve, it would appear that  $\lambda_0/2$ , or some multiple spacing, gives the greatest range of obtainable impedances. However, such spacing requires very large susceptance values to tune-out even small mismatches, when the phase is not favorable. An additional disadvantage of the half-wavelength spacing is that this tuner will be very frequency-sensitive, and hence tuning will be critical.

The same disadvantage applies to quarter-wave stub-spacing, plus the inability with this spacing to tune to a conductance greater than one. Because of these factors, a spacing in-between is usually selected as a compromise. An odd multiple of eighth-waves is the spacing most commonly used.

The triple-stub tuner consists of three of these stubs, spaced  $\lambda/4$  apart, and is capable of matching any impedance to any other impedance.

A typical construction for a Tri-Plate "line-stretcher," as it is often called, is shown in Fig. 4-11. The mechanical construction is similar to that used with the stub tuners. Here the length of line between input and output junction is varied by rotation of the center disc.

Variations of the aforementioned construction used for variable-shunt-stubs and "line-stretchers" in Tri-Plate line readily present themselves. One modification



4-10 Maximum normalized conductance  $g/Y_0$ , obtained with a double-stub tuner

would be the introduction of an air-dielectric section with the arc-shaped stub printed on both sides of a center-plate. A section of the combined outer-plates is rotated. Attached to this movable section is a spring-strip which shorts the center-conductors to the ground-planes by "wiper action".

Another type of tuner which is capable of producing a VSWR of moderate magnitude is shown in Fig. 4-12. This device, which has been called a "tab tuner", has the major advantage of having the moving parts external to the dielectric sheets. An opening is cut in the outer face of the Tri-Plate line, directly over the center-conductor. Again, it is found to be convenient to form the center-strip and, hence, the opening as well, in an arc. If the input and output of the slot in the outer-conductor are gradually tapered, such an opening will be essentially reflectionless. The introduction of a tab over the slot will produce a discontinuity. By using two or more separately-variable tabs, a versatile variable-transformer is obtained. A device of this sort will radiate if precaution is not taken to shield the area over the slot. Another marked disadvantage is that the entire assembly requires being boxed-in if the tabs are not placed symmetrically on the ground-planes.

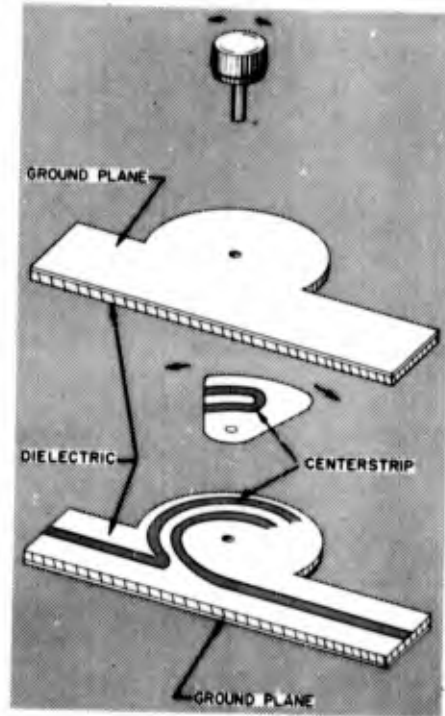
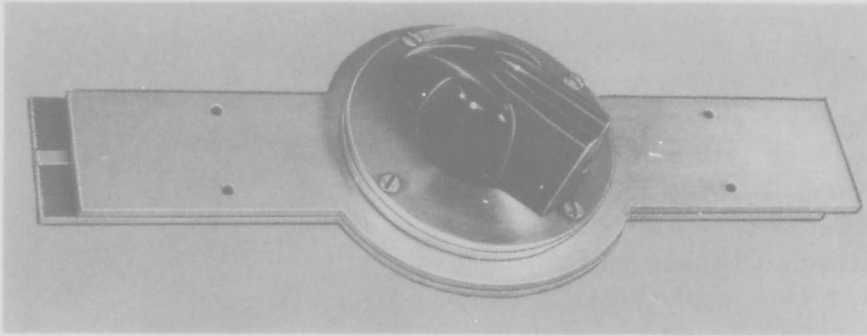


Fig. 4-11 Tri-Plate "line stretcher"

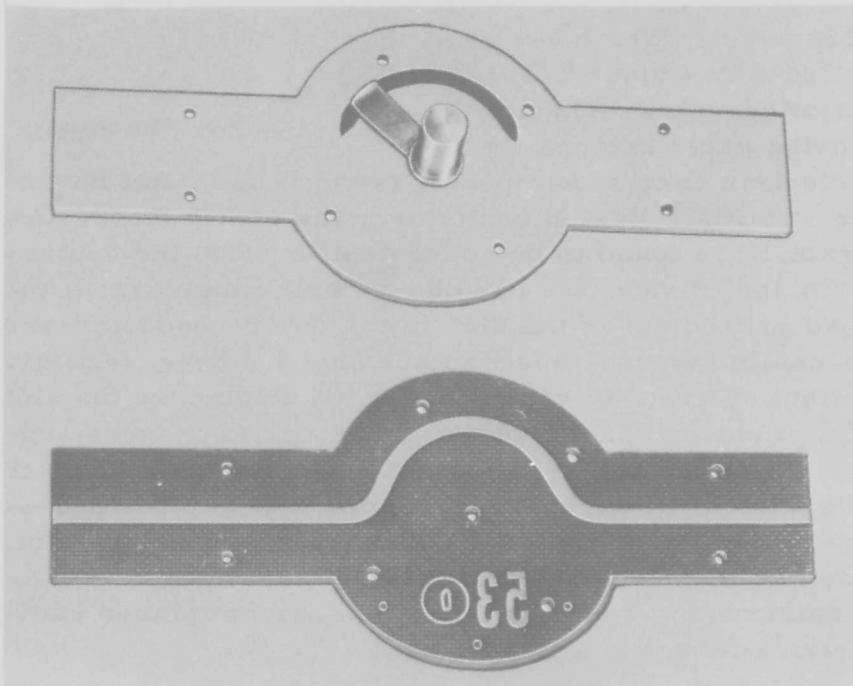
#### 4-4 Crystal Holders

One of the major problems encountered when using crystals at microwave frequencies is that of designing





a) assembled



b) slot, tab, and centerstrip configuration

Fig. 4-12 Tri-Plate "tab tuner"

a crystal-mount which provides both RF and DC paths through the crystal. A further problem is that of locating the crystal in the transmission line so that a good impedance match is obtained. In the simple, fixed, tuned, Tri-Plate crystal-mount shown in Fig. 4-13, the quarter-wavelength line behind the crystal is shorted to the ground-planes of the Tri-Plate line by an eyelet. This provides the necessary DC-return path for the rectified crystal current. The RF is by-passed by means of a built-in capacitor in the crystal-holder mount.

The useful bandwidth of this right-angle crystal-mount, matched to a 50-ohm Tri-Plate line, depends on the characteristics of the matching elements. It is not advisable to allow the length-of-line between the short-circuit and the crystal to approach a half-wavelength, since the susceptance introduced is quite large

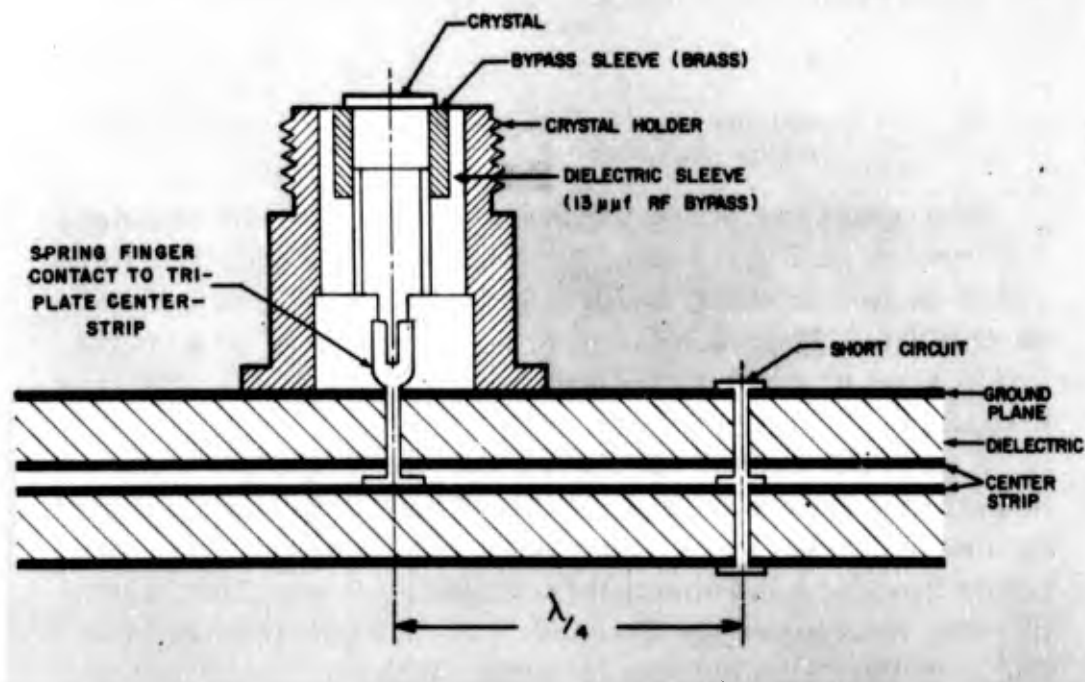


Fig. 4-13 Simple, fixed, tuned, Tri-Plate crystal mount

and varies with frequency, making a good match difficult to obtain. "A" in Fig. 4-14 shows a crystal holder with the short-circuit adjusted for best match. "B" in the same figure shows a crystal holder with the tip of the crystal cut off and with the short-circuit similarly adjusted for the best match. Fig. 4-15 is the admittance plot for these two crystal holders. Frequency-spread is much less with the modified crystal, due to the decrease in RF path-length.

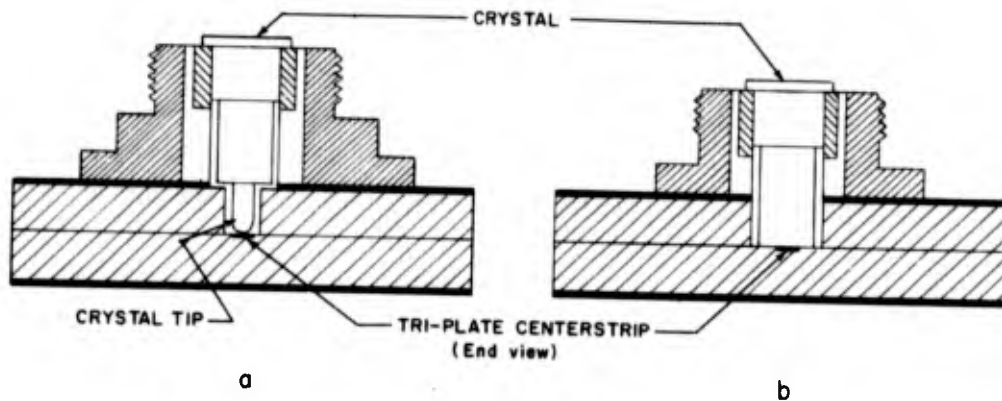


Fig. 4-14 Crystal holders in Tri-Plate line with a) crystal tip intact, and b) crystal tip cut-off

The standing wave ratios of these crystal holders are shown in Fig. 4-16. The three curves plotted here refer to the crystal, before and after modification, and to the final match by use of a shunt-stub. The right-angle type of crystal holder can be used at L-, S-, and C-bands.

A crystal holder designed for a "Tripolar" type of crystal is shown in Fig. 4-17. The "Tripolar" crystal is designed to work from a 65-ohm coaxial line, and lends itself to broadband-mixer applications. The IN369A crystal developed by Sylvania has a built-in broadband DC-return, simplifying design of the crystal holder. Although this is an in-line holder, it could be adapted easily to the right-angle type.

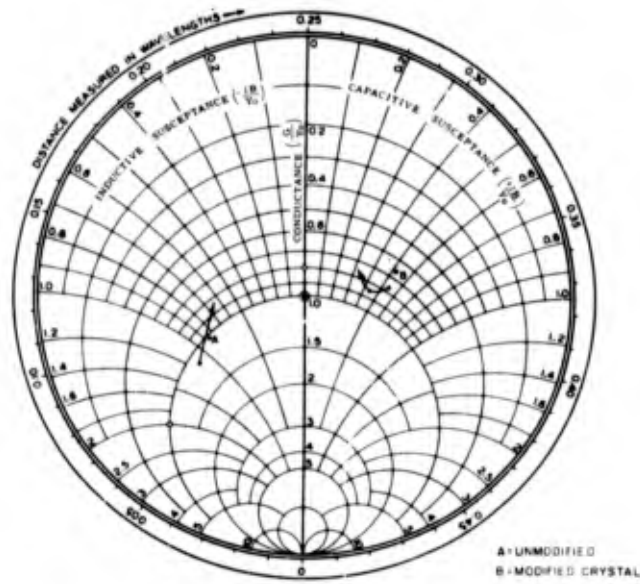


Fig. 4-15 Admittance Plot for crystals shown in Fig. 4-14

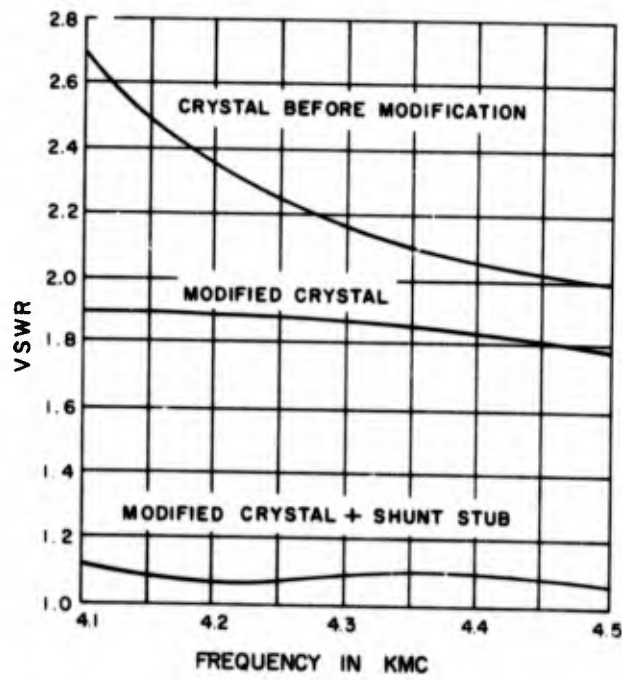


Fig. 4-16 VSWR for unmodified and modified crystals in Tri-Plate crystal holders shown in Fig. 4-14

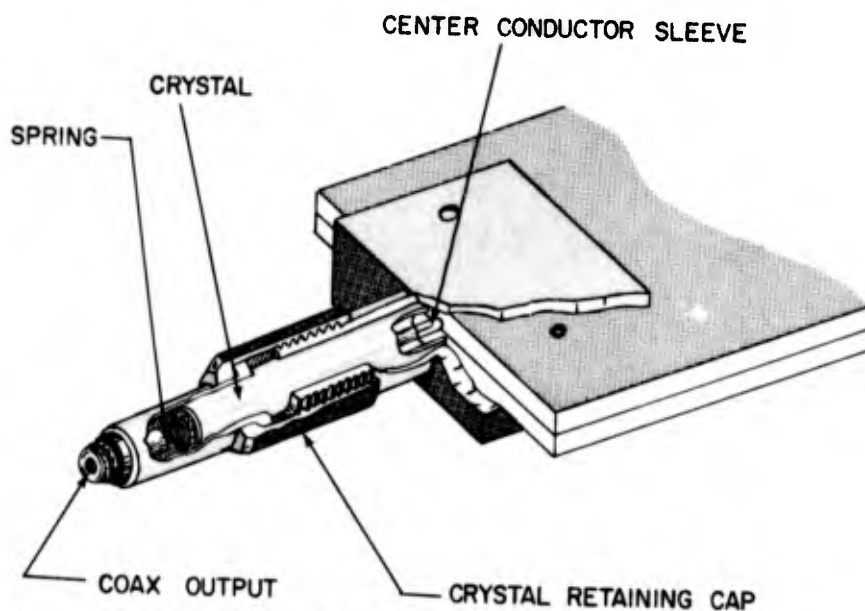


Fig. 4-17 Crystal holder for "Tripolar" crystal

Standing wave ratios for four crystals of this type, in Tri-Plate crystal holders, are shown in Fig. 4-18, plotted against frequency. It should be noted that three of the four crystals plot rather closely together, while the fourth plots differently. (The crystals tested were purchased during their developmental state.) The RF input-power required to produce 1.0 milliamperes of crystal current is approximately 1.2 milliwatts. This compares well with conventional crystals.

#### 4-5 POWER DIVIDERS

The planar form of Tri-Plate transmission makes it ideal for power-dividing networks in high-frequency transmission systems. This type of transmission line has already been used extensively in applications such as the distribution of power to the elements of an antenna and as an equal power-splitter for local-oscillator output to each mixer of the multichannel-systems characteristic of electronically-scanned radars.

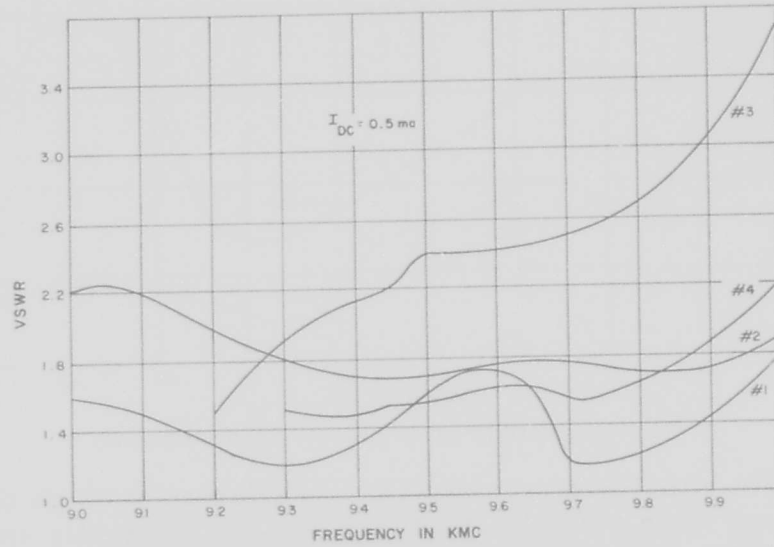


Fig. 4-18 VSWR for four 1N369A ("Tri-polar") crystals in a Tri-Plate crystal holder

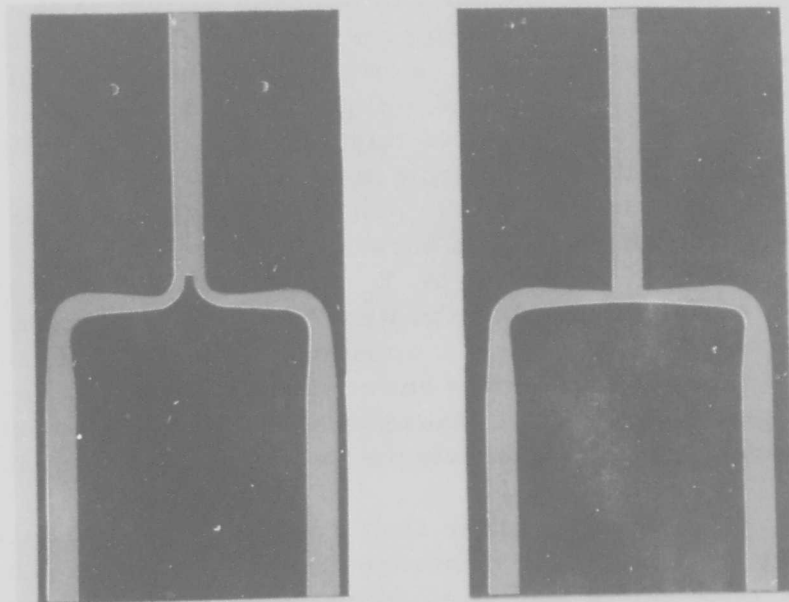


Fig. 4-19 Two centerstrip configurations for simple power dividers: a) in-line, and b) tee

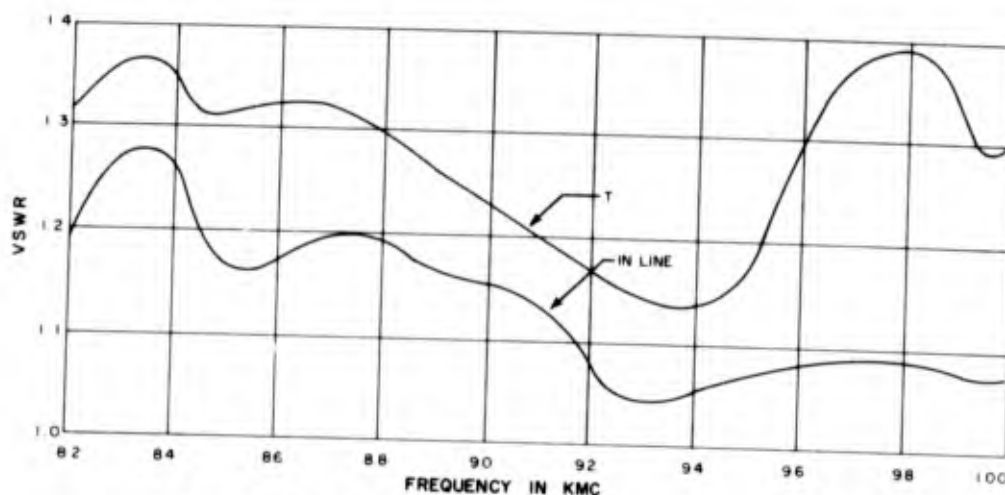


Fig. 4-20 VSWR for power dividers shown in Fig. 4-19

The simplest power divider is a junction at which the energy from a single-input line is divided equally into two branch-lines. Two possible center-conductor configurations for this type of junction are shown in Fig. 4-19. The power divider shown at the bottom is in the form of a "T" and is analogous to the coaxial "T". The power divider at the top is an "in-line" junction which is, for practical purposes, unique to strip transmission lines. The counterpart of this divider in coaxial line would be costly and difficult to construct.

The branch arms of the junctions illustrated in this figure are effectively in parallel. If admittance at the junction is represented by  $Y_0/2$ , the main arm would have a characteristic admittance equal to  $Y_0$  for the matched condition. Measurements of VSWR vs. frequency for the power dividers shown in the above figure are compared in Fig. 4-20. These results show the inherently superior match-characteristics of the "in-line" junction.

Power divisions other than equal can be obtained easily by adjustment of branch-line admittances. The ratio of power in each branch-line will be proportional to the admittance ratios. Representing the respective branch-line admittances by  $Y_1$  and  $Y_2$ , it follows that:

$$Y_1/Y_2 = P_1/P_2 \quad (4-1)$$

and for matched conditions:

$$Y_1 + Y_2 = Y_0 \quad (4-2)$$

Similarly, a strip transmission line may be subdivided into three or more arms. The general expression would then be:

$$Y_1 + Y_2 + Y_3 \dots Y_n = Y_0 \quad (4-3)$$

and equal power in each branch-line would demand that:

$$Y_1 = Y_2 = Y_3 = Y_n = Y_0/n. \quad (4-4)$$

The network at the left in Fig. 4-21 is a three-branch power divider in which the admittance for each individual branch-line is  $Y_0/3$ . It can easily be seen that any variety of power divider can be used with any other to obtain a desired power-distribution. The network at the right of this figure (4-21) consists of three "in-line" power dividers resulting in equal amounts of power being delivered to each of four branch-arms. Obviously, power in each arm will be in-phase since each arm presents a path of equal length. The power-divider combination shown in Fig. 4-22 is a series of three unequal power-divisions designed to obtain equal power in each of the four parallel arms. It must be remembered that the power-split at a junction is proportional to the respective characteristic admittances of the branch arms. With the input-line admittance  $Y_0$ , each successive junction would have branch-arm admittances of  $3 Y_0/4$  and  $Y_0/4$ ;  $2 Y_0/4$  and  $Y_0/4$ ; and  $Y_0/4$  and  $Y_0/4$ . The junctions are here arranged in tandem, and the phase of energy delivered to each of the parallel arms is dependent upon the electrical distance between junctions.



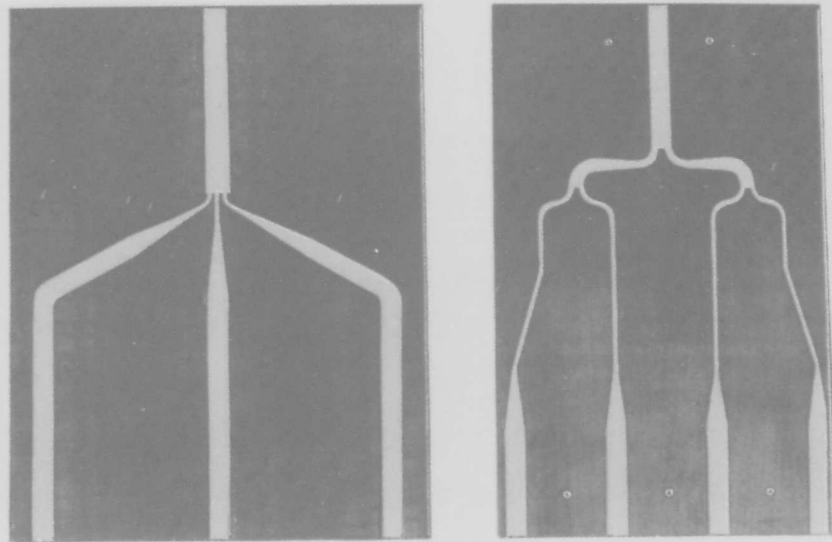


Fig. 4-21 Two possible combinations of power dividers: (Left) three equal in-line divisions, and (right) three divisions into four equal lines.

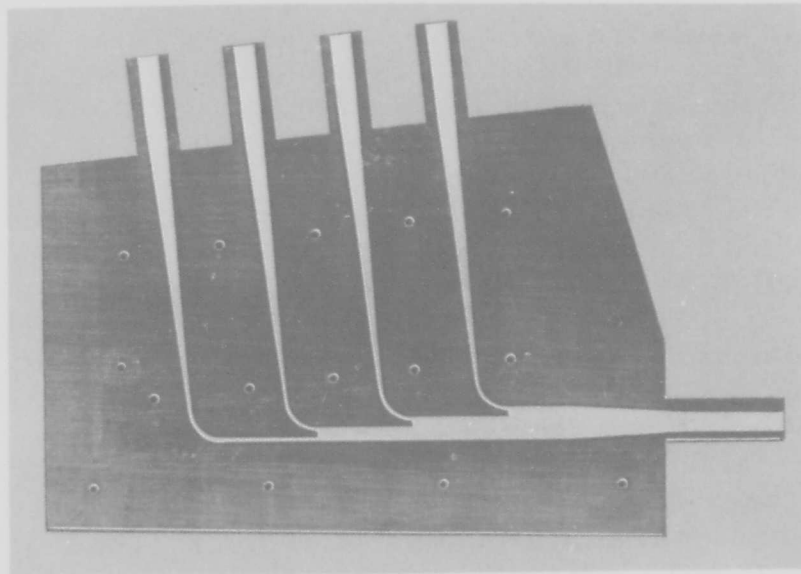


Fig. 4-22 Series of three unequal power dividers designed to obtain equal power in each of four parallel arms

Transformer sections may readily be applied in the construction of power-division networks in Tri-Plate or other strip-transmission line. One presented by R. M. Barrett of the Air Force Cambridge Research Center<sup>1</sup> is shown in Fig. 4-23. The network consists of quarter-wave line sections connecting successive junctions. Since the impedance of a quarter-wave transformer section is the geometric mean of the input and output impedances, (that is:

$$Z_T = \sqrt{Z_{in} Z_{out}}$$

a quarter-wave line of characteristic impedance  $Z_0$  may be used to join successive junctions, where the branch impedance and the input-arm impedance are also equal to  $Z_0$ . Looking from the output end of a line where two lines of characteristic impedance  $Z_0$  are joined, one sees a parallel impedance of  $Z_0/2$ . A quarter-wavelength down the line, the impedance would be  $2 Z_0/2$ , satisfying requirements for match at this junction. The primary advantage of this network is, of course, that a single characteristic impedance is maintained throughout.

A similar power divider developed at Sanders Associates, Inc., employing quarter-wave transformers to maintain a single impedance, is shown in Fig. 4-24, while the match-characteristics of this power divider are shown in Fig. 4-25. A 50-ohm coaxial transition is used to split equal amounts of power into two 50-ohm arms which are a quarter-wavelength long at the frequency of interest. These arms extend to T-branches which further divide the energy into four 50-ohm lines,

<sup>1</sup>Electronics, June 1952

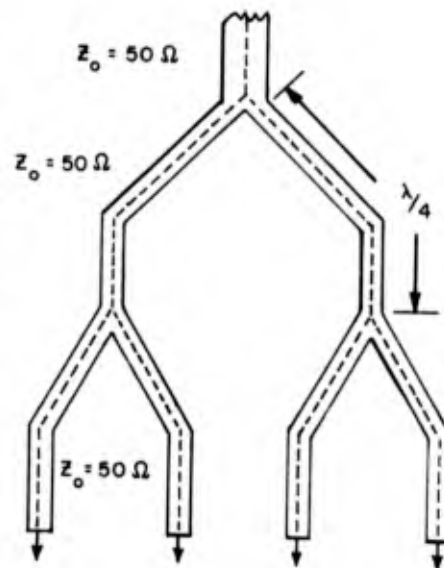


Fig. 4-23 Power division network consisting of quarter-wave line sections connecting successive junctions

(4-5)

leading to output transitions. Thus, equal amounts of energy are delivered to four different lines. The length of the four output-arms is not critical and could very conveniently be shortened.

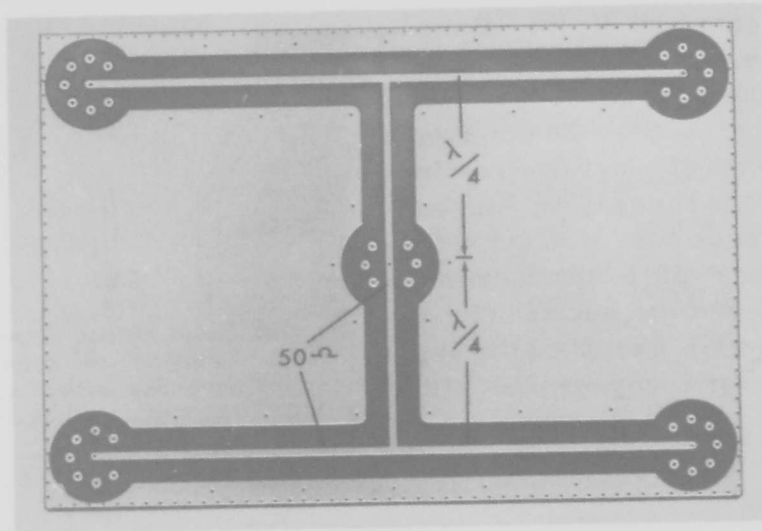


Fig. 4-24 Four-way power division in Tri-Plate line

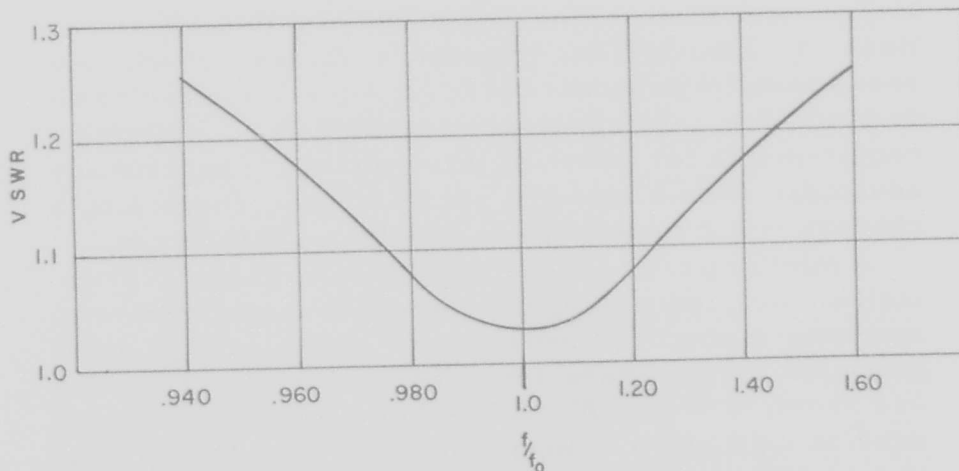


Fig. 4-25 VSWR for four-way power divider shown in Fig. 4-24

## 4-6 Bridge Circuits

Many microwave applications require the use of so-called "hybrids", such as the matched magic-tee, 3-DB short-slot coupler, and hybrid ring or "rat race". All of these devices may be represented by the symmetrical four-terminal-pair network shown in Fig. 4-26. Ideally, at the design frequency, a matched load will be presented to any pair of input-terminals, provided the two adjacent terminal-pairs are terminated in matched loads. In addition, power fed into these input-terminals will divide equally between the two matched loads and no power will appear at the fourth, or opposite, pair of terminals. The latter is commonly called the isolation arm.

In practice, the ideal is most nearly approached by the matched waveguide magic-tee. Good isolation and match are obtained over a relatively wide frequency-band. Where size is of importance, however, and the power level is permissible, a Tri-Plate hybrid ring can be used to good advantage. Such rings have been made and tested at L-, S-, C-, and X-band frequencies. The material used was copper-clad 1/16-inch-thick teflon-fiberglass (GB112T), giving a total line thickness of only 1/8-inch. Fig. 4-27 illustrates the center-conductor configuration of a Tri-Plate hybrid ring.

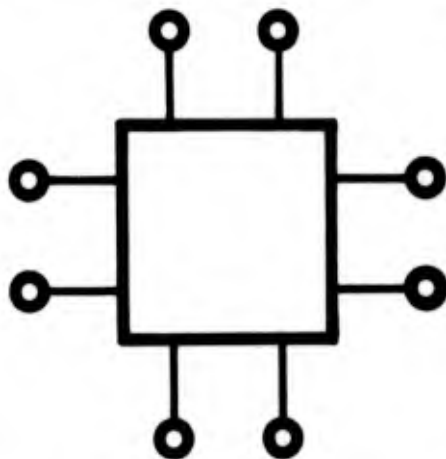


Fig. 4-26 Symmetrical four-terminal-pair network

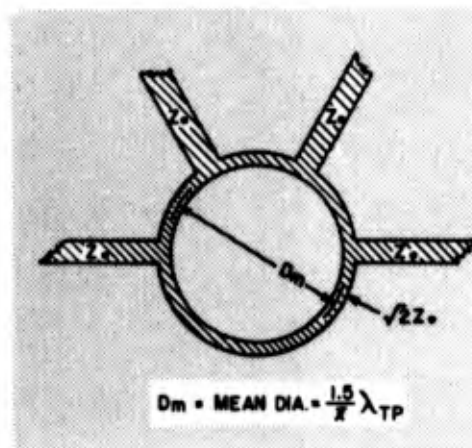


Fig. 4-27 Center-conductor configuration of a Tri-Plate hybrid ring

Because the four arms are in shunt with the ring, it is necessary to make the characteristic impedance of the ring larger than that of the arms by a factor of  $\sqrt{2}$ , in order to obtain a reasonably good match over a broad frequency-band. Unlike a matched waveguide-magic-tee, the isolation is a function of the electrical spacing of the arms and is, therefore, more frequency sensitive. Maximum isolation is obtained when the arm-spacing is exactly equal to a quarter-wavelength, since the voltage incident on the isolation-arm from one side of the ring is then exactly equal in amplitude, but opposite in phase, to the voltage incident on that arm from the other side of the ring. Ideally, complete cancellation occurs and no power enters the isolation arm. In practice, junction effects and imperfect loads on the two output-arms prevent the realization of perfect isolation, irrespective of the type of transmission line used to make the ring.

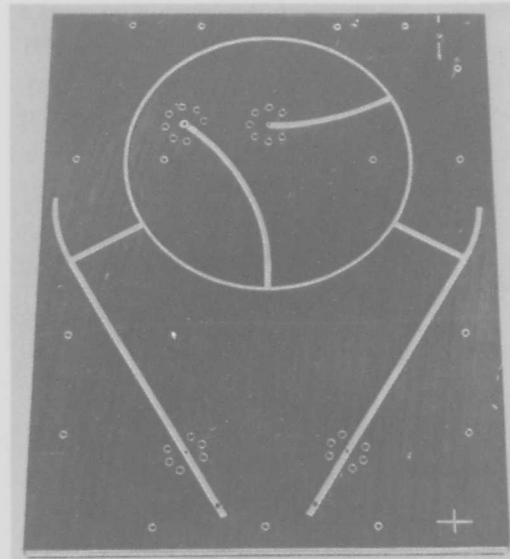


Fig. 4-28 Center conductor configuration of a band-balanced mixer

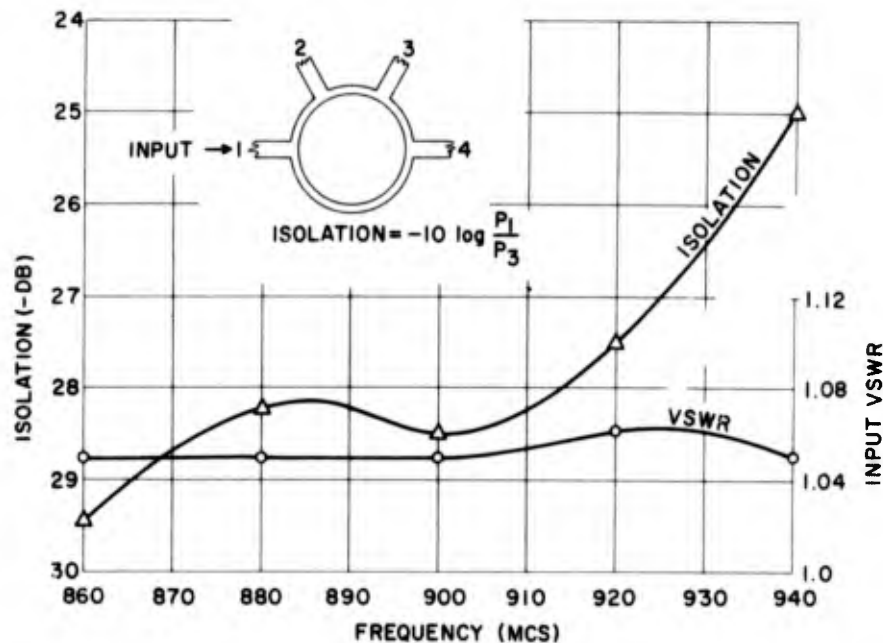


Fig. 4-29 Isolation and input VSWR versus frequency, for an L-band hybrid ring

The illustration in Fig. 4-28 of a balanced mixer which incorporates a Tri-Plate hybrid-ring, the design-frequency of which is 900 MC, clearly demonstrates what can be saved in weight, size, and cost by fabrication in microwave strip-transmission line. The overall dimensions of the mixer, including the protrusion of the four type-N connectors, are only 8-1/2" x 6-3/8" x 7/8". This same mixer, fabricated in conventional coaxial line, would be less compact, much heavier, and, because of machining and fabrication problems, considerably more costly.

The hybrid-ring design used in the above-described balanced mixer was evaluated separately over a 9% frequency-band centered about 900 MC. Input VSWR and isolation, as a function of frequency, are plotted in Fig. 4-29. The maximum difference in the power output of each of the coupled arms was only 0.3 DB. While

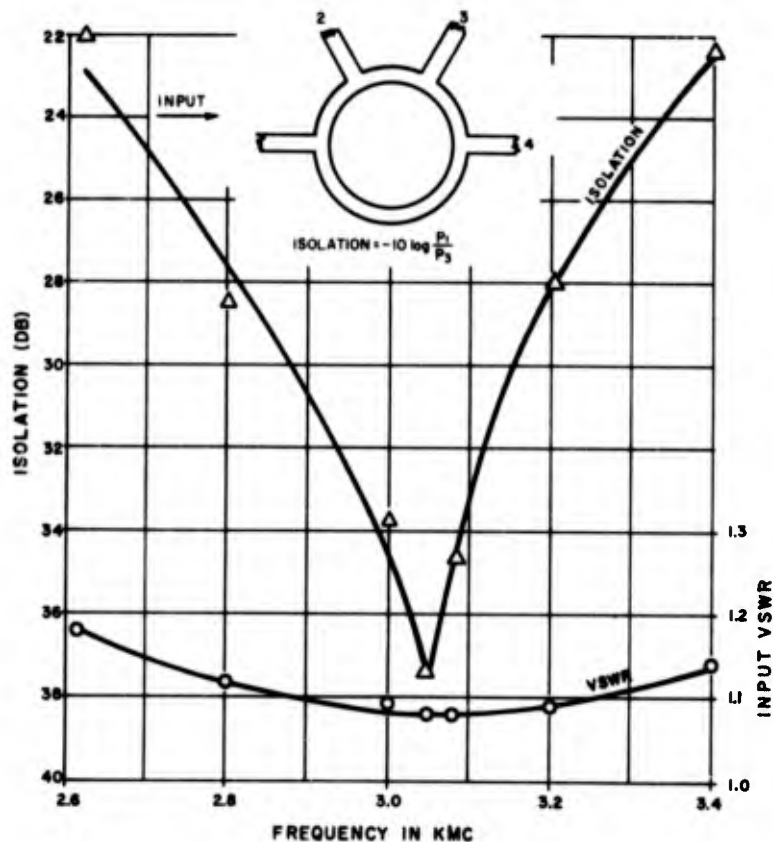
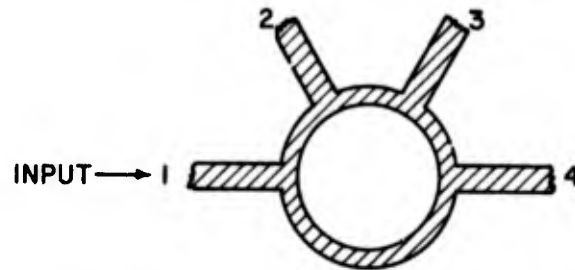


Fig. 4-30 Isolation and input VSWR versus frequency, for an S-band hybrid ring

the match of this ring was very good over the entire frequency-band, the isolation was only reasonably good. Very probably, this was due to the presence of reflections introduced at the Tri-Plate-line to coaxial-line junctions, which could not be independently matched out. The isolation curve is not, therefore, indicative of the optimum performance of which the ring, itself, is capable. The mean diameter of the ring is 4.097 inches and the characteristic impedance is 70.7-ohms. The four 50-ohm arms are terminated in type-N coaxial transitions.

Similar hybrid-rings have been made and evaluated at S-, C-, and X-bands. Isolation and input VSWR curves for an S-band ring, over a 27% band, are shown in Fig. 4-30. In this case, the four 50-ohm arms were constructed with 3/16th-inch lap-joints. Loads and double-stub



FREQUENCY (MC)	INPUT VSWR	RELATIVE POWER (DB)			
		P <sub>1</sub>	P <sub>2</sub>	P <sub>3</sub>	P <sub>4</sub>
4100	1.19	0	-3.2	-44	-3.1
4300	1.09	0	-3.1	-49	-3.1
4500	1.23	0	-3.1	-39	-3.2

Fig. 4-31 Coupling and input VSWR data for a C-band hybrid ring

tuners were connected to three coaxial Tri-Plate-line transitions, and at each test-frequency all three load-combinations were individually matched out on a Tri-Plate slotted line to a VSWR of 1.03, or less, prior to connecting them to the three output-arms of the ring. Any reflections from the Tri-Plate-line to coaxial-line junctions were, therefore, taken into account and minimized. As a result, the experimental isolation curve has the same general shape and exhibits the rather high frequency-sensitivity of the theoretical isolation curve for a waveguide hybrid ring. The impedance match was very broadband, as it should be. Were the loads completely reflectionless, some deviation from the measured values, particularly those of isolation, would be expected.

Data for a C-band hybrid ring, measured over a 9.3% frequency band centered at 4300 MC, is given in the table which forms part of Fig. 4-31. The characteristic impedance of the four arms was 30-ohms, and the measurement procedures were the same as those used for the S-band ring.



An X-band hybrid ring, with arm-impedances tapered from 50-ohms at the ring to 30-ohms at the four lap-joints was measured from 9150 MC to 9600 MC. The data is tabulated in Fig. 4-32. (The subscripts apply to the arms of the ring as they did in Fig. 4-31.)

#### 4-7 Directional Couplers

The directional coupler is another form of hybrid network which has a variety of uses in microwave circuits. Since much literature <sup>2, 3, 4</sup> is available which describes directional-coupler theory and techniques, this section will be confined to strip-transmission line adaptations of the conventional type of coupler. The couplers to be described are fabricated in accordance

FREQUENCY (MC)	INPUT VSWR	RELATIVE POWER (DB)	
		P <sub>1</sub>	P <sub>2</sub>
9150	1.15	0	-36
9375	1.12	0	-39
9600	1.05	0	-32.5

Fig. 4-32 Isolation and input VSWR for an X-band hybrid ring

with one of the following two techniques. Both the main and the auxiliary, or coupling, arms may be etched on the inner faces of the two laminates which make up a single Tri-Plate line, or, in the sec-

ond method, the center-conductor of one Tri-Plate line may be the main arm, and the center-conductor of a separate line may form the auxiliary arm of the coupler. In the latter case, the two lines are stacked together and coupling is accomplished through holes or slots etched in the ground-plane which is between or common to the two lines.

The first method is preferable from the standpoint of economy and ease of fabrication, but occasions arise where the second type of fabrication is necessary. With the second type of fabrication of directional couplers, mode suppression in the region of coupling is necessary to prevent leakage.

#### Branch Line Coupler

The branch-line coupler is useful for obtaining flat coupling in the range of 3 to 10 DB and for directivity of better than 20 DB over an 8 to 10% frequency band.

<sup>2</sup>M. I. T. Radiation Laboratory Report 724, December 1945.

<sup>3</sup>Peter Sferrazza "Directional Couplers," 1954 Convention Record of the IRE, Part 8, p. 115.

<sup>4</sup>C. G. Montgomery, "Technique of Microwave Measurements," Vol. II, Radiation Laboratory Series, 1947.

Thus, it can be used as a substitute for the hybrid ring discussed in the previous section.

Figure 4-33 is a photograph of a typical Tri-Plate branch-line coupler with four Type-N coaxial fittings at the terminals. The coupling section of this unit consists of two 50-ohm lines joined by two 92-ohm branch-lines each  $\lambda/4$  in length and spaced  $\lambda/4$  apart. Coupling and directivity for this unit are shown in Fig. 4-34. Directivity is better than 20 DB over a 9% band, and

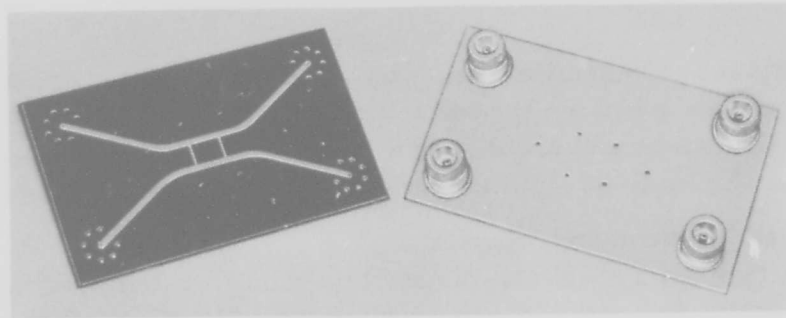


Fig. 4-33 Tri-Plate branch-line coupler

coupling is constant at 5.5 DB. The measured value of coupling is in perfect agreement with the value calculated from the equation given by Sferrazza<sup>5</sup>,

$$\text{Coupling} = 10 \log \frac{4Y^2}{4 + Y^4 + Y^6} \quad (4-6)$$

where  $Y$  is the ratio of characteristic admittance of the branch arm to that of the main arm. Deviations from the optimum quarter-wavelength spacing between branch-lines will affect directivity. Similarly, deviations in length of the branch-lines will affect coupling.

Data for the 3 DB branch-line coupler shown in Fig. 4-35 is given in Fig. 4-36. In this unit, the use of transformer sections in the main lines allows a characteristic impedance in the branch-lines which is equal to that of

<sup>5</sup>Sferrazza, loc. cit.

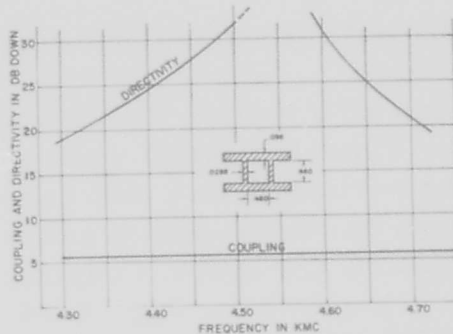


Fig. 4-34 Coupling and directivity for branch-line coupler shown in Fig. 4-33

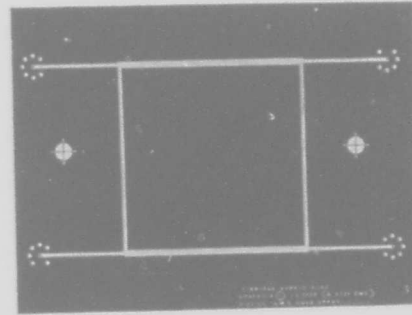


Fig. 4-35 3 DB branch-line coupler in Tri-Plate line

the input and output arms. The isolation characteristics are not as good as those of the hybrid ring. However, there is some physical space saved with this component since the loop-periphery measures only one wavelength.

#### Quarter-Wave Stub Coupler

A typical Tri-Plate directional coupler consisting of two stubs spaced  $\lambda/4$  apart, capacitively coupled to the main line, and directly coupled to the auxiliary line, is shown in Fig. 4-37. Some of the energy introduced into the main line at A is capacitively coupled to the auxiliary line by the stubs. This energy arrives at point D in phase and is, therefore, reinforced, regardless of stub spacing. In the reverse direction, the path length is twice the stub spacing (S) and the energy arrives at point C in phase-opposition, and is, therefore, cancelled. The stub lengths are kept as short as is practicable in order to obtain the best match-characteristics in the auxiliary line. The usable bandwidth of this type of coupler is insufficient for some applications and may be increased by the use of more stubs. Coupling is controlled by varying the gap spacing (E). The coupler shown has 20 DB coupling and 18 DB directivity at 4.2 Kmc for a gap spacing (E) of .015 inches.

#### Parallel-Line Couplers

The parallel-line coupler is useful over an octave of

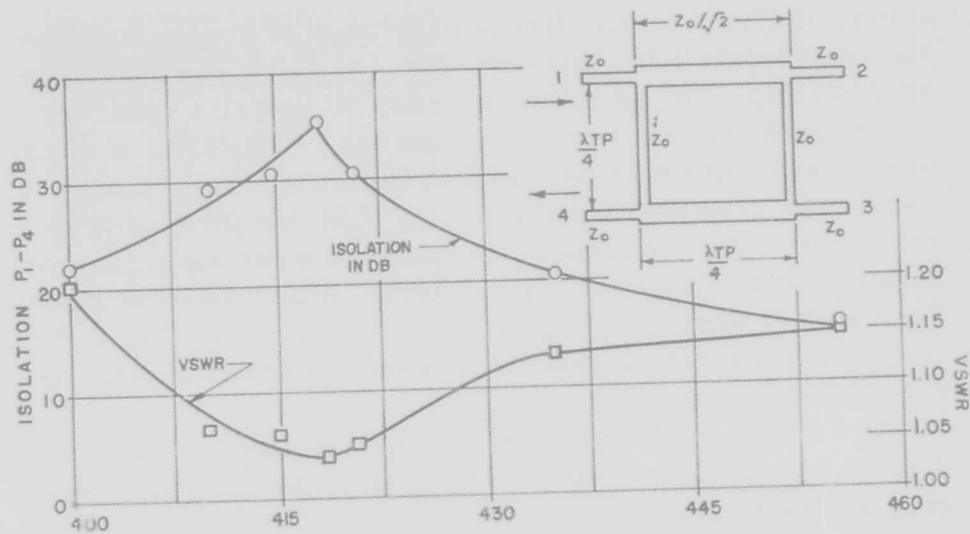


Fig. 4-36 VSWR and isolation for 3 db Branch-line coupler shown in Fig. 4-35

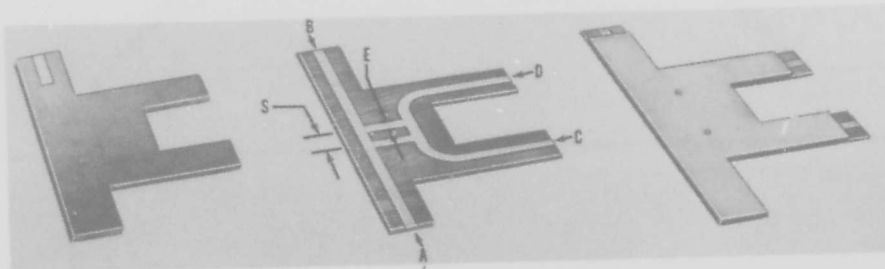


Fig. 4-37 Tri-Plate quarter-wave stub coupler

frequencies and can be designed to give coupling values in the range of 10 to 40 DB. This type of coupler consists of a straight section of line, (A-B) in Fig. 4-38, very close to which (in lateral spacing) is placed a parallel and auxiliary line (C-D). A voltage will be induced in the auxiliary line when energy travels from A to B in the main line and a portion of that energy will be delivered to the terminal at C. The reverse-coupling

action of this contra-directional type of coupler is explained in detail by Oliver<sup>6</sup>. The length of the auxiliary or coupling arm is usually made to equal a quarter-wavelength at the center frequency. Provided a good impedance match is secured at the output terminal (B) and at the coupling terminal (C), flat coupling and directivity characteristics are obtained over an octave of frequencies. Coupling, directivity, and VSWR data for the coupler shown in Fig. 4-38 are plotted in Fig. 4-39, fully demonstrating the wide-band characteristics of parallel-line couplers.

For large coupling, the effect of coupling upon the characteristic impedance of the two lines must be taken into account. A complete treatment of these effects and how to compensate coupled lines is given by Seymour Cohn<sup>7</sup>.

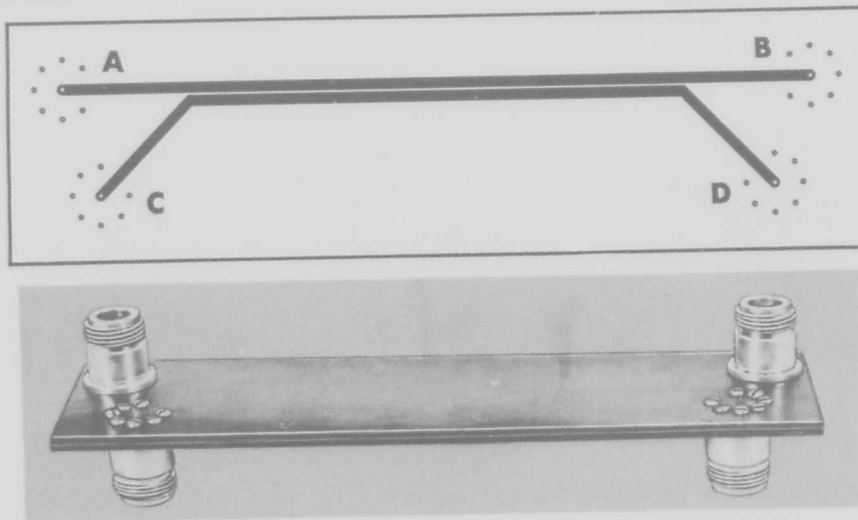


Fig. 4-38 Parallel-line directional coupler showing (a) center-strip configuration and (b) assembled coupler

#### *Long-Slot Coupler*

The long-slot directional coupler is another embodiment of the second type of coupler-fabrication previously mentioned. Two Tri-Plate transmission lines are used

<sup>6</sup>B. M. Oliver, "Directional Electromagnetic Couplers," IRE Proceedings, Vol. 42, pp. 1686-92, November 1954.

<sup>7</sup>S. B. Cohn, "Shielded Coupled-Strip Transmission Line," IRE Transactions on Microwave Theory and Techniques, Vol. MTT-3, October, 1955.

and coupling is accomplished by means of a single slot etched in the ground-plane which is common to both lines. The slot leaks energy from the main line to the auxiliary line at all points along its length. In the forward direction, these waves are in phase, and are mutually reinforced, while in the reverse direction, the waves are random in phase and cancellation takes place. Analysis shows that if the slot is an integral number of half-wavelengths long and is carefully tapered at both ends to prevent reflection, perfect directivity is attainable. Fig. 4-40 is a sketch showing the construction of a long-slot coupler in Tri-Plate line. A coupler of this type, with a slot width of  $.062\lambda$  and a slot length of  $3\lambda$  at 5 Kmc was constructed and tested at Sanders Associates, Inc. At the design frequency, both coupling and directivity measured 23 DB.

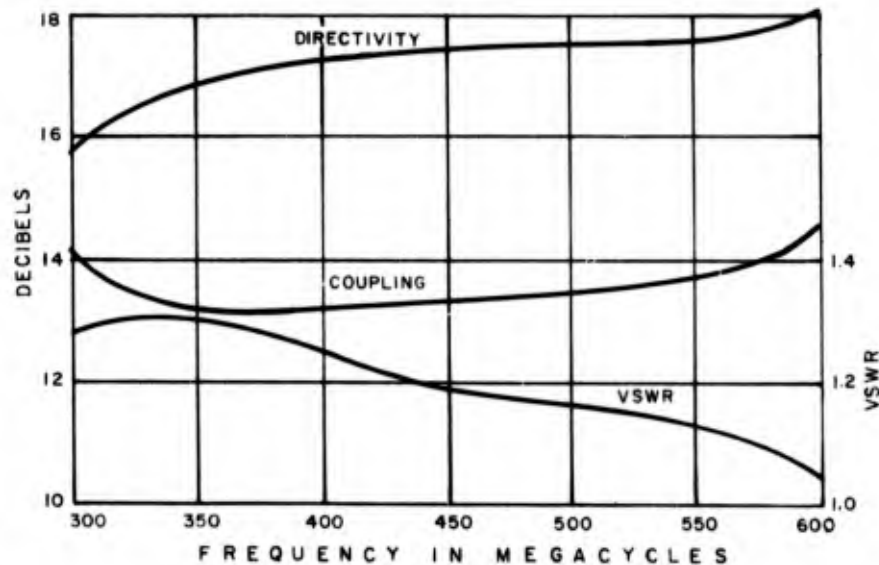


Fig. 4-39 Coupling, VSWR, and directivity for parallel-line coupler shown in Fig. 4-37



Fig. 4-40 Construction of a long-slot in Tri-Plate line

### Bethe-Hole Coupler

The Bethe-hole directional coupler shown in Fig. 4-41 consists of two Tri-Plate lines assembled, one on the other, with a single coupling-hole etched in the common ground-plane. In this coupler, both the electric and transverse magnetic field components are coupled. Magnetic coupling is twice as strong as electric coupling

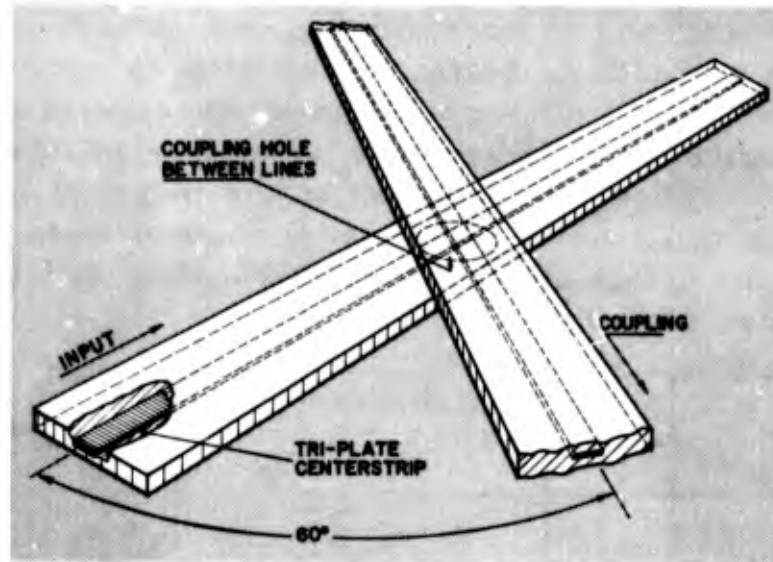


Fig. 4-41 Bethe-hole coupler fabrication in Tri-Plate line

for a circular hole, and the electric coupling is independent of the angle between the two transmission lines. Since magnetic coupling varies as the cosine of the angle between the two transmission lines, at an angle of  $60^\circ$  the two coupled fields are equal. Thus, on one side of the coupling hole, the fields cancel, while on the other side, the fields reinforce each other. A plot of coupling versus hole-size etched in the ground-plane between two 50-ohm Tri-Plate lines is shown in Fig. 4-42. Data measured for a Bethe-hole coupler with a  $3/16$ " coupling hole is shown in Fig. 4-43. The optimum angle for directivity for this coupler over the frequency band of interest was  $65^\circ$ . This characteristic is probably due to physical asymmetry in the region of the coupling hole.

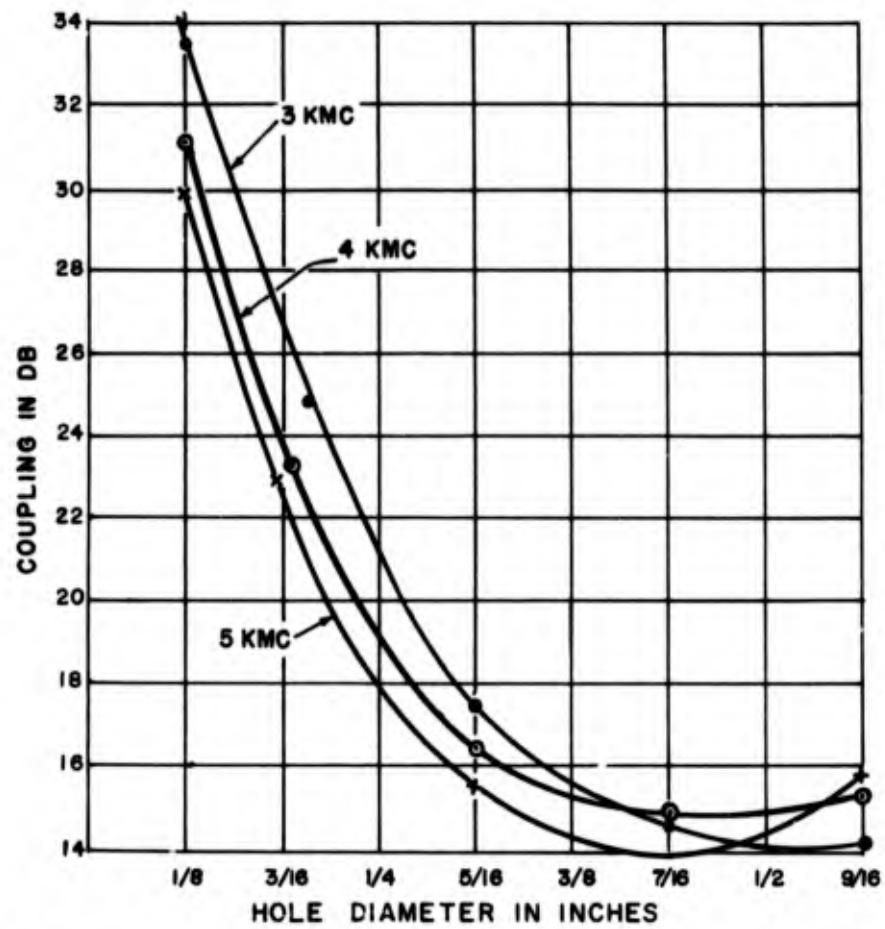


Fig. 4-42 Coupling versus size of holes etched in ground plane common to two Tri-Plate lines

FREQUENCY IN KMC	COUPLING DB	DIRECTIVITY DB
3	30.5	19.5
4	28.6	13
5	27.8	11

Fig. 4-43 Data measured for Bethe-hole coupler with a 3/8" coupling hole



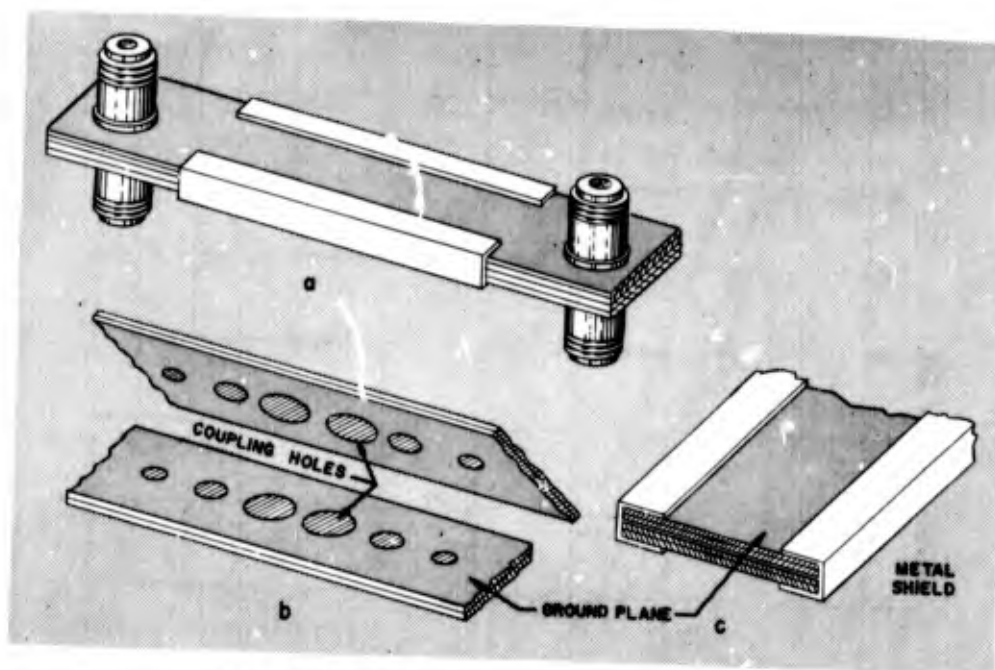
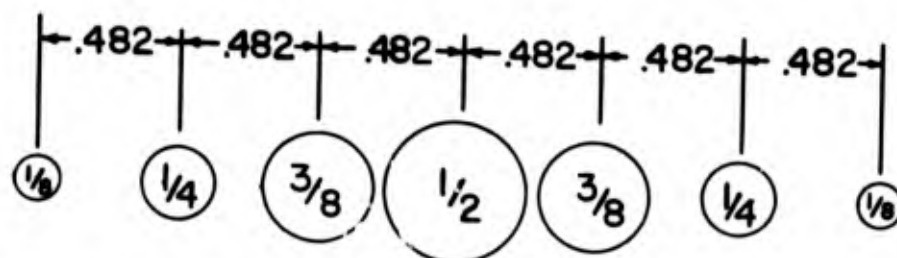


Fig. 4-44 Multihole coupler in Tri-Plate line



FREQUENCY IN KMC	COUPLING DB	DIRECTIVITY DB
3	11.7	27.8
4	9.0	27.4
5	4.7	20.0

Fig. 4-45 Frequency characteristics for multi-hole coupler shown in Fig. 4-43

### *Multihole Coupler*

The multihole coupler is another device which is fabricated from two Tri-Plate lines which are coupled together by means of holes through the common ground-plane. Multihole couplers are useful because, with more than two coupling elements, directivity characteristics can be attained that are less sensitive to changes in wavelength. An additional advantage is the increase in coupling since, with identical coupling elements, the amount of power induced in the auxiliary line is proportional to the square of the number of elements. An adaptation of "binomial" distribution to a multipath coupler fabricated in Tri-Plate line is shown in Fig. 4-44. The frequency characteristics of this coupler are tabulated in Fig. 4-45.



## CHAPTER FIVE

### FILTERS

#### 5-1 General Considerations

The techniques used in the design of Tri-Plate filters have been adapted from those conventionally used with coaxial line. In practice, it has been found that the designer is limited to a fairly simple but adequate combination of series-lines, shorted or open shunt-lines, and series-capacitors formed by small gaps or overlapping lines. Shunt elements can be realized by suitable lengths of transmission line etched at right-angles to the main line. (Short lengths of open-circuited line are capacitive while short lengths of short-circuited line are inductive). These microwave elements can be used to approximate the behavior of lumped-elements over a limited frequency-band.

#### 5-2 Behavior of simple sections of line

Before considering practical filter structures, it should be pointed out that a simple section of transmission line can be made to approximate the behavior of a lumped-inductance or capacitance. The input impedance of a lossless line of characteristic impedance  $Z_0$  and length  $l$ , when short-circuited at one end, is

$$Z = jX = jZ_0 \tan \frac{\omega l}{v} \quad (5-1)$$

where  $\omega$  and  $v$  are, respectively, the angular frequency and the velocity of propagation along the transmission line. The admittance of the line is

$$Y = 1/Z = jB = -jY_0 \cot \frac{\omega l}{v} \quad (5-2)$$

When the section of line is open-circuited, the input impedance becomes

$$Z = jX = -jZ_0 \cot \frac{\omega l}{v} \quad (5-3)$$

and correspondingly the input admittance is

$$Y = jB = jY_0 \tan \frac{\omega l}{v} \quad (5-4)$$

A plot of the reactance for a short-circuited line and susceptance for an open-circuited line is shown in Fig. 5-1. Reactance for an open-circuited line and susceptance for a short-circuited line would be shown by an identical curve displaced to the left by

$$\frac{\pi}{2} \frac{c}{l}.$$

The slope of the curve shown in Fig. 5-1 is given by the expressions

$$\frac{dX}{d\omega} = Z_0 \frac{l}{v} \sec^2 2 \frac{\omega l}{v} \quad (5-5)$$

$$\frac{dB}{d\omega} = Y_0 \frac{l}{v} \sec^2 2 \frac{\omega l}{v} \quad (5-6)$$

Since the slope in the vicinity of the origin remains relatively constant, the expression which follows, for slope at the origin ( $\omega = 0$ ), may be used.

$$\frac{dX}{d\omega} = Z_0 \frac{l}{v} \quad (5-7)$$

$$\frac{dB}{d\omega} = Y_0 \frac{l}{v} \quad (5-8)$$

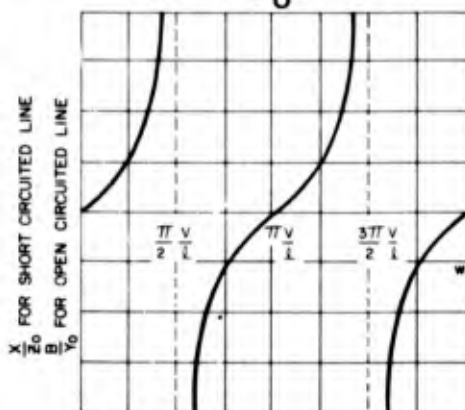
Thus, a short section, (less than  $\lambda/4$  at the frequency of interest), of short-circuited transmission line can be used to approximate an inductance. The slope given

by Eq. (5-7) must be made equal to the inductance as follows:

$$L = Z_0 \frac{l}{v} \quad (5-9)$$

Similarly, a capacitance can be designed by using a short ( $< \lambda/4$ ) section of open-circuited line, where the slope of the susceptance function shown in Eq. (5-8) is made to equal C:

$$C = Y_0 \frac{l}{v} = \frac{l}{Z_0 v} \quad (5-10)$$



5-1 Reactance for a short-circuited line and susceptance for an open-circuited line

### 5-3 Short-line filters

It is possible to obtain short-line low-pass and high-pass microwave filters from low-frequency structures by substituting microwave components for the lumped elements of the low-frequency filter. Short-line filters of this type are useful because they are comparatively small, especially at lower frequencies, and spurious responses and rejections are much higher in frequency for these filters than for the resonant-line type.

A typical low-frequency ladder-network with "constant-k" intermediate-sections and "m-derived" end-sections, which can be used as a model for a low-pass microwave filter design, is shown in Fig. 5-2 compared to the equivalent center-conductor configuration in Tri-

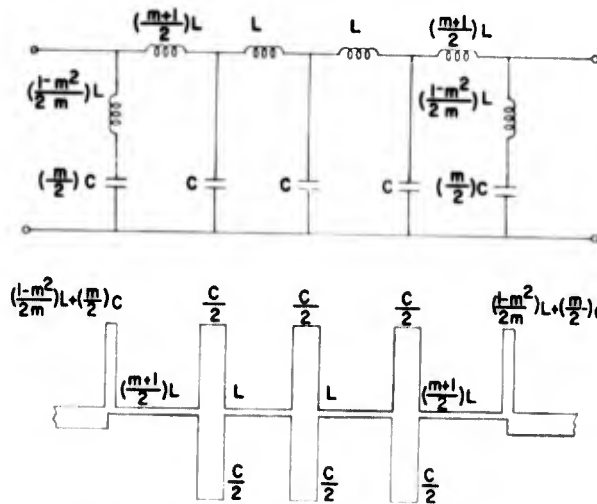


Fig. 5-2 Comparison of a typical low frequency ladder-network for a low-pass filter with the equivalent center-conductor configuration in Tri-Plate line

Plate line. The succeeding Fig. 5-3 shows a typical ladder-network from which a high-pass microwave filter can be derived, similarly compared to its equivalent in Tri-Plate line. Such a ladder-network is composed of a cascade arrangement of symmetrical T or  $\Pi$  units, embodying the principle properties of the filter. To procure a satisfactory frequency response, however, several such symmetrical units must be combined. Using the formulas presented in Section 5-2 for short (less than  $\lambda/4$ ) sections of open- or short-circuited transmission line, center-conductor configurations can be derived that will provide the same electrical characteristics as provided by the lumped units. Fig. 5-4 compares a single symmetrical lumped-constant T-section for a low-pass filter with the equivalent center-conductor configuration in Tri-Plate line.

In a short review of the "constant-k" filter, it is recalled that a "constant-k" type of reactance-network is one in which  $Z_1$  and  $Z_2$  are inverse reactance arms. That is,

$$Z_1 Z_2 = K^2$$

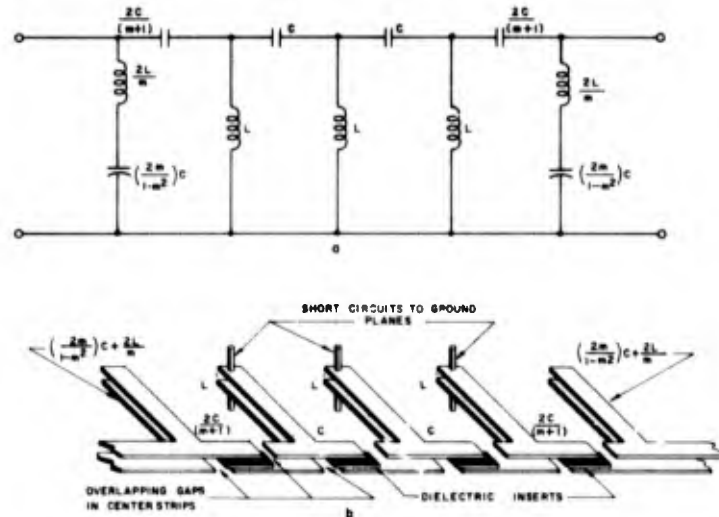


Fig. 5-3 Comparison of a typical low-frequency ladder-network for a high-pass filter with the equivalent center-conductor configuration in Tri-Plate line

The constant ( $K^2$ ) is independent of frequency and has the dimensions of a resistance squared. Therefore, replacing  $K^2$  by  $R^2$ , for a simple low-pass filter

$$Z_1 = j\omega L \quad (5-11)$$

$$\text{and } Z_2 = 1/j\omega C \quad (5-12)$$

since  $Z_1 Z_2 = R^2$ , where  $R$  may have any convenient value. The image impedance of a T-section (as shown in Fig. 5-4) is

$$\begin{aligned} Z_1 &= R \sqrt{1 - (\omega L/2R)^2} \\ &= R \sqrt{1 - (f/f_0)^2} \end{aligned} \quad (5-13)$$

where  $f$  is any frequency of interest and  $f_0$  is the frequency of cut-off. When  $f = f_0$ ,  $Z_1 = 0$ , and there is infinite attenuation, if  $L$  and  $C$  have no resistance.

The image impedance for a  $\Pi$  section is

$$Z_1' = \frac{R}{\sqrt{1 - (\omega L/2R)^2}} = \frac{R}{\sqrt{1 - (f/f_0)^2}} \quad (5-14)$$

When  $f = f_0$ ,  $Z_1'$  becomes infinite.



The filter composed of one such section, either T or  $\Pi$ , should show an attenuation, above cut-off, approaching 12 DB per octave. Attenuation is increased by approximately 6 DB for each additional section.

For the high-pass filter of the "constant-k" type:

$$Z_1 = 1/j \omega C \quad (5-15)$$

$$Z_2 = j \omega L \quad (5-16)$$

and  $Z_1 Z_2 = R^2$ , and  $L/C = R^2$ .

Image impedance for a T-element is

$$\begin{aligned} Z_1 &= R \sqrt{1 - (1/2R \omega C)^2} \\ &= R \sqrt{1 - (f_0/f)^2} \end{aligned} \quad (5-17)$$

where  $f_0 = 1/(4 \pi \sqrt{LC})$ .

The image impedance for a  $\Pi$  section is

$$\begin{aligned} Z_1' &= \frac{R}{\sqrt{1 - (1/2R \omega C)^2}} \\ &= \frac{R}{\sqrt{1 - (f_0/f)^2}} \end{aligned} \quad (5-18)$$

Since single T or  $\Pi$  sections rarely provide enough attenuation in the stop band, filters are usually composed of multiple sections. All sections in the filter are matched at each junction on an image-impedance basis.

Terminating end-sections are usually "m-derived", a modified form of the "constant-k" section. In addition to providing a much flatter terminal image impedance for the filter, "m-derived" end-sections provide an extremely sharp cut-off, with a high rejection point at a frequency a short distance (within the stop-band) from the cut-off frequency. In a multiple-section filter, the flat pass-band response, sharp cut-off characteristics, and the attenuation peak near cut-off provided by the

"m-derived" terminal half-sections are combined with the high, increasing, attenuation of the intermediate "constant-k" sections. A filter composed solely of "m-derived" sections may not have a sufficiently high insertion loss throughout the stop-band, since the attenuation constant for an "m-derived" filter-section decreases farther within the stop-band.

The "m-derived" filters involve a number of multipliers; namely, the factors  $m_1 m_2 \dots m_n$  by which the series components of a "constant-k" prototype are to be multiplied to derive a filter which has one frequency of infinite attenuation  $f_\infty$ . The series-arm of the "m-derived" filter is

$$Z_{1m} = mZ_{1K} \quad (5-19)$$

where  $Z_{1K}$  is the series-arm of the "constant-k" prototype. For the same "m-derived" section, the shunt-arm becomes.

$$Z_{2m} = \frac{1-m^2}{4m} Z_{1K} + \frac{Z_{2K}}{m} \quad (5-20)$$

where  $Z_{2m}$  denotes the shunt-arm of the "m-derived" filter, and  $Z_{2K}$  the shunt-arm of the prototype "k" section.

The actual value of (m) is obtained on the basis of the frequency at which the "m-derived" filter is expected to attenuate most sharply. The relation between (m), cut-off frequency ( $f_0$ ), and the frequency of peak attenuation, ( $f_\infty$ ) is obtained by setting Eq. (5-20) equal to zero ( $Z_{2m} = 0$ ) with the result

$$m = \sqrt{1 - \left(\frac{f_0}{f_\infty}\right)^2} \quad \text{for low pass filters, and}$$

$$m = \sqrt{1 - \left(\frac{f_\infty}{f_0}\right)^2} \quad \text{for high pass filters.} \quad (5-21)$$

Terminal "m-derived" half-sections should be designed with a value of (m) equal to 0.6 to provide constant image-impedance characteristics in the pass-band. Image-impedance is held within 4% over most of the

band. For optimum results, the end-sections should be designed to present attenuation peaks that are staggered with relation to each other.

#### 5-4 Practical Design procedure for low-pass filters

Before outlining, in practical form, a procedure to be applied to the design of short-line filters, both low- and high-pass, it must be pointed out that there is at least one other useful approach to this problem. In Chapter 27, Vol. II, of Very High Frequency Techniques, <sup>1</sup> Seymour Cohn describes a design-procedure for the varying-impedance low-pass filter. However, this method is not applicable to the high-pass filter.

The following procedure, somewhat similar to that outlined by Lt. James E. Butler in his U. S. Naval Post-graduate School thesis "Design of Strip Transmission Line Systems and Antennas", will be presented as the solution of a practical design problem. The result of the following outline will be a design for a low-pass filter which will cut-off at 1300 MC and will reject all frequencies through 3fc. A 50 DB rejection in the stop-band is required and the input and output terminals must be matched to a 50-ohm line.

A 50-ohm Tri-Plate line composed of two 1/16-inch sheets of teflon-fiberglass, clad with 1-oz. copper, will have the following parameter values: (see Fig. 1-4).

$$b = 1/8''$$

$$t/b = \frac{.0027''}{.125''} = .022''$$

$$\sqrt{\epsilon} = 1.58$$

$$w = .088''$$

1. Design a prototype intermediate-section as shown in Fig. 5-4.

a. The inductive component of the equivalent low-frequency prototype is here represented by a short section of Tri-Plate line terminated by transverse elements. The value of L (series inductance) is dependent on  $Z_1$

<sup>1</sup>Splitting the shunt capacitance reactance into two equal stubs on either side of the line shortens the necessary physical length of the stubs and therefore places spurious responses farther away from cut-off into the stop-band.

and increases with decreasing line width. ( $Z$  should be as high as practicable in order to keep the length of the line to a minimum.) A line-width of .010 inches is a

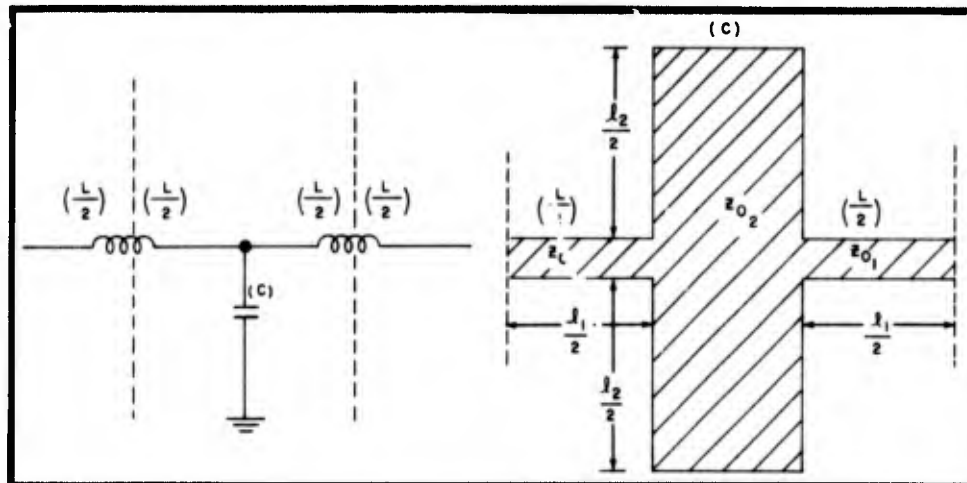


Fig. 5-4 Comparison of a symmetrical lumped-constant T-section for a low-pass filter with the equivalent center-conductor configuration in Tri-Plate line

good compromise for etching accuracy and alignment between image circuits. A Tri-Plate transmission line having a line-width of .010 inches, a ground-plane spacing of 1/8-inch, and a dielectric medium of teflon-impregnated-fiberglass, would have a characteristic impedance of 116 ohms.

The series inductance of a low-pass prototype is given by the expression

$$L = \frac{R}{\pi f_0} \quad (5-22)$$

and the reactance by

$$X_L = 2\pi f_0 L = 2R \quad (5-23)$$

Equating (5-23) in (5-1) and solving for " $l_1$ ":

$$l_1 = \frac{v}{\omega} \arctan \frac{2R}{Z_1} \quad (5-24)$$

$$= \frac{3 \times 10^{10}/1.58}{2\pi \times 1.3 \times 10^9} \arctan \frac{100}{116}$$

$$= 1.654 \text{ cm.} = .651''$$

b. The capacitive components of the equivalent low-frequency prototype are represented in Tri-Plate line by transverse sections of line (refer to Fig. 5-4). An open-circuited stub-length must be selected that will present an adequate susceptance to all frequencies within the required stop-band. The length

$$\frac{l_2}{2}$$

is a quarter-wavelength long at the mean-frequency between the upper limit of the stop-band and the frequency of cut-off:

$$\frac{l_2}{2} = \frac{\lambda_m}{4} \quad (5-25)$$

where  $\lambda_m$  is the line wavelength at the mean frequency, ( $f_m$ ). Since

$$f_m = \sqrt{f_0 f_2} \quad (5-26)$$

$$\frac{l_2}{2} = \frac{v}{4\sqrt{f_0 f_2}} \quad (5-27)$$

$$= \frac{3 \times 10^{10}/1.58}{4\sqrt{1.3 \times 10^9 \times 6.5 \times 10^9}}$$

$$= 1.63 \text{ cm} = .641''$$

The shunt capacity of a low-pass filter is given by the expression

$$C = \frac{1}{\prod f_0 R} \quad (5-28)$$

and the reactance,

$$X_c = \frac{1}{2\pi f_o C} = \frac{R}{2} \quad (5-29)$$

Equating (5-29) to (5-3) and solving for  $Z_{o2}$ , impedance for each half of the shunt capacitive reactance is found\*:

$$\begin{aligned} Z_{o2} &= R \tan \frac{\omega \lambda_2}{v} & (5-30) \\ &= 50 \tan \frac{2\pi \times 1.3 \times 10^9 \times 1.63}{3 \times 10^{10} / 1.58} = 42 \Omega \end{aligned}$$

2. Design an "m-derived" half-section similar to that shown in Figure 5-2:

a. The value of .6 will be used for "m", since that value presents the flattest image impedance over the pass band. The series inductance for the "m-derived" half-section is added to the adjacent series inductance which forms part of the neighboring constant-k section. The length of high impedance line used here must equal the combined inductance ( $\frac{m+1}{2}$ ) L. The line length is found as follows:

$$\begin{aligned} l_{m1} &= \frac{v}{\omega} \arctan \left( \frac{m+1}{Z_{o1}} \right) R & (5-31) \\ &= \frac{3 \times 10^{10} / 1.58}{2\pi \times 1.3 \times 10^9} \arctan \frac{30}{116} \\ &= .587 \text{ cm.} = .231" \end{aligned}$$

b. The length of the shunt portion of the "m-derived" end-section ( $l_{m2}$ ) is made a quarter-wavelength at the peak frequency,  $f_\infty$ , where

$$f_\infty = \frac{f_o}{\sqrt{1-m^2}} = \frac{1625 \text{ megacycles per second}}{\text{second}} \quad (5-32)$$

$$l_{m2} = \lambda_{TP} / 4 = 2.92 \text{ cm.} = 1.15" \quad (5-33)$$

where  $\lambda_{TP}$  equals wavelength in Tri-Plate transmission line.

The characteristic impedance of the stub is calculated from equation (5-20).

$$X_{m2} = \frac{1-m^2}{2m} X_L + \frac{2X_c}{m} \quad (5-34)$$

and since  $X_L = 2R$  and  $X_c = \frac{R}{2}$ ,

$$\begin{aligned} jX_{m2} &= j \left( \frac{1-m^2}{m} \right) R - j \frac{R}{m} \\ &= -jmR \end{aligned} \quad (5-35)$$

Therefore, from equation (5-3)

$$\begin{aligned} Z_{m2} &= m R \tan \frac{\omega \lambda_{m2}}{v} \\ &= 30 \tan \frac{2\pi \times 1.3 \times 10^9 \times 2.92 \times 1.58}{3 \times 10^{10}} \\ &= 92 \text{ ohms.} \end{aligned} \quad (5-36)$$

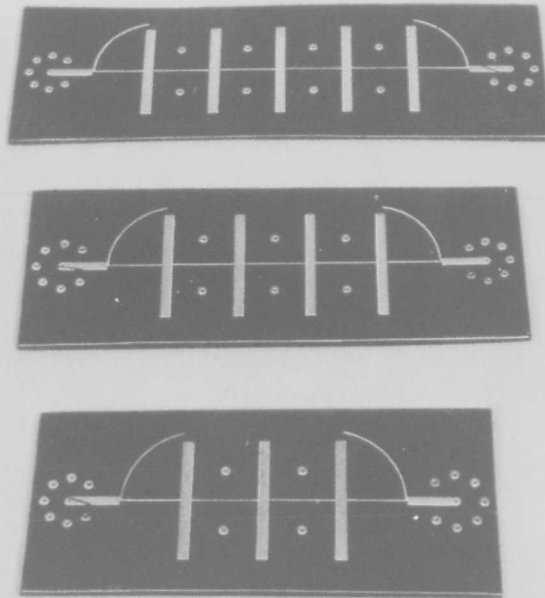


Fig. 5-5 Centerstrip configurations of three low-pass filters designed to cut-off at 1.3 KMC

Low-pass filters (with  $m$ -derived end-sections and with three, four, and five constant- $k$  intermediate sections), which were designed (in accordance with the outlined procedure) to cut off at 1.3 KMC, were fabricated at Sanders Associates, Inc. in 50-ohm Tri-Plate line. The centerstrip configurations are shown in Fig. 5-5, while Fig. 5-6 shows an external view of one of these filters. Attenuation versus frequency is plotted for all three filters in Fig. 5-7. The first spurious response for all three filters occurs at approximately 3.7

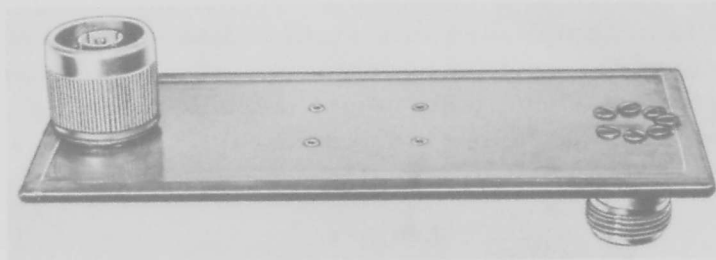


Fig. 5-6 Tri-Plate low-pass filter with cut-off frequency at 1.3 KMC

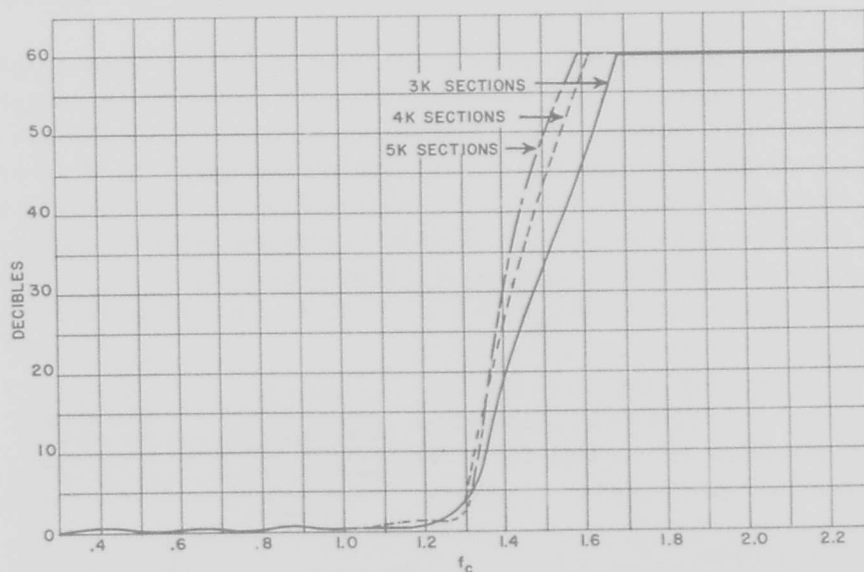


Fig. 5-7 Attenuation vs. frequency for three low-pass filters fabricated in Tri-Plate line with three, four, and five intermediate sections



times cut-off, at a point where the spacing between stubs is approaching one-half wavelength. The next spurious response occurs where the stubs themselves are one-half wavelength long. This response occurred at about 4.5 times cut-off frequency. (These spurious responses can be eliminated by cascading this filter with another having a higher cut-off frequency and no coincident spurious responses.)

### 5-5 High-pass filters

The design of a constant-k section for a high-pass filter is accomplished in a similar manner, although in this case, the section is composed of a series capacitance and a shunt inductance, as shown in Fig. 5-3. These capacitance and inductance values are calculated from the following expressions:

$$L = \frac{R}{4\pi f_0} \quad \text{henries} \quad (5-37)$$

$$C = \frac{1}{4\pi f_0 R} \quad \text{farads} \quad (5-38)$$

The shunt-inductance of the low frequency prototype is represented here by a short length of short-circuited stub. The series-capacitance can be most easily fabricated in the line by cutting alternate gaps in the two (facing) center-conductors of the line, and inserting a thin low-loss dielectric strip between the center-conductors where they overlap. A cross-sectional view of this configuration is shown in Fig. 5-8. A sheet of thin, low-loss dielectric, such as teflon is used for the insert. The capacity of this device is then computed from the formula for parallel-plate capacity:

$$C = .0885 \frac{A}{d} \epsilon r$$

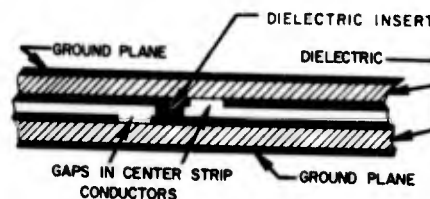


Fig. 5-8 Cross-sectional view of a series-capacitance fabricated in Tri-Plate line

where (A) is the plate area and (d) the thickness of the insert (separation between centerstrips) in centimeters. This expression neglects fringing capacitances, but in most practical designs these can be ignored.

The m-derived end-sections have the same relationship to the intermediate-sections in high-pass as in low-pass filters, and perform identical functions.

#### 5-6 Resonant-line filters

A band-pass filter is easily obtained in Tri-Plate transmission line by separating two identical series capacities by approximately a half-wavelength. A series capacity can be obtained by one of several methods depending upon the magnitude of the desired capacity. Smaller capacities are obtained by interrupting the center-conductor with a small gap. (Expressions for the reactance of a series gap are given in Section 2-4). When slightly higher capacitive values are desired, they can be obtained by reshaping the two adjacent terminals of the gap so that they dovetail. To obtain relatively large series capacities, a center-conductor overlap is needed in which the two overlapping center-conductors are separated by a thin sheet of dielectric material. These two methods of increasing series capacity are shown in Fig. 2-15.

The behavior of a single-element resonant-line filter in Tri-Plate line may best be understood by referring to the impedance chart shown in Fig. 5-9. Let us interrupt the center-conductor (of a match-terminated, lossless line) with a gap, the normalized reactance (X) of which is  $-j3.0$  at the frequency of interest. At the point of discontinuity, the impedance (Z) will equal  $1-j3$ , which is located at "a" on the chart. Moving along the transmission line toward the generator, the apparent impedance values will trace the path of constant standing wave ratio on the chart which is shown by the arc "abc". At the point c on the arc, which represents a point along the transmission line about  $.46\lambda$  away from the original

gap, the impedance of the gap plus that of the line appears as  $1 + j3$ . (This is the conjugate of the impedance at "a"). An identical gap may be inserted here to effect a cancellation of the reactance. On the chart we are then shifted back to the matched point at 0 at the center of the chart.

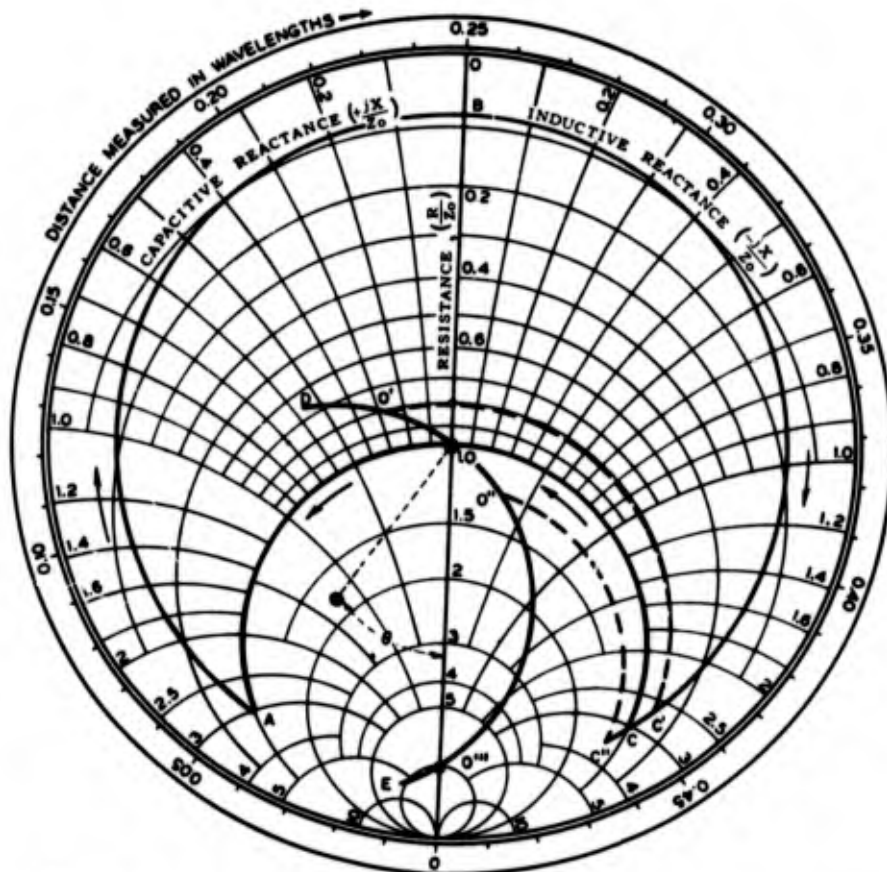


Fig. 5-9 Impedance chart showing behavior of a single-element resonant line filter fabricated in Tri-Plate line

Impedance values will vary with changes in frequency. The locus of this variation in impedance with frequency is described by the arc of circle, "de", the radius of which, in terms of VSWR, equals

$$\frac{(4 - 2 \tilde{X}^2) + (\tilde{X} \sqrt{4 + \tilde{X}^2})}{(4 + 2 \tilde{X}^2) - (\tilde{X} \sqrt{4 + \tilde{X}^2})} \quad (5-39)$$

and the center of which lies on a straight line which passes through "0" and makes an angle with the real axis of

$$\theta = \tan^{-1} \left( \frac{-2}{\tilde{X}} \right) \quad (5-40)$$

A small decrease in frequency would have the effect of moving point C to C' on the chart, causing the filter to appear shorter electrically. The impedance, referred to the point of the first discontinuity, now plots at O'. at the point of intersection between the arc "dc" and a circle of constant resistance passing through C'. Similarly, an increase in frequency will move C to C'', increasing the electrical length of the filter and changing the impedance to O''. The insertion loss characteristics of a single filter section may be determined from this construction.

The design procedure for bandpass filters is given in several sources<sup>1, 2, 3</sup>. Probably the simplest design procedure is that for the Butterworth type of filter given by Southworth. For a filter of one or more direct-coupled cavities, the expression for the normalized reactance of the end gaps is

$$\tilde{X}_{1, n+1} \cong \sqrt{\frac{4}{\pi}} Q_L \sin \frac{\pi}{n} \quad (5-41)$$

and the reactance for all intermediate gaps is given by

$$\tilde{X}_m \cong \frac{2 \sqrt{2}}{\pi} Q_L \sqrt{\cos \frac{\pi}{n} - \cos \sqrt{\frac{2(m-1)\pi}{n}}} \quad (5-42)$$

where

$Q_L$  = loaded Q (defined as the center frequency divided by the 3 DB bandwidth,

$n$  = number of sections, and

$m$  = the serial number of the gap.

The length of line between gaps is computed from the general expression

$$l_{m, m+1} = \frac{\lambda_{TP}}{2} + \frac{\lambda_{TP}}{4\pi} \tan^{-1} \left[ \frac{2}{\tilde{X}_m} + \tan^{-1} \frac{2}{\tilde{X}_{m+1}} \right] \quad (5-43)$$

where  $\lambda_{TP}$  is the center frequency wavelength in the transmission line. These equations assume a lossless structure and their accuracy will decrease with increased losses.

The unloaded  $Q$  of a TEM transmission line is related to the attenuation in the line by

$$Q_u = \frac{\beta}{2\alpha} \quad (5-44)$$

where

$\beta$  = the phase constant, and  
 $\alpha$  = the attenuation in nepers.

Expressing  $\alpha$  in DB per unit length,  $Q_u$  becomes

$$Q_u = \frac{27.3}{\alpha \lambda_{TP}} \quad (5-45)$$

The loaded and unloaded  $Q$ 's of a resonant circuit are related by

$$\frac{Q_L}{Q_u} = 1 - \sqrt{T} \quad (5-46)$$

where  $T$  is the power transmission coefficient, defined as the ratio of power output of the filter to that available at the power input.

Fig. 5-10, (a plot of equation (5-46)), shows how insertion loss at resonance increases with an increase in the ratio of loaded to unloaded  $Q$ . A typical 50-ohm Tri-Plate line constructed of 1/16" sheets of teflon fiberglass, (GB112T), has an unloaded  $Q$  of about 300 at 3 KMC. Thus, a resonant filter with  $Q = 100$  should have an insertion loss of 3.25 DB at resonance. Transmission

losses of this magnitude have an additional effect on the filter performance. When a loss occurs between two such reactances, the reactance of the second discontinuity no longer cancels that of the first one. An appreciable VSWR will be measured at the resonant frequency and thus an additional loss will be produced due to reflection. To prevent reflection (VSWR = 1) in a lossy filter would require unequal capacitances for the series gaps. Such a device would be non-reciprocal.

These factors must be taken into account when designing bandpass filters in Tri-Plate line.

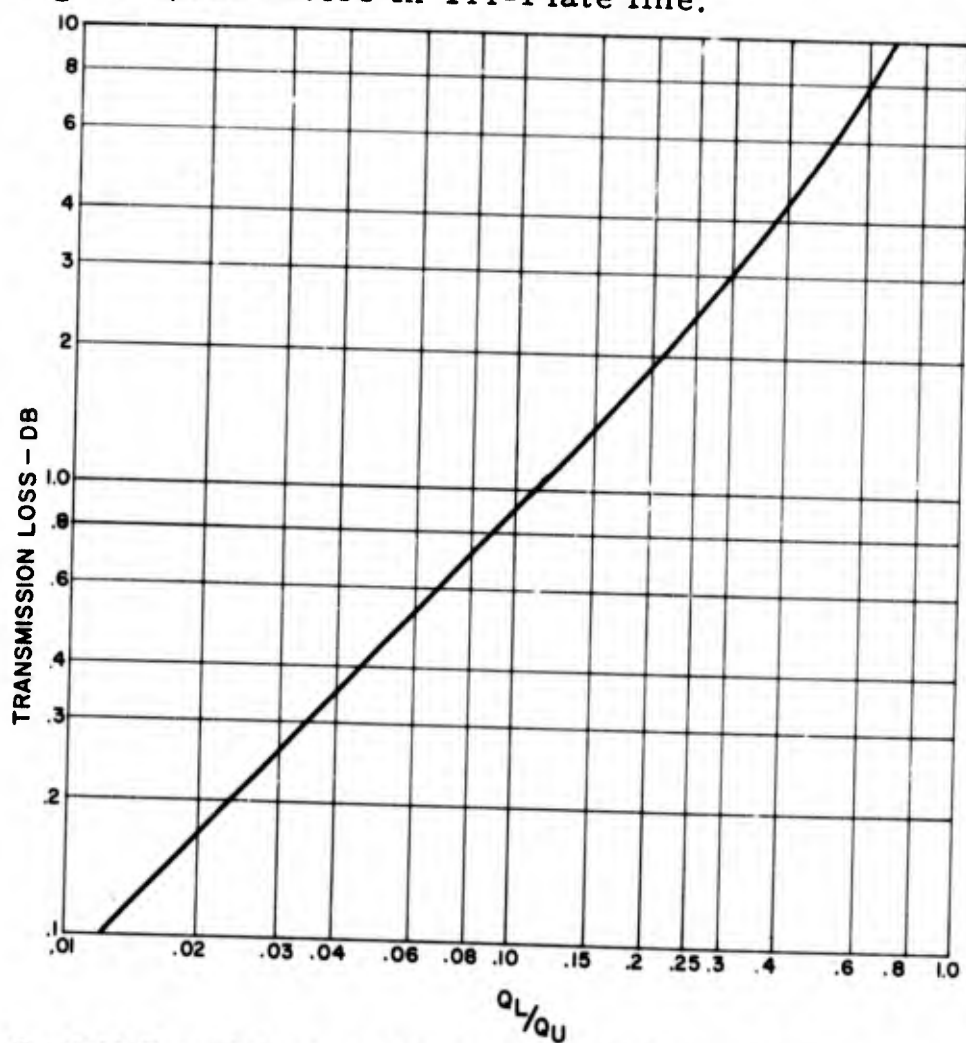


Fig. 5-10 Transmission loss at resonance for TEM transmission line filters

A discussion of typical dielectrics and their properties is given in Chapter VII. Reference to the unloaded  $Q$  curves for various dielectrics, in Fig. 7-7, will aid in the determination of the choice of dielectric. The curves will also give an estimate of the line losses to be expected. Inspection of these curves ( Fig. 7-7) and those in Fig. 5-10 show that the use of a dielectric-filled line of this type is generally restricted to filters requiring low to moderate values of unloaded  $Q$ .

## CHAPTER VI

### ANTENNAS

#### 6-1 General Considerations

Slot radiators photo-etched on Tri-Plate transmission line are particularly useful for flush-mounted arrays in aircraft. Even where standard types of radiators are desirable, Tri-Plate power dividers will usually be advantageous because of ease of design and fabrication.

Various possible radiating devices for Tri-Plate transmission line are suggested in Figs. 6-1 and 6-2.

#### 6-2 Single Resonant Slots

For a narrow resonant half-wave slot radiating on both sides of its ground-plane, the resonant resistance  $Z_S$  is given by:

$$Z_D Z_S = \frac{(120\pi)^2}{4} \quad (6-1)$$

where  $Z_D$  is the resonant impedance of the equivalent dipole and  $120\pi$  is the impedance of free space. The variation of resistance and reactance of a slot antenna as a function of  $\lambda$  will be the same as that of the conductance and susceptance of a dipole antenna. For a half-wave slot, the input resistance has a maximum near the resonant point. The effect of widening the slot will be to reduce the rate of change of reactance just as for a dipole. The "Q" of equivalent slots and dipoles will, in fact, be equal.

In many applications, it is undesirable to have the slot radiate on both sides of the ground-plane, and it is

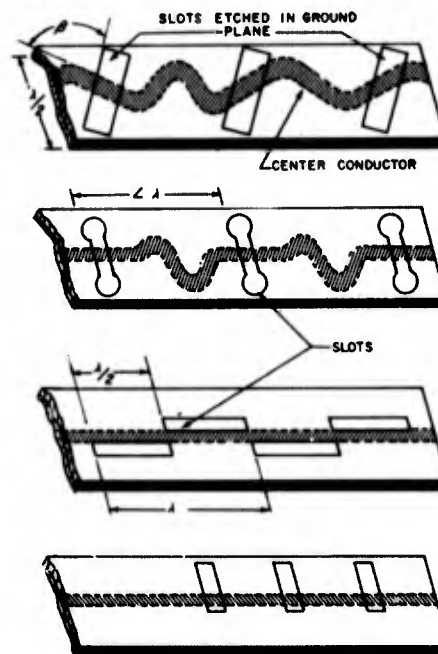
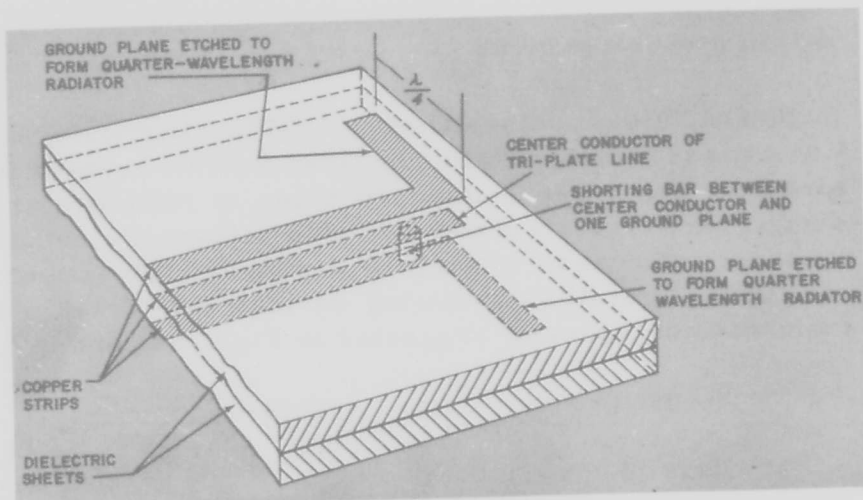
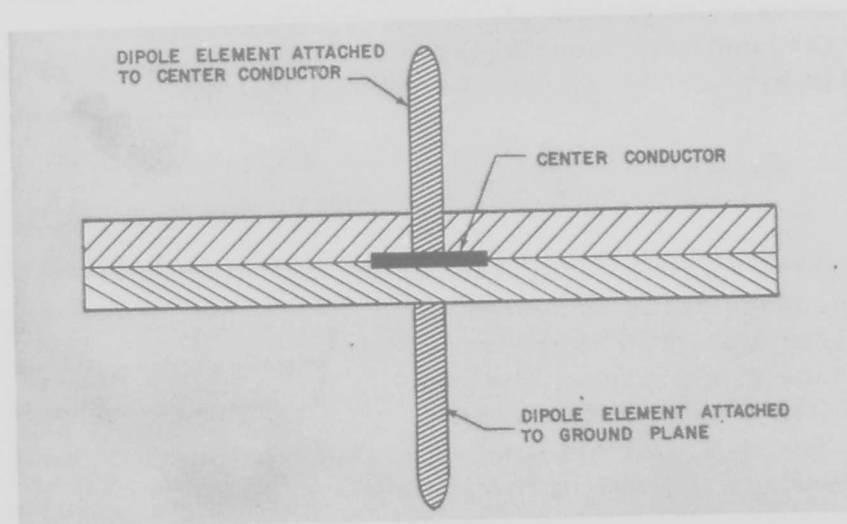


Fig. 6-1 Various radiating devices for Tri-Plate transmission line. (Patent applied for.)





a



b

Fig. 6-2 Two possible dipole radiating devices for Tri-Plate transmission line (Patent applied for.)

common to add a cavity on one side of the ground-plane. If the depth of this cavity is adjusted to present an infinite impedance across the slot, it is obvious that the slot-impedance will be doubled. If the cavity depth is

less than approximately  $\lambda/4$  deep, zero conductance will still be shunted across the slot and the resonant resistance will still be doubled, but the reactive component of slot impedance will be modified, resulting in a change in resonant frequency and an increase in  $Q$ . The shunting reactance of the cavity can be calculated from the equation:

$$Z = jR_c \tan \beta S \quad (6-2)$$

where  $R_c$  is the characteristic resistance of the cavity transmission line, and  $\beta S$  is the electrical length of the cavity.

Tri-Plate antennas may consist of resonant slots etched in one or both of the ground-planes. When slots are etched opposite to each other on the two ground-planes, the symmetry of the TEM mode in the line is not disturbed and the measured impedance of the antenna will be approximately equal to the result given by Eq. (6-1). If the slot is etched in one ground-plane only, the mode symmetry will be disturbed and some of the energy not radiated by the slot will be retransmitted along the line in either direction in the parallel-plane TEM or TE modes. Unless effective conducting walls, consisting of either continuous metal walls or mode-suppressing screws, are provided, this energy will be radiated from the edges of the line. However, discontinuities presented to the new slot-generated modes will modify the measured slot-impedance.

Figs. 6-3, 6-4, 6-5, and 6-6 show slot resistance and reactance as a function of frequency and mode-screw placement for a 7 1/2-inch L-band slot. Fig. 6-7 shows a typical L-band single-slot antenna fabricated in 1/4-inch Tri-Plate line. The slot is  $\lambda/2$  long and  $.02\lambda$  in width, at the center frequency of 900 MC. In addition, the slot is offset from the center-conductor by  $.2\lambda$  to obtain the best impedance-match to a 50-ohm line. An

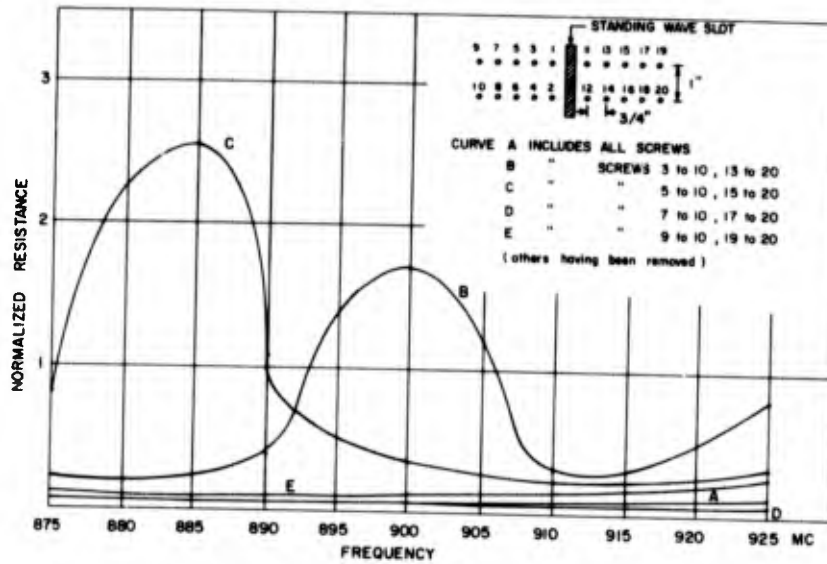


Fig. 6-3 Slot resistance as a function of frequency and mode screw placement for a 7 1/2-inch L-band standing-wave slot.

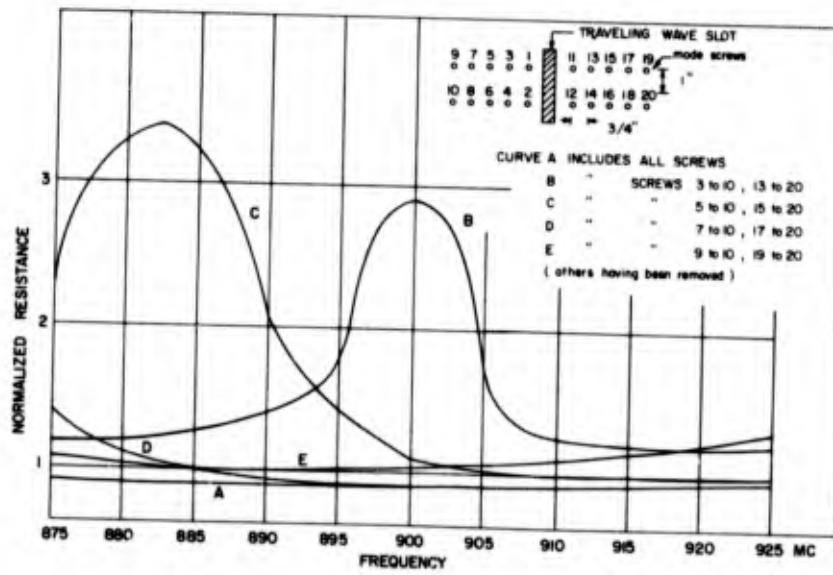


Fig. 6-4 Slot resistance as a function of frequency and mode screw placement for a 7 1/2-inch L-band traveling-wave slot.

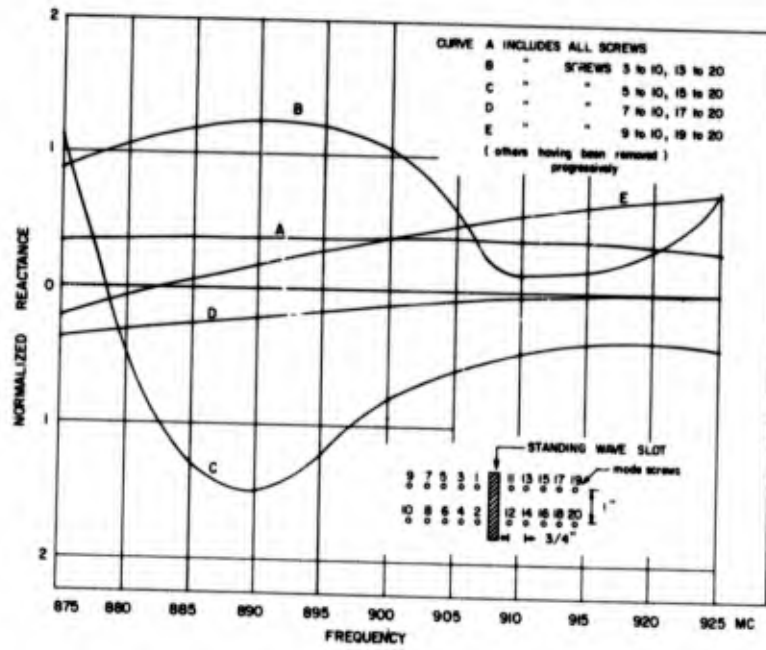


Fig. 6-5 Slot reactance as a function of frequency and mode screw placement for a 7 1/2-inch L-band standing-wave slot.

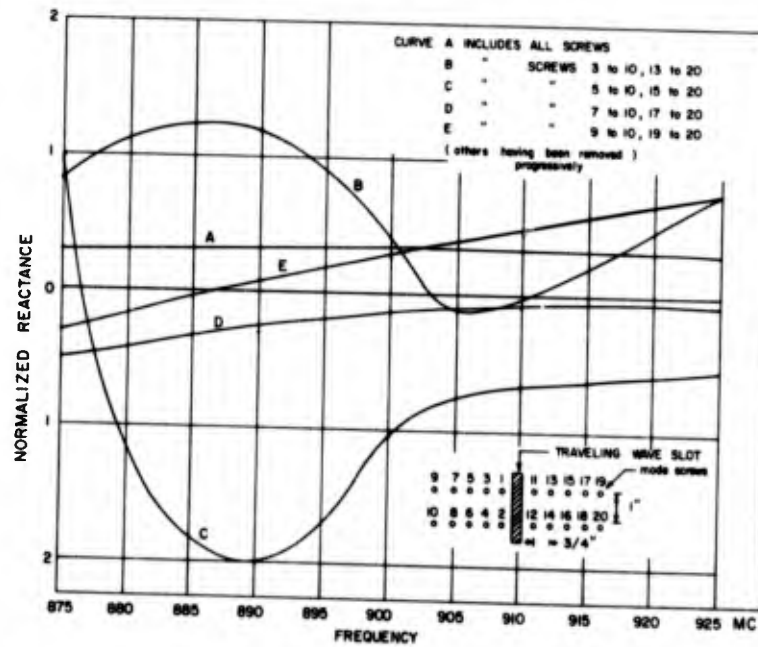


Fig. 6-6 Slot reactance as a function of frequency and mode screw placement for a 7 1/2-inch L-band traveling-wave slot.

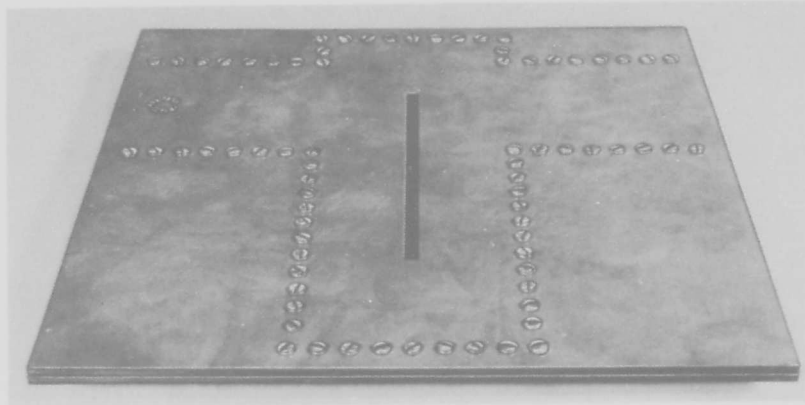


Fig. 6-7 A typical L-band slot, series fed from 50-ohm Tri-Plate line.

impedance slot for this antenna is shown in Fig. 6-8. With the aid of the sketch of this same single-slot antenna in Fig. 6-9, the following conclusions have been made in regards to mode-screw placement. Distance "a" should be not more than one-half inch. (With a spacing of less than one-half inch, no advantage is gained.) Distance "b" decreases bandwidth if made small, but increases waveguide mode-propagation if made large. Resonant length is inversely proportional, while bandwidth is directly proportional, to distance "c". The prototype of this L-band single-slot antenna showed a VSWR of no more than 1.75 over a 2.2% band.

With continuous mode-suppressing walls, the radiation conductance of a slot may be calculated<sup>1</sup>. However, for a slot design which is usable in two-dimensional arrays, continuous mode-suppressing walls are sufficiently difficult to achieve as to nullify many of the advantages of Tri-Plate line for antennas. Hence, mode suppression in all antenna-slots fabricated in Tri-Plate line to date has been achieved by the use of shorting pins. All parameters, including the number, size, and location of the shorting pins, have been adjusted empirically. Eyelets, rivets, or screws have been used for this purpose.

<sup>1</sup>Arthur A. Oliver, "The Radiation Conductance of a Series Slot in Strip Transmission Line". 1954, IRE Convention Record, Part 8.

Fig. 6-10 shows this technique of mode suppression applied to a series-slot developed at X-band. Fig. 6-11 is a plot of the volt standing wave ratio versus frequency for this slot, which was centered at 9375 megacycles. The figure illustrates the increased bandwidth obtainable at higher frequencies for typical ground-plane spacings.

### 6-3 Slot Arrays

A natural consequence of the development of the X-band series-slot antenna-element was its application to a 16-element, 4x4, E- and H-plane broadside array.

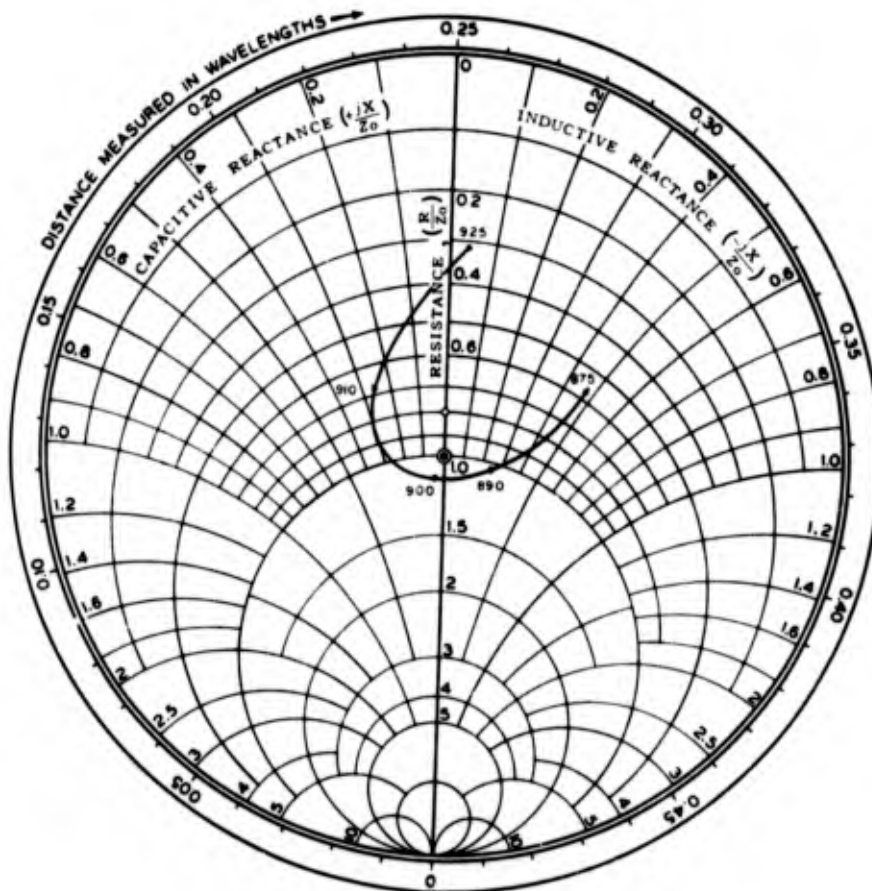


Fig. 6-8 Impedance plot for the L-band slot shown in Fig. 6-7.

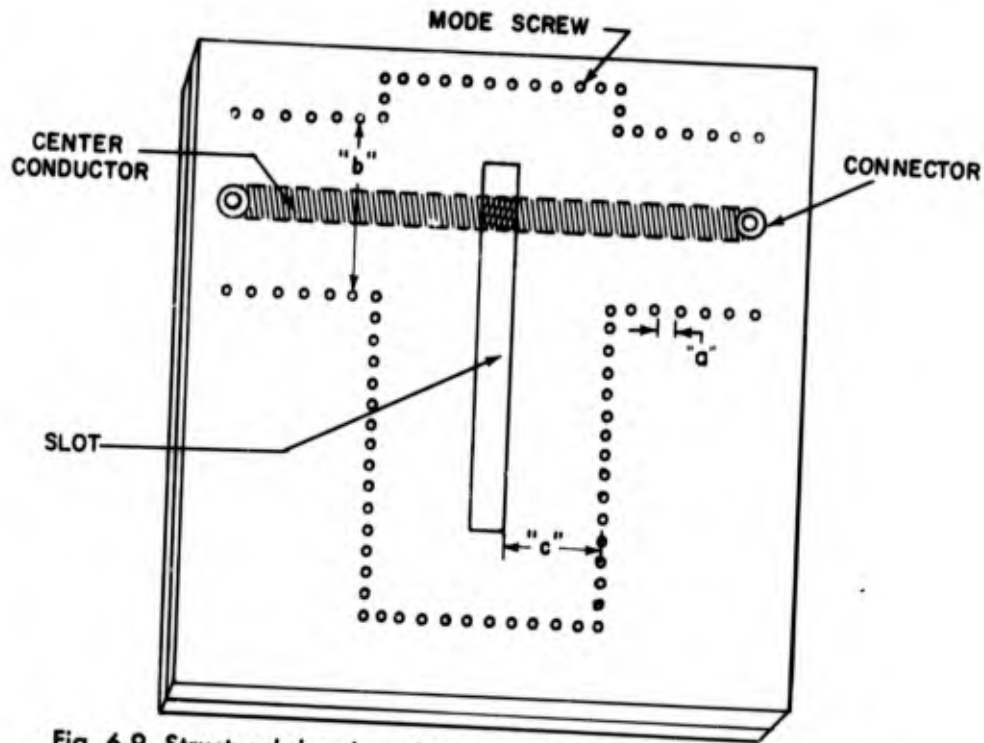


Fig. 6-9 Structural drawing of L-band series slot shown in Fig. 6-7.

It was felt that such an array would have sufficient directivity and gain to demonstrate its capabilities as a compact flush-mounted antenna for aircraft.

For elements fed, in phase, and with uniform amplitude distribution, maximum broadside gain requires that the center-to-center spacing of adjacent elements be a half-wavelength in air. To achieve this, in a practical manner, requires a dielectric constant of 4 for the feed-line material. Since, at the design frequency of 9375 MC, teflon-fiberglass (GB112T) has a dielectric constant of  $\approx 2.5$ , it was necessary to compromise in this respect.

The progressive 4-way power divider, described in Section 4-5, was especially designed to feed, in phase, (using a minimum area) the elements of a 4-slot H-plane array.

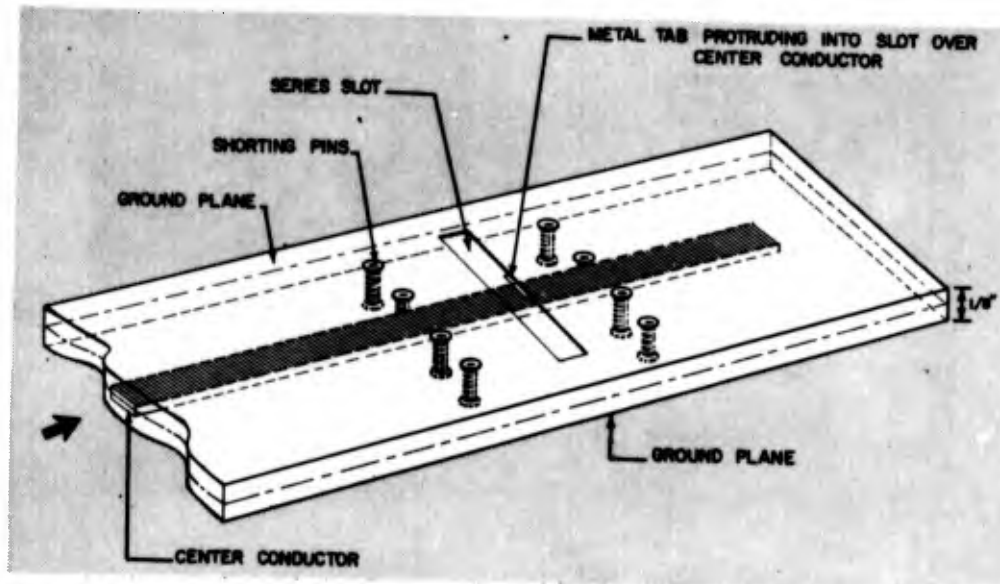


Fig. 6-10 X-band series slot

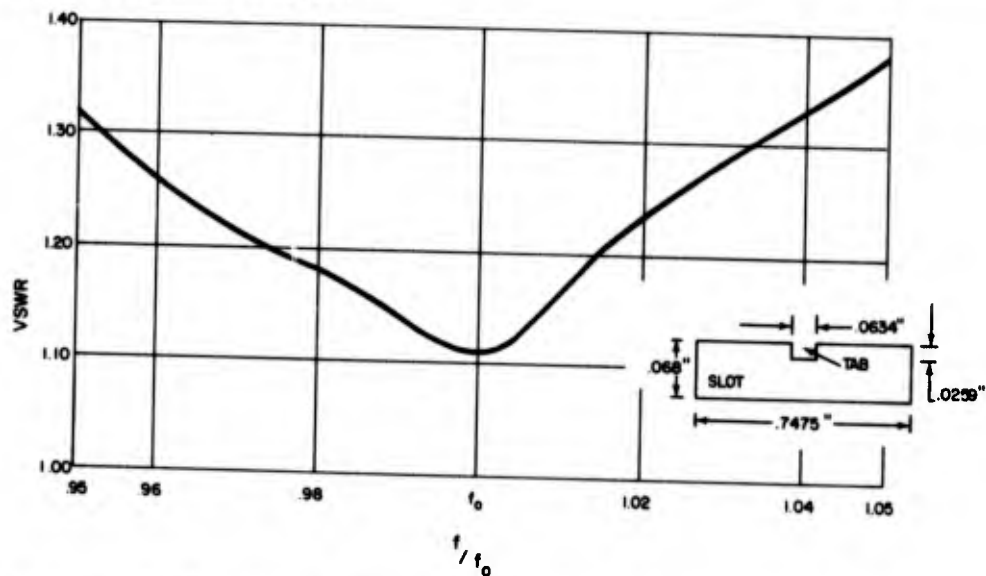


Fig. 6-11 VSWR versus frequency for the X-band series slot shown in Fig. 6-10

The 4x4 array was to employ four such four-slot H-plane arrays stacked one under another. The center-to-center spacing of the slots in the E-plane was determined solely by the space required for the progressive 4-way power divider. The result was a center-to-center spacing of 0.750", or about 0.6 of the wavelength in air.



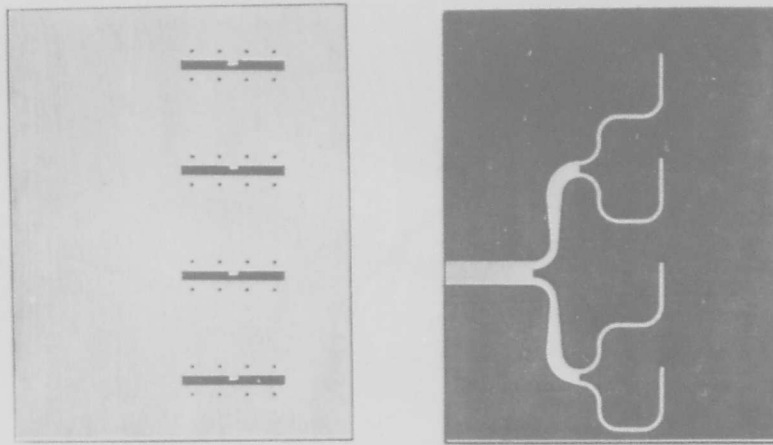


Fig. 6-12 4-slot E-plane array and its associated power divider

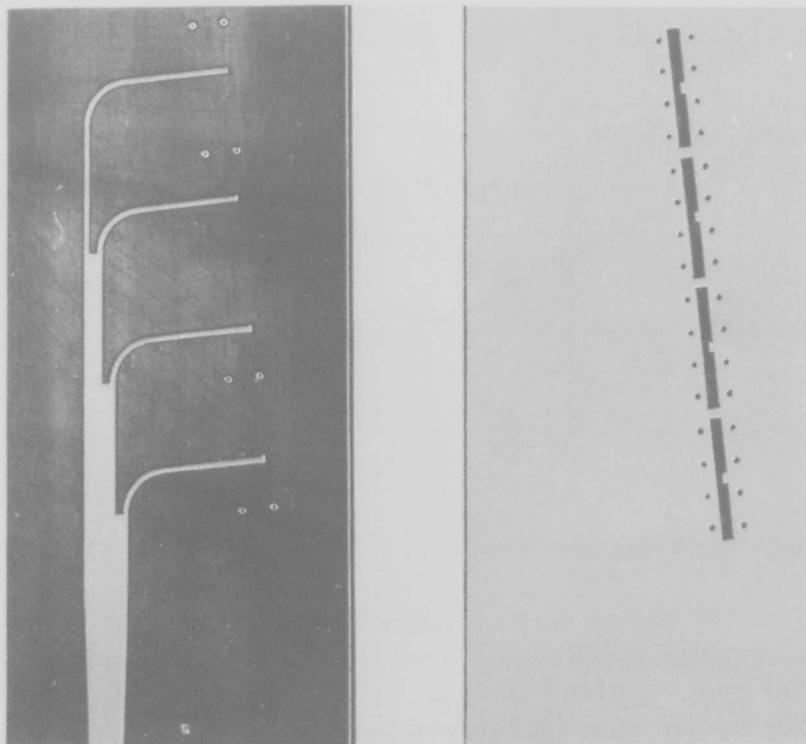


Fig. 6-13 4-slot H-plane array and its associated power divider

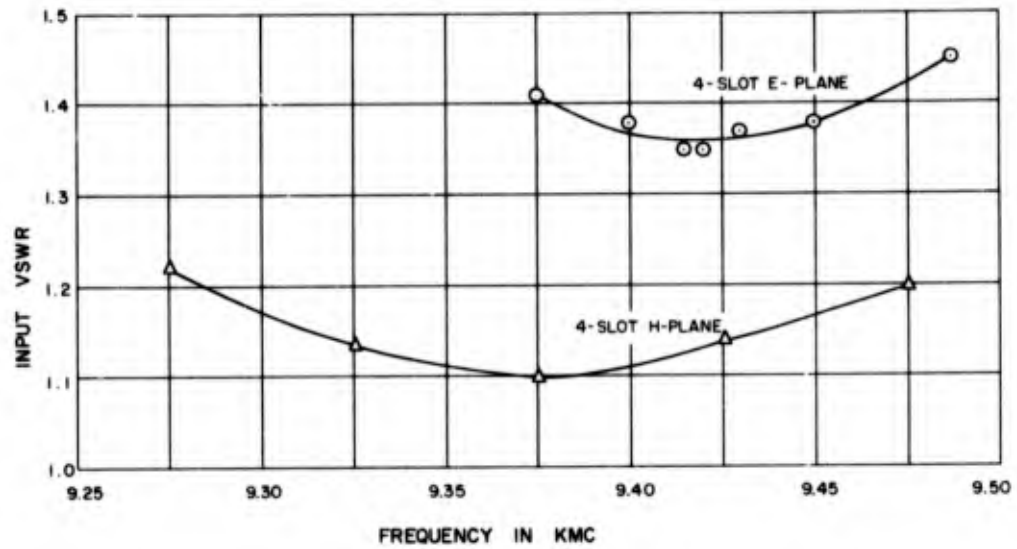


Fig. 6-14 Input VSWR versus frequency for four-slot E- and H-plane arrays

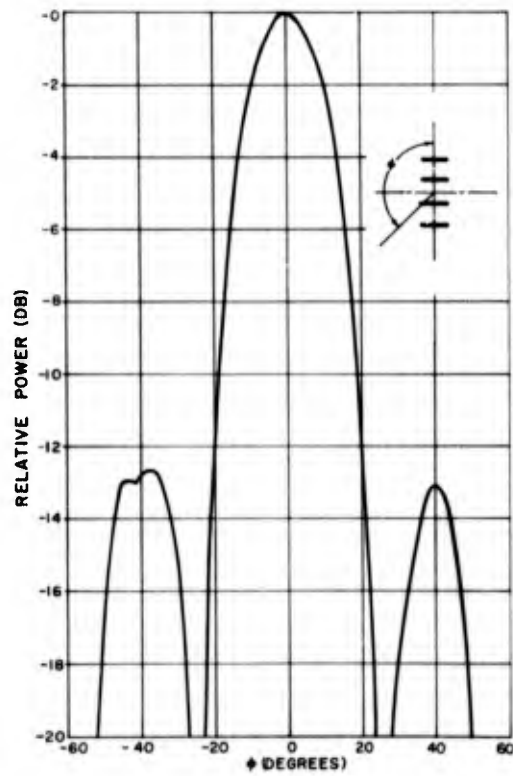


Fig. 6-15 E-plane radiation pattern of four-slot E-plane array

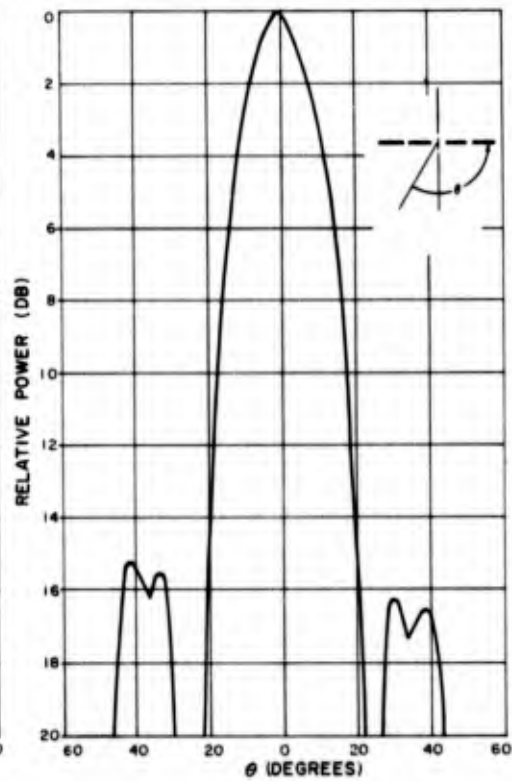


Fig. 6-16 H-plane radiation pattern of four-slot H-plane array

While the input VSWR of 1.10 for the 4-slot H-plane array at the design frequency of 9375 MC was reasonably good, the VSWR of 1.41 for the 4-slot E-plane array was rather high. The latter was attributed to mutual coupling between adjacent slots in the E-plane. Since the voltage across an individual slot decreases to zero at the two ends, there is inherently less coupling between adjacent slots in the H-plane than there is in the E-plane. This voltage-taper effect was further evidenced by the H-plane array's having side lobe intensities approximately 3 DB lower than those of the E-plane array. The half-power beamwidth of the 4-slot E-plane array was  $23.5^\circ$ , while that of the 4-slot H-plane array was about  $20.0^\circ$ .

The composite 4 x 4 array feed-system and slots are shown in Fig. 6-17. It is apparent that the feed-system is a combination of the power-dividers used in the two types of 4-slot arrays. Input VSWR is shown in Fig. 6-18.

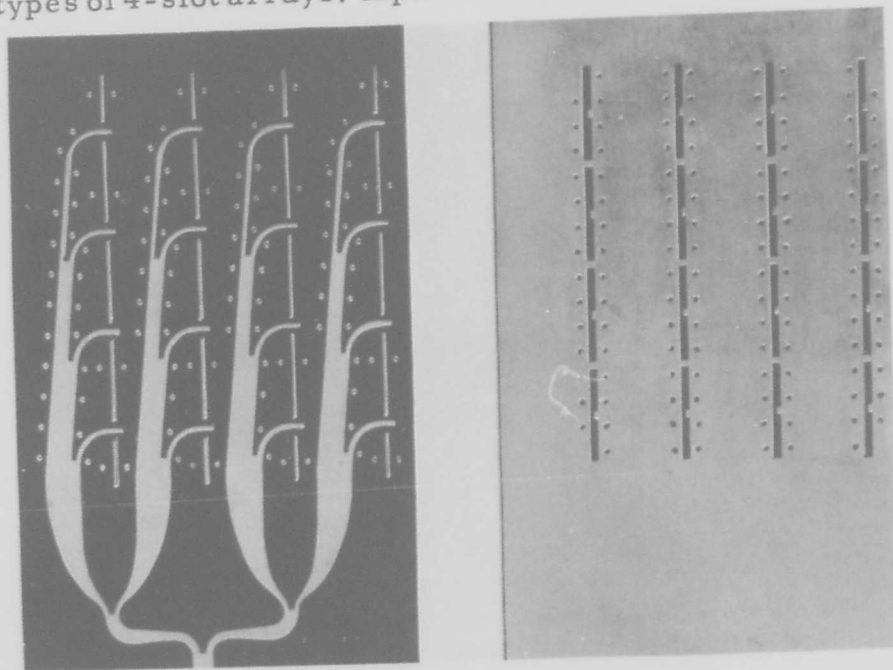


Fig. 6-17 Composite 4 x 4 slot-array (a) feed, and (b) slots

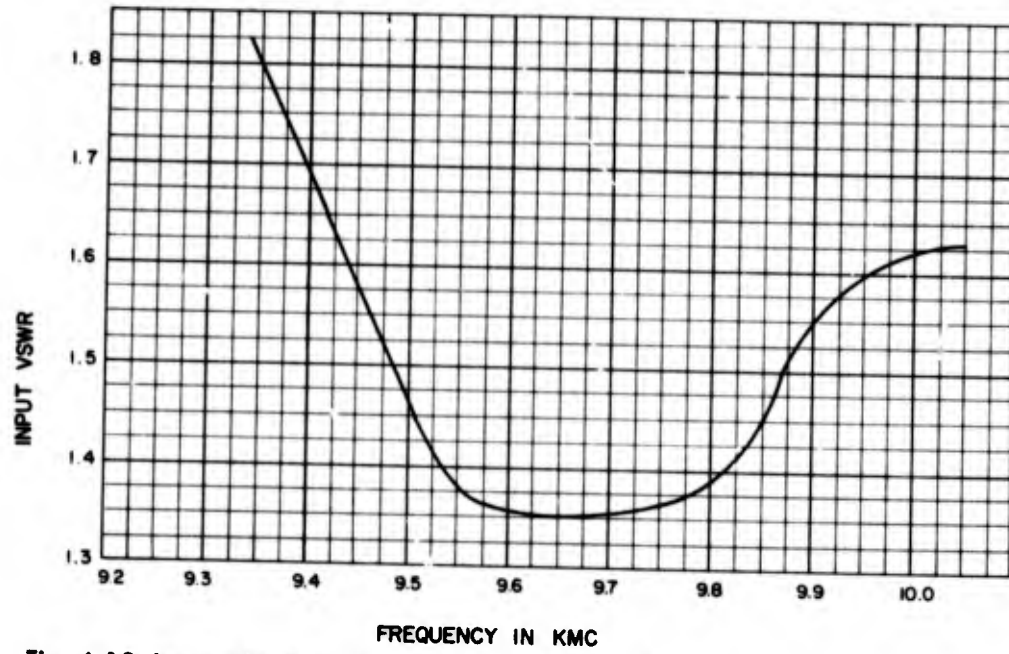


Fig. 6-18 Input VSWR for array shown in Fig. 6-17

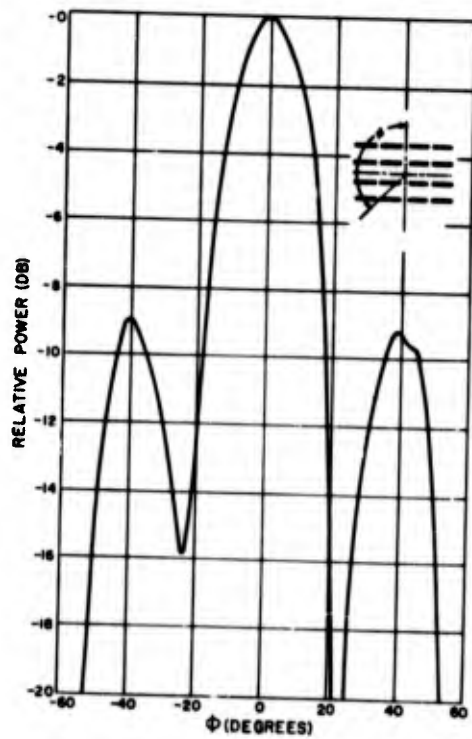


Fig. 6-19 E-plane radiation pattern of 4 x 4 slot array

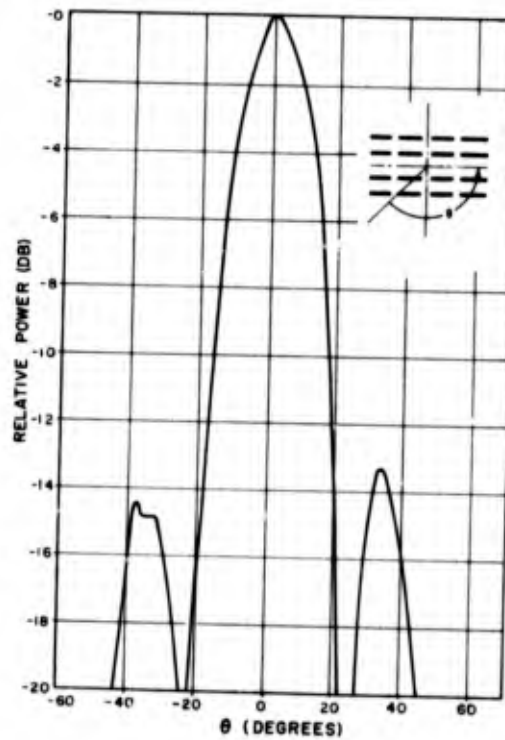


Fig. 6-20 H-plane radiation pattern of 4 x 4 slot array

E- and H-plane radiation patterns for this array are presented in Figs. 6-19 and 6-20 respectively.

Comparing the E- and H-plane patterns of the 4 x 4 array with those for the E-plane and H-plane arrays shown in Figs. 6-15 and 6-16, it is evident that the main lobes of both sets of plots are practically identical. However, the sidelobes in both planes of the 4 x 4 array are appreciably larger than those in the separated plane patterns. The E-plane sidelobes increased from approximately -12.5 DB to -9.0 DB, while the higher of the two H-plane sidelobes increased from about -15.2 DB to -13.3 DB. These higher sidelobe intensities were due primarily to mutual coupling between diagonal slots. Diagonal slots were not, of course, present in the individual arrays.

In an effort to reduce the E-plane sidelobes, a 4 x 6 array employing an E-plane power-taper was designed. Two such arrays, consisting of six 4-slot H-plane arrays stacked one under another, were fabricated in anticipation of evaluating their performance for a military radar. This array and its entire feed-system, including a 6-way, tapered power-divider, are illustrated in Fig. 6-21.

The six-way power-divider was designed to feed the six 4-slot H-plane arrays, in phase, at the design frequency of 9375 MC and to have a 1-2-3-3-2-1 power taper in the E-plane. E- and H-plane radiation patterns of one of these arrays are shown in Figs. 6-22 and 6-23, respectively. Comparing Figs. 6-19 and 6-22, it is noticeable that the effects, in the E-plane, of going from the 4 x 4 array to the larger 4 x 6 array with the above E-plane power-taper were a decrease in the half-power beamwidth from about 23.5° to 15.3° and a substantial decrease in the two sidelobes from approximately -9.0 DB to -13.4 DB and -16.4 DB. With respect to the H-plane, a comparison of Figs. 6-20 and 6-23 shows that the half-power beamwidth remained 20.0°, and the two sidelobes were only slightly reduced, going from -13.3

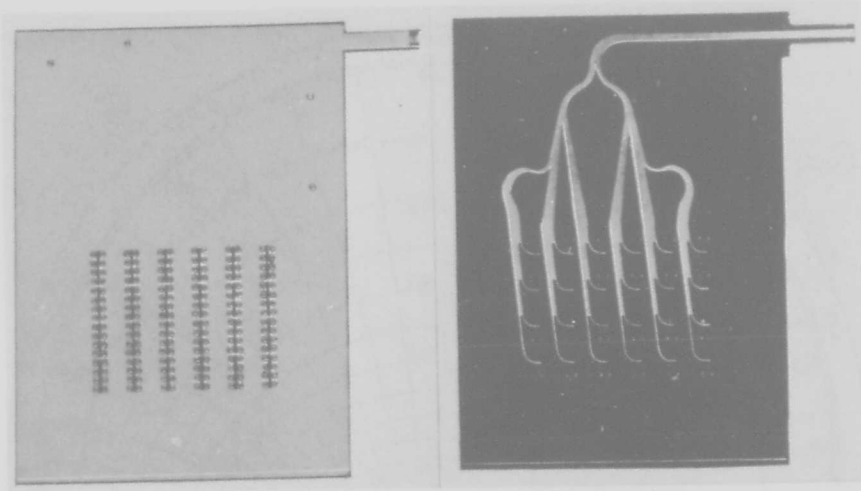


Fig. 6-21 4 x 6 slot array and feedline

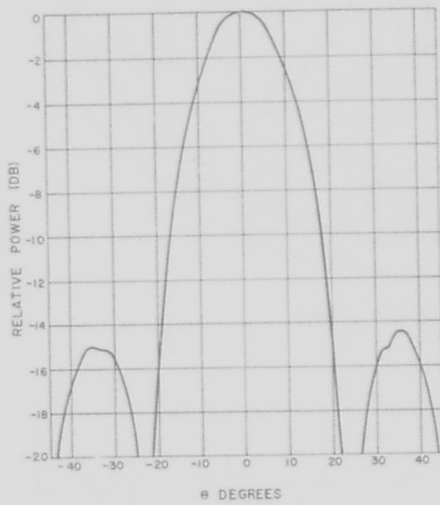


Fig. 6-22 E-plane radiation pattern of 4 x 6 slot array

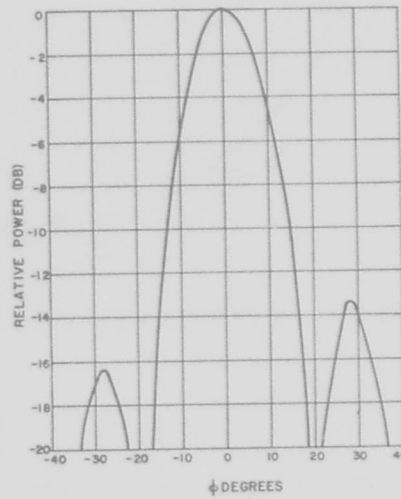


Fig. 6-23 H-plane radiation pattern of 4 x 6 slot array

DB and -14.6 DB to -14.5 DB and -15.0 DB.

Admittance plots of the two 4 x 6 arrays are presented in Fig. 6-24. The reference plane for each was approximately one-half inch on the input side of the initial power -

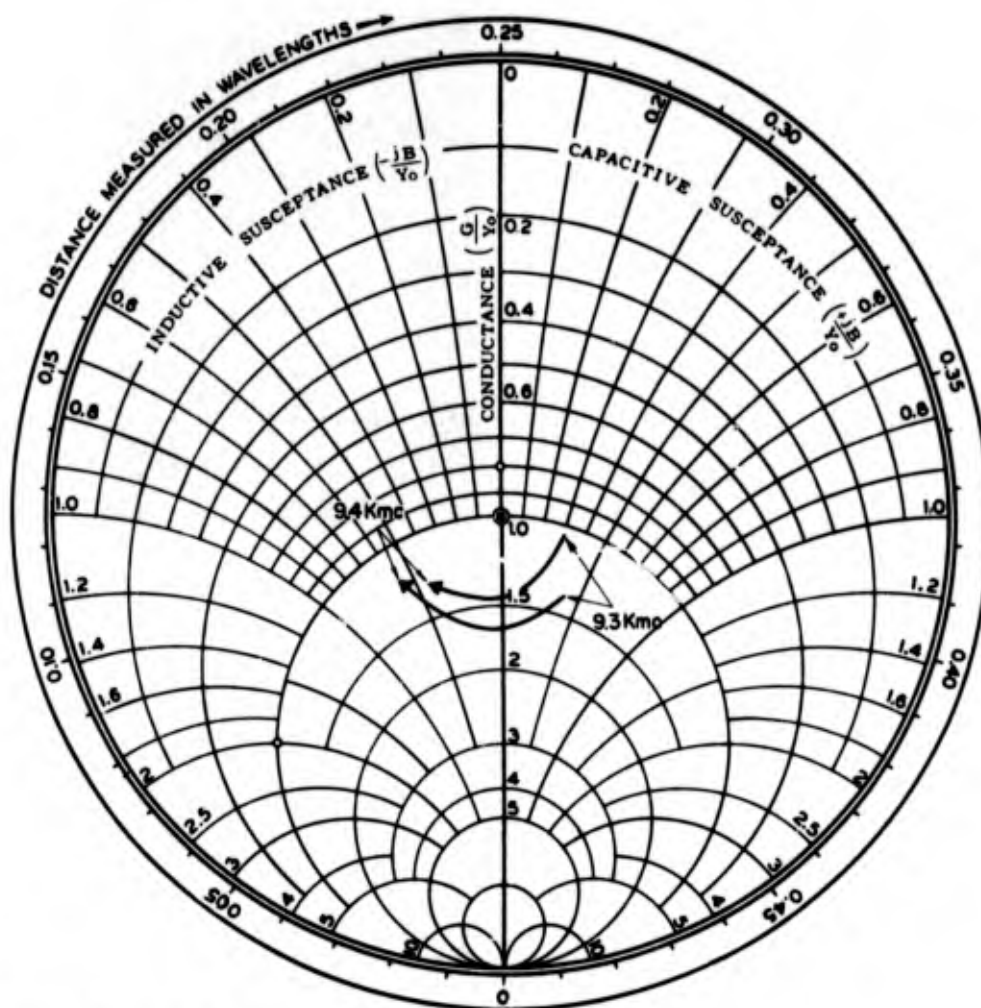


Fig. 6-24 Admittance plots of two 4 x 6 slot arrays

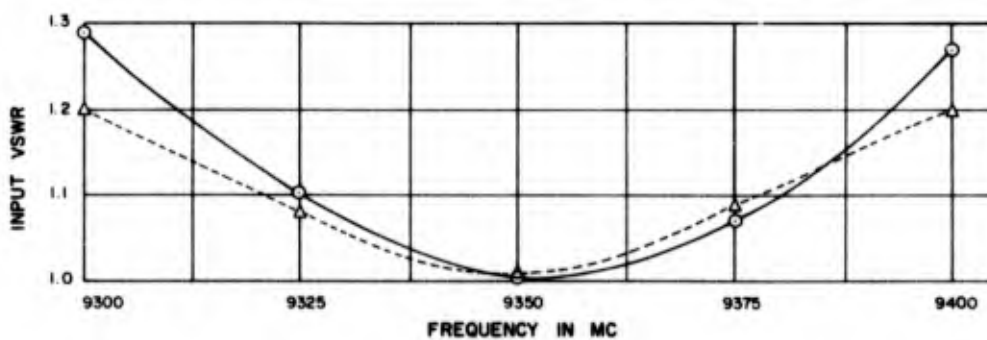


Fig. 6-25 Input VSWR versus frequency for the two halves of a twin X-band array

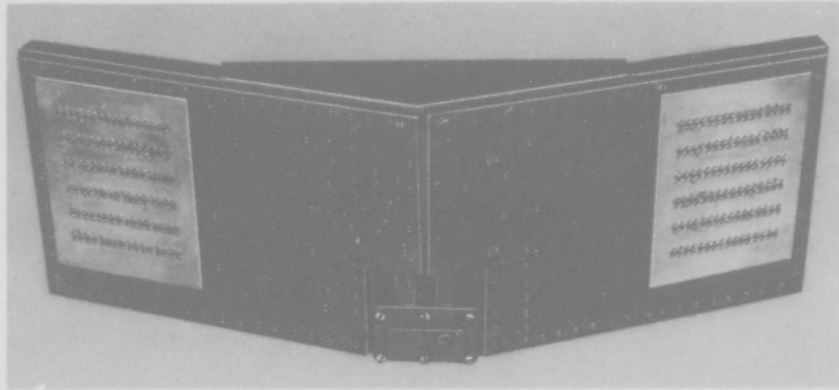


Fig. 6-26 Twin X-band Tri-Plate array

split. VSWR was corrected for line attenuation. The final input VSWR, as a function of frequency, for these two arrays is shown in Fig. 6-25. Fig. 6-26 is a photograph of the complete twin-X-band Tri-Plate array. Each array has a separate waveguide transition.





## CHAPTER SEVEN

### MEASUREMENTS, MATERIALS, AND FABRICATION TECHNIQUES

#### 7-1 General Considerations

Much of the effort which has been devoted to Tri-Plate transmission line development was directed toward evolving basic techniques of measurement, design and assembly. Considerable space will therefore be devoted to a description of the processes employed in the design and production of this form of microwave transmission line.

Tri-Plate is composed of two thin sheets of dielectric, each of which has metallic foil, usually copper, bonded to both sides. Portions of the metal are etched away from one side of each of these laminated sheets to form a center-conductor, leaving a complete copper plate on the other side to form a ground-plane. One of these laminated sheets is etched to form a mirror image of the other sheet. (The advantages of this type of construction are described in Chapter One.) The two sheets are then assembled into a composite laminate so that the two photoetched copper center-conductor strips effectively become a single conductor sandwiched between two sheets of dielectric and two copper ground-planes.

The fabrication of Tri-Plate components involves the following steps: selection of the proper dielectric and metallic conductor; bonding of the metal foil to the dielectric; layout of the baseplate for photographing; photography; photo-etching; cutting and trimming; and finally, assembly. Prior to these steps must come the engineering development involving the verification of design data by means of electrical measurements. The subject of measurement techniques will be treated before undertaking a description of the mechanical processes of production.

### 7-2 Measurement Techniques

In Tri-Plate line, as in more conventional coaxial and waveguide systems, measurement of impedance by slotted-line techniques is probably the most practical and informative technique for discovering the capabilities of the line or components. In addition, the accuracy of this method, which is within a few per cent, is adequate for all but the most rigorous requirements. The Tri-Plate slotted-line section, and, therefore, the techniques used with it, are similar to those used in coaxial and waveguide mediums. In Tri-Plate line, however, the probe is not inserted into the interior of the line. The energy sampled is present in a slot cut in the top wall of a metal case enclosing the line, as shown in Fig. 7-1. In order to insert the probe into a slot in the top of the transmission line, as is done in more conventional media, it would be necessary to remove some of the dielectric. The minus 30 db coupling obtained by external probing at the surface of the dielectric sheet (with ground-plane removed) has been found satisfactory for most measurements.

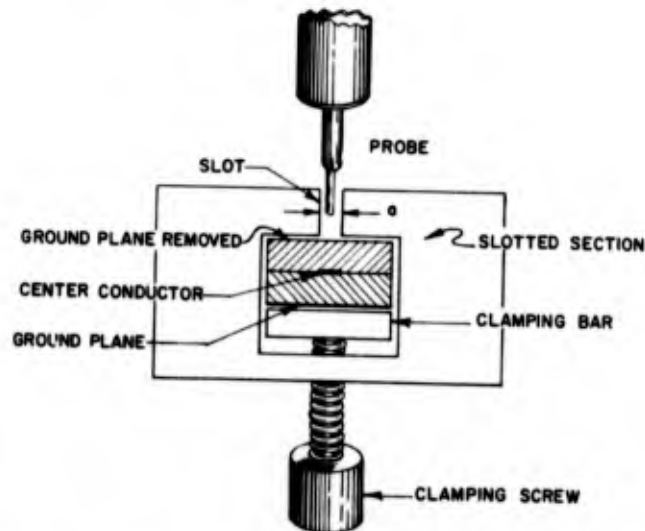


Fig. 7-1 Probe, slotted metal case, and Tri-Plate line with top ground-plane etched away.

To obtain more coupling, it is possible to probe the line laterally, rather than from above. In view of the field distribution in Tri-Plate line, as shown in Fig. 7-2, such an approach might cause less disruption of the field. In addition, this method is advantageous insofar as it allows the probe to approach closely to the center-conductor. However, aside from the physical difficulties of cutting away the solid dielectric line, coupling will change rapidly with movement perpendicular to the ground-planes, as shown in the theoretical curve of field distribution in Fig. 7-3. A small displacement of a lateral probe, up or down, during axial travel introduces a relatively large percentage of error. As a result, probe position is critical.

Introduction of a longitudinal slot in the top plate of the line produces effects similar to those encountered in coaxial and waveguide slotted sections. The characteristic impedance is changed due to slot influence on unit-length-capacitance in the line. However, the change in impedance is small and causes no significant reflection if the ends of the slot are adequately tapered as is conventionally done in waveguide slotted sections.

The propagation constant of the line is also affected by the slot, since the dielectric medium is now composed of air in addition to solid dielectric, and therefore the

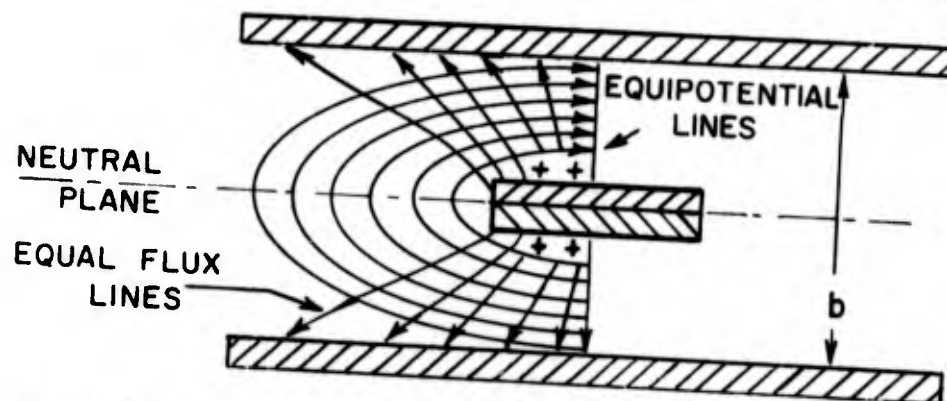


Fig. 7-2 Field distribution in Tri-Plate line.

wavelength in the slotted section is changed. In addition, due to the asymmetrical change in dielectric, as well as the unbalancing of potential between the outer plates, field distribution is disrupted to a certain extent, and energy will tend to be radiated from the edges of the line. The effects of unbalanced potential are counteracted by the metal case which encloses the slotted line in the probe carriage. The internal width of the case into which the line is inserted is reduced, so that at the highest frequency used, its dimension in this plane is below cutoff for the fundamental waveguide mode excited by the unbalance. Fig. 7-4 is a cross-sectional view of a Tri-Plate line (with topground-plane removed) enclosed in a slotted metal section fabricated for the standing-wave detectors used for Tri-Plate measurements. The

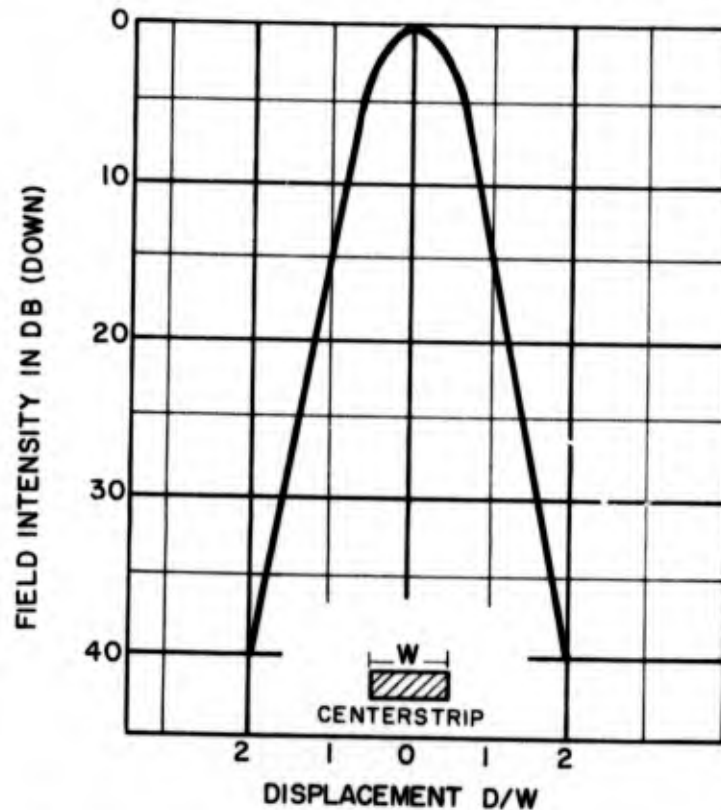


Fig. 7-3 Measurement of current on outer plates of Tri-Plate line.

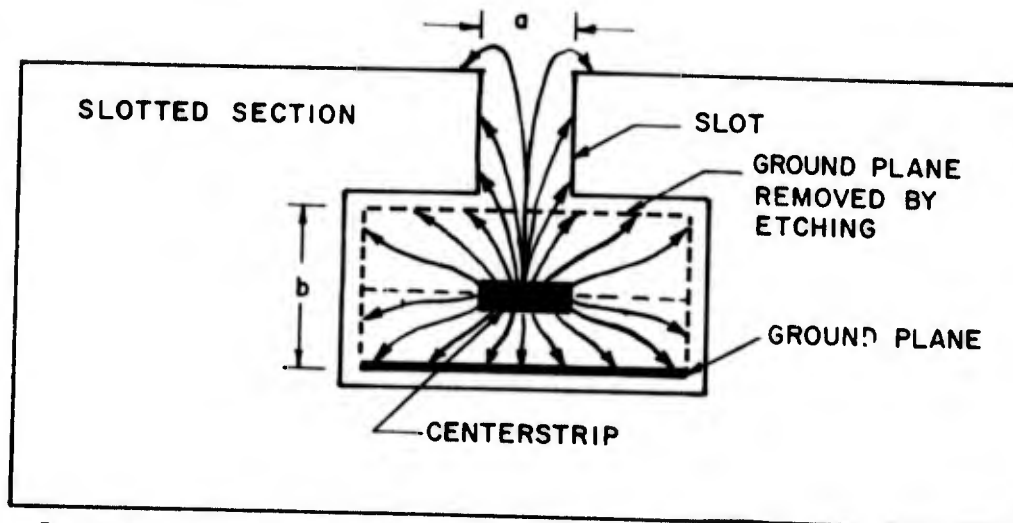


Fig. 7-4 Cross-sectional view of Tri-Plate line enclosed in slotted metal section, showing field configuration through line, slot, and etched ground-plane.

drawing shows the field configuration in the slot. The top wall of the metal case should be sufficiently thick so that the major portion of the field will be contained in the slot.

Measurements have been made to determine the correction factor for wavelength in the slotted section. In a slotted section where the slot-width ( $a$ ) is 1/8-inch, and ground-plane separation ( $b$ ) is 1/8-inch, the following correction values were found:

Material	Freq. (MC)	$\lambda_o$	$\lambda_{TP}$	$\lambda_{SL}$	$\frac{\lambda_{TP}}{\lambda_{SL}}$
Teflon glass GB112T	9375	3.2 cm.	2.02 cm.	2.07 cm.	.976
Teflon glass GB112T	3000	10.0 cm.	6.38 cm.	6.56 cm.	.974
Rexolite 2200	9375	3.2 cm.	1.99 cm.	2.05 cm.	.972
Rexolite 2200	3000	10.0 cm.	6.21 cm.	6.375 cm.	.974

where  $\lambda_o$ ,  $\lambda_{TP}$  and  $\lambda_{SL}$  are the wavelengths in air, the solid dielectric Tri-Plate line, and the slotted Tri-Plate section respectively.

Since the characteristic impedance of the line is dependent upon the line's capacitance per unit-length, a given line can be used for any frequency, provided that the width of the line, ( $S$ ), is such as to be below cutoff for other modes at the highest frequency to be used. This indicates a primary advantage of Tri-Plate slotted lines: in addition to the possibility of using the same line over a wide range of frequencies, lines of varying impedance can be inserted in the case with little difficulty.

Certain practical approaches to the design of Tri-Plate slotted-line sections have been evolved. The slotted section consists of a length of standard Tri-Plate line, of the desired impedance, from which the top ground-plane has been partially removed. The line is inserted into a slotted metal case which is so dimensioned that the Tri-Plate line's center-conductor is centered under the slot cut in the top wall of the metal case. As previously mentioned, the internal width of the metal slotted section is such as to be below cutoff for undesired modes at the highest frequency to be used. The section is then mounted on a probe carriage in the same manner as a conventional waveguide slotted-section, as shown in

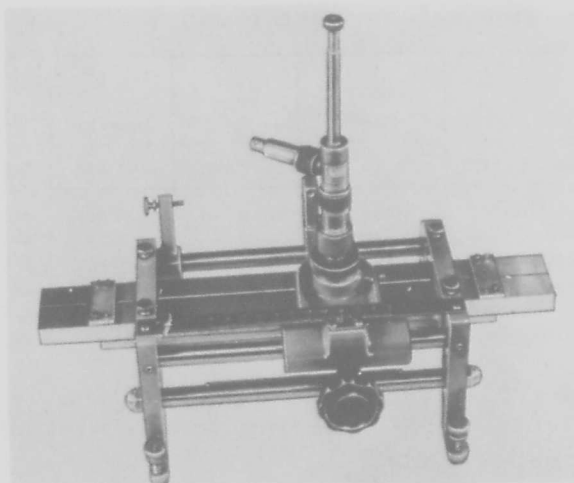


Fig. 7-5 Tri-Plate slotted line enclosed in slotted metal case and mounted on probe carriage.

Fig. 7-5. The probe is adjusted so that it travels in a plane just above the exposed dielectric surface of the etched Tri-Plate line. The Tri-Plate line extends beyond the ends of the metal slotted section and the upper and lower halves of the Tri-Plate line are cut to provide a lap-junction at each end. The slot should be wide enough to give adequate coupling. For example, for a line with ground-plane separation of 1/8-inch, a slot width of 1/8-inch will give 30 db coupling.

### 7-3 Dielectric Materials

Dielectric materials must be considered from the mechanical and chemical as well as from the electrical point of view. The mechanical and chemical properties of a dielectric which have a bearing on its use in Tri-Plate line include the range of operating temperature, the mechanical strength and stability, the inertness to solvents, and the water absorption properties. In addition, a dielectric should have a high degree of homogeneity in composition, and consecutive lots should show a dependable repeatability in characteristics. There must be sufficient chemical stability to prevent changes with time and unavoidable environmental effects. There must be sufficient mechanical strength. Expansion coefficients must be reasonably similar to those of the metallic conductors to prevent warping when the metal is etched off one side. The factor of bondability to metals must also be taken into account.

The basic electrical properties essential for use in Tri-Plate lines are a low dissipation factor, a sufficiently low dielectric constant over the frequency range of interest, and a high intrinsic dielectric strength. These factors should not differ widely with changes in frequency, and environment.

Loss tangents and values for the dielectric constants for numerous materials can be found in tables included in "Dielectric Materials and Applications", edited by A. Von Hippel<sup>1</sup>. These parameters should be appropriate for the particular realization in mind. For instance, in a delay line a high dielectric constant is desirable to



decrease the length of the line. A high dielectric constant is also desirable for the miniaturization of components, provided that in both these uses, there is also a reasonable loss tangent.

Up to the present, the most useful low-loss high-frequency dielectric has been teflon (polytetrafluoroethylene) and its glass - or quartz-filled laminates or mixtures. Teflon<sup>2</sup> is a low-loss material with a low dielectric constant and a high intrinsic dielectric strength. It can withstand ambient temperatures from approximately -110°F to 500°F. The dielectric constant is approximately 2.1 in the range of interest for microwave strip-transmission lines and the loss tangent approaches .00015 in the same range. Pure teflon has a high coefficient of expansion and a marked tendency to flow under load.

Quartz- or glass-filled teflon lines have added strength and a lower coefficient of expansion. Teflon-laminate<sup>3</sup> GB112T which is approximately 65% teflon and 35% continuous-filament glass base, has a dielectric constant of about 2.5 in the frequency range of interest and a loss tangent between .0017 and .0020. Quartz-filled teflon has a very similar value for the dielectric constant but considerably less loss. Another very-low-loss dielectric (approximately .001 loss tangent at 10 KMC) is Rexolite 1422, a cross-linked polystyrene<sup>4</sup>. The dielectric constant is 2.54. Rexolite is hard, fabricates easily, has considerable mechanical strength, but has a lower maximum operating temperature than teflon (near 230°F). Rexolite 2200, which is the glass-filled laminate of 1422, has a much greater sheer strength and warps less than Rexolite 1422 after etching. Glass-filled Rexolite has a loss tangent which is considerably more than that of Rexolite 1422 and approaches that of teflon-glass (GB112T), however, the Rexolite-glass mixture is a more homogenous material than the GB112T.

<sup>2</sup>E. I. DuPont de Nemours and Co., Inc., Polychemicals Dept., Wilmington, Del.

<sup>3</sup>Continental-Diamond Fibre Co., Bridgeport, Pa.

<sup>4</sup>Rex Corporation, West Acton, Mass.

Another dielectric which has been used is an alloy of dimethyl silicone and styrene copolymer resin. Silicone-alloy C-989<sup>5</sup> has a dielectric constant, at 100 mc, of 2.48 and a loss tangent of .0009. Advantages of the silicone-alloy over teflon include a substantially lower cold flow, relative ease of machining, and low cost. In addition, this alloy is water-repellent. However, silicone-alloy C-989 has a comparatively low melting point (near 200°F) and is soluble in many chemical solvents.

Fig. 7-6 shows measured attenuation in db per foot for four typical Tri-Plate copper-clad dielectrics compared with the calculated figure for pure teflon in the frequency range from one to ten kilomegacycles. Curves for unloaded Q values for the same materials are shown in Fig. 7-7.

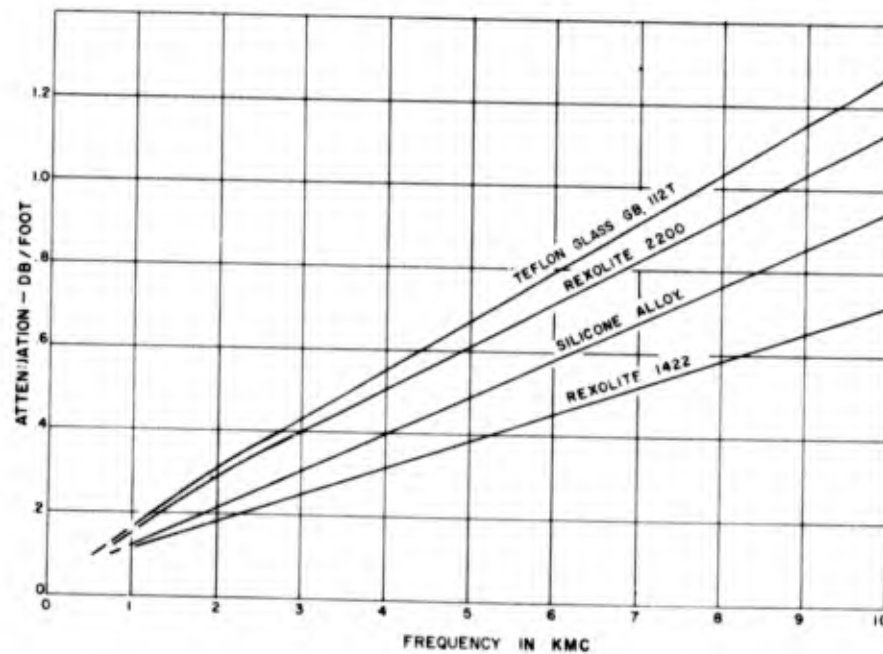


Fig. 7-6 Attenuation in DB per foot for four 50-ohm Tri-Plate lines fabricated from four different copperclad dielectrics, compared with the calculated figure for pure teflon.

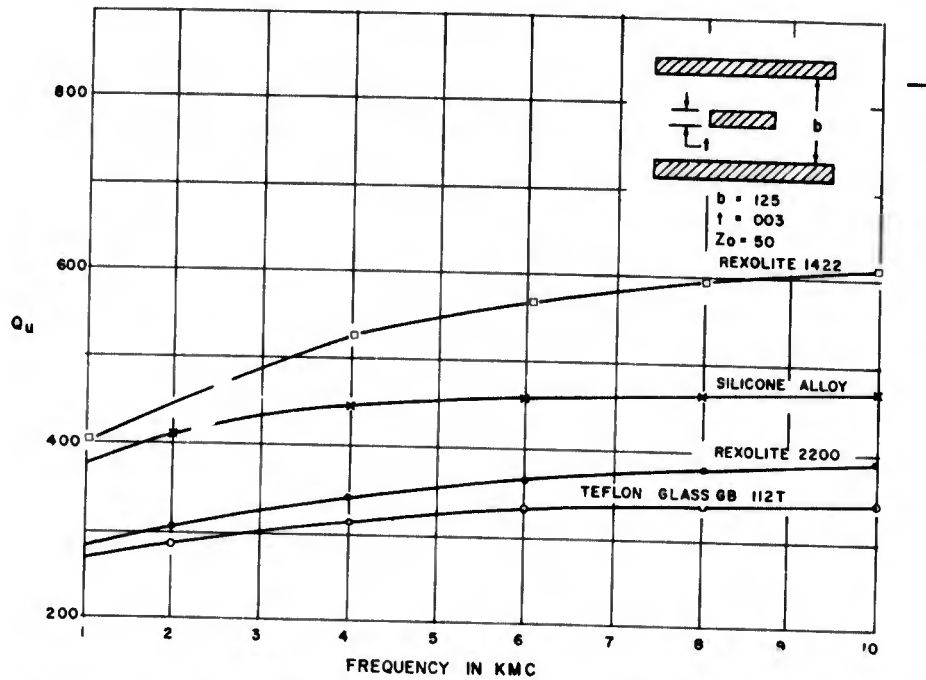


Fig. 7-7 Unloaded Q values for four 50-ohm Tri-Plate lines fabricated from four different copperclad dielectrics.

#### 7-4 Metallic Materials and Bonding

Copper foil is the conductor most commonly used for Tri-Plate ground-planes. Aluminum is easily obtainable as foil and is cheap, but is difficult to solder. In addition, aluminum is somewhat more difficult to etch.

The copper foil is used in nominal thicknesses of 1.35 or 2.7 mils (one and two ounces respectively). Heavier foil, which gives a better protective cover to the line, can be used, but this increases etching time and decreases etching accuracy because of undercutting. The bond between foil and dielectric should be able to withstand a minimum of three pounds pull per inch-wide strip without peeling, though an ability to withstand a considerably greater pull is desirable. The bond, which is usually the result of pressure and an adhesive, must be able to withstand high temperatures and allow soldering. A thin oxide coating on the copper will increase bond strength in most cases. The bond obtained by the alternative techniques of spraying or plating the metal surface onto the dielectric is normally weak.

Until recently, the slippery surface of teflon has made bonding to copper difficult, while teflon-laminates or mixtures presented less trouble in this regard. The problem has been overcome by a newly discovered method of treating the surface prior to bonding<sup>6</sup>. The teflon is immersed in a bath of metallic sodium dissolved in liquid anhydrous ammonia, washed and dried. After treatment, the teflon can be cemented to various metals with conventional bonding agents.

#### 7-5 Fabrication

A series of illustrations, Fig. 7-8 through 7-18, show the design, etching, and assembly of an S-band hybrid ring. These figures will clarify the following discussion.

The original drawing of a microwave component to be fabricated in Tri-Plate line is the step which requires the most attention to detail, since the final microwave printed circuit will be an exact scaled-down copy of the drawing. Fig. 7-8 shows finishing touches being made on the S-band hybrid-ring drawing.

The design is laid out, preferably with hard pencil, on a photographic baseplate. It is possible to make the design with pen and ink on bristol board, cardboard or heavy paper. However, line accuracies are difficult to hold with the latter materials. For good results, photographic masters must retain their dimensions rigidly in spite of environmental changes. The usual baseplate design is four times the size of the etched component. After photographing, the overall tolerance must be within five thousandths of an inch. However, with trained personnel and the proper equipment this tolerance can be invariably achieved.

Materials that form a good base for accurate line drawings and retain their size under normal environmental changes are: Plax Corporation's Polyflex, the surface of which must be modified to obtain a mat surface; Stabilene (Mylar) film, which is distributed by Keuffel & Esser Co.; and Lumarith, distributed by the Celanese Corp.



Fig. 7-8 Finishing touches on base-plate for S-band hybrid ring.

of America. Keuffel & Esser Co. also distribute a plastic-impregnated glass cloth which is very stable dimensionally but is somewhat more difficult to work with than the other materials.

In those areas where the copper conducting surface must be retained on the etched laminate, the baseplate must appear dark to the camera. For this reason, a contrasting ink or material must be applied to the surface of the drawing. There are several such materials which photograph well and are easily applied. Probably the most important of these is Zipatone, a thin red acetate-film with a wax surface which can be cut to any desired shape. With this material, outlines can be followed with a knife, substantially decreasing the amount of error which is the inevitable result of pencil thickness. The film is placed on the baseplate and pressure is applied to fix it to the surface. A roller or burnishing tool is used to remove air bubbles from between the two surfaces.

The film can then be cut along the pencil outline with a knife and straight-edge as shown in Fig. 7-8. (Radial cutters are used for cutting curved lines.) The technician must develop a sure sense of touch so that the cut may be the right depth to avoid injuring the master and yet to make sure the film is completely severed. The unwanted film is then stripped away. This material is easy to work with, adheres to the surface permanently but is easily removed and reworked. Corrections can be made by patching-in additional Zipatone and recutting. Large areas can be covered with this material where it is desired to maintain the metal laminate unetched.

Cutlines or edges for the cutting out of the Tri-Plate component must be included in the etching and therefore must form part of the original master. The outlines, as shown in Fig. 7-8, are usually made with narrow tape (precut to the desired thickness) such as pressure-sensitive, photographic Scotch Tape. In addition, there are available, for locating screw or eyelet holes, transparent or easily separated tapes on which are printed small black rings or washers<sup>7</sup>. Other aids include pre-cut narrow and curving lines<sup>8</sup>.

Dimensional accuracy can be achieved by scaling the baseplate drawing several times larger than the size of desired microwave circuit. The drawing scale to be used is dependent upon several factors such as the overall size of the Tri-Plate circuit, the dimensional tolerances required and the camera facilities available. For overall tolerances, a scale relationship between drawing and photo-negative of six to one should be quite adequate. A scale relationship of 4:1 is often sufficient and is more convenient, when tolerances allow, due to the decreased size of the baseplate drawing. A scale ratio of 2:1 is generally inadequate. When gaps as small as .003" or line widths of .005", for instance, are desired, the higher scale ratios are necessary.

In cases where tolerances must be very close, and the camera cannot handle extra-large baseplate drawings, the original drawing may be reduced as much as possible and a preliminary negative made from it. A contact print is then made and used as a second baseplate or as part of a new drawing, making further reduction possible.

Precision camera facilities are not readily available and it may be necessary, with any particular drawing, to go through a trial and error process to adjust the camera and drawing to obtain the necessary accuracy. In addition, an adequate technique must be developed with regard to measuring the negatives.

After the baseplate has been prepared, cross hairs are fixed to the drawing for later reference measurements and the plate is sent to the photographer.

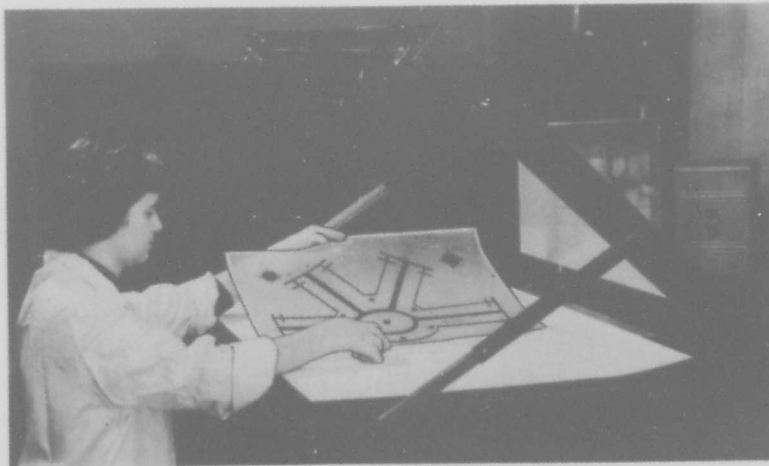


Fig. 7-9 Technician placing S-band hybrid ring baseplate in copy camera vacuum frame.

Although the present technique can be applied with almost any big camera (with due attention to spherical aberration, etc.), the best apparatus to use is a copy camera such as that shown in Fig. 7-9. In the picture,



the technician is shown placing the photo-master or baseplate within a frame from which the air can be exhausted. Removing the air holds the master flat to the surface of the frame so that there is no chance that light will undercut the master to cause blurred edges in the negative.

The typical copy camera can be set for any desired reduction within limits set by its size and length of carriage. The vacuum frame is mounted on rails, and the distance from the lens can be adjusted with some precision. Such adjustment will overcome any discrepancies in overall size which are discovered when checking the reference crosshairs on the baseplate.

Choice of film is important. With films such as Kodak PB, which is stable dimensionally, tolerances can be held below five-thousandths of an inch. Vinyl-based film is also dimensionally stable under normal environmental conditions but is thicker than the Kodak PB and has a pebbly-grained surface. During the photoetching process, a thin and smooth film is advantageous since the negative can be turned over and a reversed image can be made of the configuration on the sensitive laminate without light distortion. Such distortion occurs when light penetrates under the edges of the negative or when, as in the case of vinyl-based film, light is diffused when passing through the film itself. (Reversed images are needed to supply the double centerstrips characteristic of Tri-Plate line.)

For the most accurate work and for excellent storage-life, glass negatives can be used.

Processing the film includes careful developing to avoid the appearance of pinholes and other irregularities in the film. Some holes may appear after the most careful developing, and should be opaqued.

There are several methods of putting an image on a prepared metal-clad laminate. These include the use of



the silk screen and offset printing processes. However, to obtain the accuracy and definition required for most microwave printed circuits (where line-width tolerances of the order of .001" and line definition are important) the photo-etching technique is far superior.

The metal-clad laminated sheets must be free from pit-holes or dents. First cleaned with pumice, they are then baked to evaporate moisture from the surface pores of the metal. The sheets are cooled and the sensitive emulsion is applied to the surface. The sheets are centrifuged under heat to form an even dry film of photo-resist. It is desirable to keep the emulsion as thin as possible; when the emulsion is too thick, the etching is less accurate.

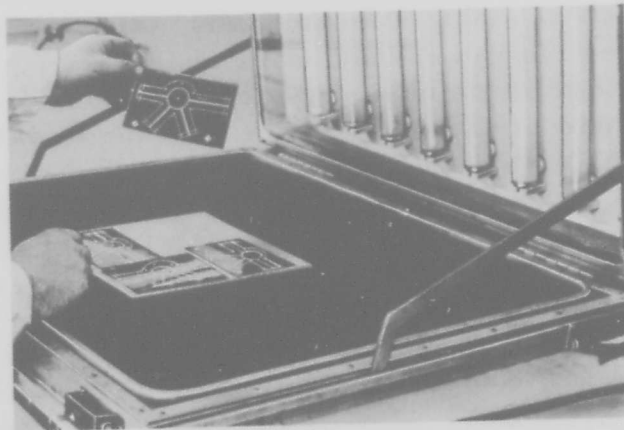


Fig. 7-10 Preparations for exposing the sensitized Tri-Plate ground-plane in ultraviolet light.

As shown in Fig. 7-10, the prepared metal-clad plate is placed in a vacuum frame, masked with the negative, and then exposed to ultraviolet light. With a perfect negative, three minutes of exposure is sufficient when using Kodak Photo Resist. With an indistinct negative, up to ten minutes exposure is possible. Time is not particularly critical with this material. However, with an emulsion such as "cold-top" enamel, exposure time is extremely critical and a high degree of definition is

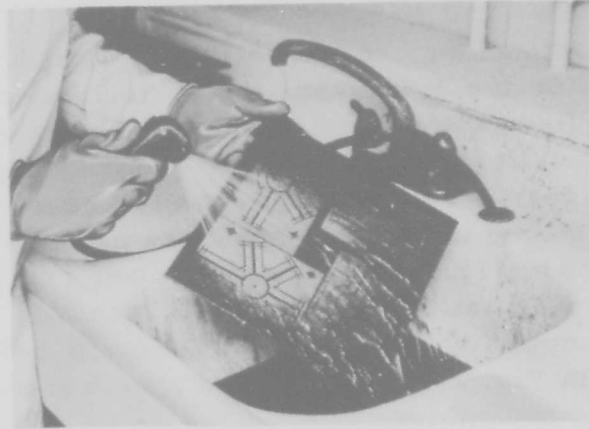


Fig. 7-11 Washing dye off exposed Tri-Plate components.

difficult to obtain. This more than offsets the advantages of this latter type of emulsion (including that of allowing a dye to be applied with the emulsion itself and thus avoiding an extra step in the process). The negatives are developed in the appropriate solution, (trichlorethylene for the Kodak Photo Resist). The Kodak negatives are treated with Kodak Photo Resist dye, which will show up irregularities (or pinholes) in the image. They are then washed, as shown in Fig. 7-11, and dried. (The dye will not wash off where the resist is polymerized.) At this time pin holes or other breaks in the surface can be retouched. Outline irregularities demand rejection of the exposure.

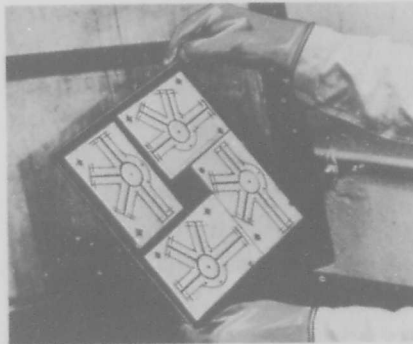


Fig. 7-12 Etched components being removed from etching tank.

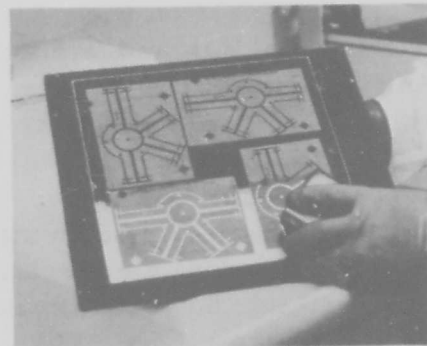


Fig. 7-13 Final cleaning to remove photo resist from copper.

After retouching, the sheets are etched in ferric chloride (for the Kodak emulsion) for approximately three minutes when the metal-clad surface is one-ounce copper, and five minutes for two-ounce copper. The solution of ferric chloride should have a Beaume strength of 42. An etched laminate is shown being removed from the solution in Fig. 7-12. The sheets are rinsed in cold running water and the photo resist removed from the unetched copper with methyl ethyl ketone and a brush, as shown in Fig. 7-13. The etched sheets are ready for cutting and assembly.

#### d) Tolerances

Before continuing with the final assembly of the line, it would be worthwhile to emphasize the importance of the close tolerances prescribed in the production process. The tolerance desirable can be determined from the wavelength, the type of circuit required, and the required accuracy of tuning. As already pointed out, tolerances must be considered in the choice of drawing dimensions for the photographic master. Also important is the dimensional stability of the material on which the drawing is made. In photographing, the dimensional stability of the negative, the absence of spherical or other distortion and the degree of definition of the camera lens are important. In the etching process, accuracy depends in part on the surface condition of the material. It must be flat and smooth to give proper definition. And finally, the negative must be held flat to the copper-clad Tri-Plate laminate to prevent distortion caused by light striking under the edges of the negative. One-ounce copper is superior to two-ounce copper in that there is a great deal less undercutting encountered during the etching process. Under ideal conditions gaps as small as .003" can be etched accurately (within .0005"). Line widths as small as .005" may be etched to the same tolerance. Undercutting, with lines thinner than .005", often causes breaks in the line.

Before the line is assembled, the copper surfaces -

both ground-planes and center-conductors - may be silver plated. While silver plating has no electrical significance, because only the non-current-carrying surfaces are exposed to plating, it has some protective value and affords a surface which is more easily soldered.

#### e) Assembly

The assembly process will vary, depending on whether a complete RF system, such as a receiver, or a simple component for test purposes is to be fabricated. Generally, separate components demand the more precise technique, since such units must be matched to other lines. Lap joints, for instance, must be accurate in dimensions to make good connections.

The first step in the assembly is to rough out the component along the cutlines with a bandsaw as shown in Fig. 7-14. The component is then inserted in a jig, such as that shown in Fig. 7-15, and shaved carefully down to the cut-lines by hand. For this job a sharp wood chisel or an Exacto-knife may be used. For some types of dielectric materials such as Rexolite, filing may be necessary.

A small high-speed drill such as that shown in Fig. 7-16 is needed to bore screw or eyelet holes in materials such as Teflon-glass (Continental Diamonds' GB112T). Because of the glass filler, this material is difficult to drill accurately. (Accuracy is necessary since the holes are often used for line-up purposes.) Cutting the holes can be done as part of a single punch operation where production-line techniques are warranted.

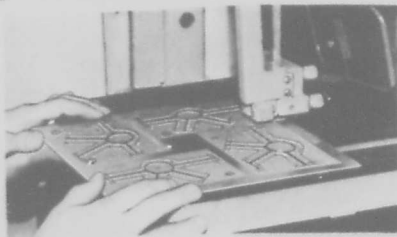


Fig. 7-14 Roughing out S-band hybrid ring along cutlines.



Fig. 7-15 Shaving hybrid ring down to cut lines.

The two halves of each component are then fitted together and the center-conductors can be expected to register to a close tolerance since the opposite sides or laminates are etched from alternate sides of the same photo-negative. Alignment to within a few thousandths of an inch is assured by matching the drill holes. This procedure is adequate from the standpoint of accuracy except for special cases. The most economical means of permanent assembly is to use small eyelets which can be inserted in the line and peened by means of an eyeletting machine as shown in Fig. 7-17. Where disassembly is necessary for measurement work or design changes, small screws can be substituted for the eyelets.

One of the final stages in the Tri-Plate line assembly process is that of cutting accurate terminations and lap-joints with the aid of a jig and knife as shown in Fig. 7-18. With some units it is desirable to enclose the edges of the Tri-Plate line. This is easily accomplished by forming soft copper channel and soldering it to the outer plates.

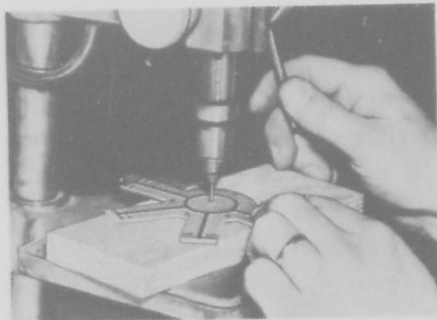


Fig. 7-16  
High speed drill bores eyelet holes in Tri-Plate hybrid ring.

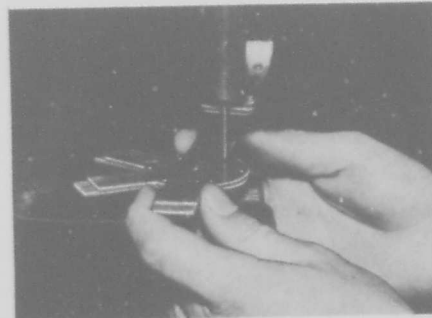


Fig. 7-17  
Assembly of Tri-Plate hybrid ring: peening eyelets.

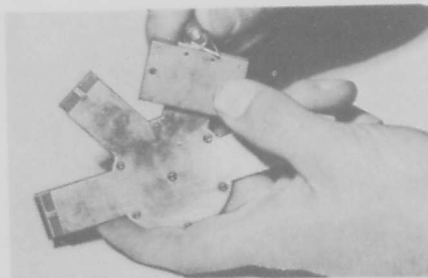


Fig. 7-18 Trimming termination of S-band hybrid ring (Notice overlap for junctions).

1

2

3

4

5

6



## REFERENCES

- Arditi, M. "Characteristics and applications of microstrips for microwave wiring," *IRE Transactions*, v. MTT-3, No. 2, March 1955, p. 31-56.
- Arditi, M. "Experimental determination of the properties of microstrip components," *Convention Record of the IRE*, March 1953, p. 27-37.
- Arditi, M. and J. Elefant. "Microstrip applied to band-pass microwave filters," *Electrical Communications*, March 1955.
- Barrett, R. M. "Etched sheets serve as microwave components," *Electronics*, v. 25, June 1952, p. 114-8.
- Barrett, R. M. "Microwave printed circuits — a historical survey," *IRE Transactions*, v. MTT-3, No. 2, March 1955, p. 1-9.
- Barrett, R. M. and M. H. Barnes. "Microwave printed circuits," *Radio and TV News*, v. 46, September 1951, p. 16.
- Begovich, N. A. "Capacity and characteristic impedance of strip-transmission lines with rectangular inner conductors," *IRE Transactions*, v. MTT-3, No. 2, March 1955, p. 127-33.
- Bowness, C. "Strip transmission lines," *Electronic Engineering*, January 1956, p. 2-7.
- Bradley, E. H. and D. R. J. White. "Band-pass filters using strip-line techniques," *IRE Transactions*, v. MTT-3, No. 2, March 1955, p. 163-9.
- Bradley, E. H. and D. R. J. White. "Band-pass filters using strip-line techniques," *Electronics*, May 1955, p. 152-5.
- Bradley, E. H. "Design and development of strip-line filters," *IRE Transactions*, v. MTT-4, April 1956, p. 86-93.
- Butler, Lt. J. E. *Design of strip transmission line systems and antennas*, U. S. Naval Postgraduate School Thesis, 1955.
- Coale, F. S. "A traveling-wave directional filter," *IRE Transactions*, v. MTT-4, October 1956, p. 256-60.
- Cohn, S. B. "Characteristic impedance of the shielded-strip transmission line," *Transactions of the IRE-PGMITT*, v. MIT-2, No. 2, July 1954, p. 52-5.
- Cohn, S. B. "Design of transmission-line filters," Chap. 27, v. II, *Very high-frequency techniques*, H. J. Reich, editor; New York: McGraw-Hill, 1947.
- Cohn, S. B. and F. S. Coale. "Directional channel-separation filters," *IRE Convention Record*, v. 4, Part 5, 1956, p. 106-12, and *IRE Proceedings*, v. 44, No. 8, August 1956, p. 1018-24.
- Cohn, S. B. "Optimum design of stripped transmission-line transformers," *IRE Transactions*, v. MTT-3, April 1955, p. 16-21.
- Cohn, S. B. "Problems in strip transmission lines," *IRE Transactions*, v. MTT-3, No. 2, March 1955, p. 119-26.



- Cohn, S. B. "Shielded coupled-strip transmission line," *IRE Transactions on Microwave Theory and Techniques*, v. MTT-3; October 1955.
- Dahlmann, B. A. "A double-ground-plane strip-line system for microwaves," *IRE Transactions*, v. MTT-3, October 1955, p. 52-7.
- Frank, N. H. "Reflections from sections of tapered transmission lines and wave guides," Radiation Laboratory Report 43-17; January 1943.
- Fromm, W. E. "Characteristics and some applications of strip-line components," *IRE Transactions*, v. MTT-3, No. 2, March 1955, p. 13-20.
- Frost, A. D., and C. R. Mingins. "Microwave strip circuit research at Tufts College," *IRE Transactions*, v. MTT-3, No. 2, March 1955, p. 10-12.
- Frost, A. D., C. R. McGeoch, and C. R. Mingins. "The excitation of surface waveguides and radiating slots by strip circuit transmission lines," *IRE Transactions*, v. MTT-4, October 1956, p. 218-22.
- Fubini, E. G., W. Fromm and H. Keen. "New techniques for high-Q microwave components," *Convention Record of the IRE, Part 8, 1954 National Convention*, p. 91-7.
- Fubini, E. G., W. Fromm, and H. Keen. "Microwave applications of high-Q strip components," *IRE Convention Record, Part 8, 1954 National Convention*, p. 98-103.
- Fubini, E. G. "Stripline radiators," *IRE Transactions*, v. MTT-3, No. 2, March 1955, p. 149-56.
- Geppert, D. V. and R. H. Koontz. "TEM mode microwave filters," *Tele-Tech & Electronic Industries*, November 1955, p. 72-3, 150-1.
- Jones, E. M. T., and J. T. Bolljahn. "Coupled-strip-transmission-line filters and directional couplers," *IRE Transactions*, v. MTT-4, April 1956, p. 75-81.
- Karakash, J. J. *Transmission lines and filter networks*, New York: MacMillan, 1950.
- Kostriza, J. A. "Microstrip components," *Proceedings of the IRE*, v. 40, December 1952, p. 1658-63.
- Marcuvitz, N. *Waveguide handbook*, MIT Rad. Lab. Series, v. 10, New York, McGraw-Hill, 1951.
- Mole, J. H. *Filter design data*, New York: Wiley, 1952.
- Montgomery, C. G. *Technique of microwave measurements*, v. 11, MIT Rad. Lab. Series, New York: McGraw-Hill, 1947.
- Mumford, W. W. "Maximally-flat filters in waveguide," *Bell System Tech. Jour.*, v. 27, October 1948, p. 684-713.
- Oliner, A. A. "Equivalent circuits for discontinuities in balanced strip transmission line," *IRE Transactions*, v. MTT-3, No. 2, March 1955, p. 134-43.

- Oliner, A. A. "The radiation conductance of a series slot in strip transmission line," Paper No. 43.3, IRE National Convention, New York City; March 1954.
- Oliner, A. A. "Theoretical developments in symmetrical strip transmission line," In *Proceedings of the Symposium on modern advances in microwave techniques*, Polytechnic Institute of Brooklyn, July 1955, p. 379-402.
- Oliver, B. M. "Directional electromagnetic couplers," *IRE Proceedings*, v. 42, November 1954, p. 1686-92.
- Packard, K. S. "Machine methods make strip transmission line," *Electronics*, September 1954, p. 148.
- Park, D. "Planar transmission lines," *IRE Transactions*, v. MTT-3, April 1955, p. 8-12, and October 1955, p. 7-11.
- Park, D. "Planar transmission lines," *IRE Transactions, Correspondence*, v. MTT-4, April 1956, p. 130.
- Pease, R. L. "Characteristic impedance of strip transmission lines with rectangular inner conductors in the low impedance region," Tufts College Interim Report No. 2 on Contract No. AF19(604)—575, January 1954.
- Pease, R. L., and C. R. Mingins, "A universal approximate formula for characteristic impedance of strip transmission lines with rectangular inner conductors," *IRE Transactions*, v. MTT-3, No. 2, March 1955, p. 144-8.
- Ragan, G. *Microwave transmission circuits*, MIT Rad. Lab. Series, v. 9, New York: McGraw-Hill, 1948.
- Reich, H. J., editor. *Very high-frequency techniques*, Radio Research Laboratory, Harvard University, 2 vols., New York: McGraw-Hill, 1947.
- Ringebach, M. E., and H. W. Cooper. "Measurement of attenuation and phase velocity of various laminate materials at L-band," *IRE Transactions*, v. MTT-3, No. 2, March 1955, p. 87-92.
- Schelkunoff, S. A. *Electromagnetic waves*, New York: Van Nostrand, 1943.
- Sferazza, P. "Directional couplers," *Convention Record of the IRE, Part 8*, 1954, p. 115.
- Slater, J. C. *Microwave transmission*, New York: McGraw-Hill, 1942.
- Sommers, D. J. "Photo-etched antennas for supersonic aircraft," *Electronics*, July 1955.
- Sommers, D. J. "Slot array employing photo-etched Tri-Plate transmission lines," *IRE Transactions*, v. MTT-3, No. 2, March 1955, p. 157-62.
- Southworth, G. C. *Principles and applications of waveguide transmission*, New York: Van Nostrand, 1950.
- Torgow, E. N., and J. E. Griemsmann, "Miniature strip transmission line for microwave applications," *IRE Transactions*, v. MTT-3, No. 2, March 1955, p. 21-30.

- Von Hippel, A. R. *Dielectrics and waves*, New York: Wiley, 1954.
- Von Hippel, A. R. *Dielectric materials and applications*, New York: Wiley, 1954.
- Whinnery, J. R., H. W. Jamieson, and Theo Eloise Robbins. "Coaxial-line discontinuities," *Proceedings of the IRE*, v. 32, November 1944, p. 695-709.
- Wild, N. R. "Photo-etched microwave transmission lines," *IRE Transactions*, v. MTT-3, No. 2, March 1955, p. 21-30.
- Wild, N. R. "Photo-etched microwave transmission lines," *Tele-Tech and Electronic Industries*, February and March 1955.